UNIVERSIDADE ESTADUAL DE CAMPINAS
FACULDADE DE CIÊNCIAS MÉDICAS

CARLOS FERNANDO ODIR RODRIGUES MELO

METABOLÔMICA E LIPIDÔMICA DOS PROCESSOS INFECCIOSOS DO VÍRUS DA ZIKA e DENGUE, DO MOSQUITO AO PACIENTE.

METABOLOMIS AND LIPIDOMIC OF BOTH ZIKA AND DENGUE VIRUS INFECTIOUS PROCESSES; FROM MOSQUITO TO THE PATIENT.

CAMPINAS
2019

CARLOS FERNANDO ODIR RODRIGUES MELO

METABOLÔMICA E LIPIDÔMICA DOS PROCESSOS INFECCIOSOS DO VÍRUS DA ZIKA e DENGUE, DO MOSQUITO AO PACIENTE.

METABOLOMIS AND LIPIDOMIC OF BOTH ZIKA AND DENGUE VIRUS INFECTIOUS PROCESSES; FROM MOSQUITO TO THE PATIENT.

Tese apresentada à Faculdade de Ciências Médicas da Universidade Estadual de Campinas como parte dos requisitos exigidos para a obtenção do título de Doutor em Ciências.

Thesis presented to the Faculty of Medical Sciences of the State University of Campinas as part of the requirements required to obtain the title of Doctor of Science

ORIENTADOR: PROF. DR. RODRIGO RAMOS CATHARINO

ESTE EXEMPLAR CORRESPONDE À VERSÃO FINAL DA TESE DEFENDIDA PELO ALUNO CARLOS FERNANDO ODIR RODRIGUES MELO, E ORIENTADA PELO PROF. DR. RODRIGO RAMOS CATHARINO.

CAMPINAS

2019

Ficha catalográfica
Universidade Estadual de Campinas
Biblioteca da Faculdade de Ciências Médicas
Maristella Soares dos Santos - CRB 8/8402

M491a

Melo, Carlos Fernando Odir Rodrigues, 1985-
Metabolômica e lipidômica dos processos infecciosos do vírus da Zika e Dengue, do mosquito ao paciente / Carlos Fernando Odir Rodrigues Melo. – Campinas, SP : [s.n.], 2019.

Orientador: Rodrigo Ramos Catharino.
Tese (doutorado) – Universidade Estadual de Campinas, Faculdade de Ciências Médicas.

1. Zika vírus. 2. Vírus da dengue. 3. Dengue hemorrágica. 4. *Aedes aegypti*. 5. Metabolômica. I. Catharino, Rodrigo Ramos. II. Universidade Estadual de Campinas. Faculdade de Ciências Médicas. III. Título.

Informações para Biblioteca Digital

Título em outro idioma: Metabolomis and lipidomic of both Zika and Dengue virus infectious processes; from mosquito to the patient
Palavras-chave em inglês:
Zika virus
Dengue virus
Hemorrhagic dengue fever
Aedes argypti
Metebolomic
Área de concentração: Fisiopatologia Médica
Titulação: Doutor em Ciências
Banca examinadora:
Rodrigo Ramos Catharino [Orientador]
Karina Cogo Müller
Daniel Fabio Kawano
Daisy Machado
Rejane Maria Tommasini Grotto
Data de defesa: 23-09-2019
Programa de Pós-Graduação: Fisiopatologia Médica

Identificação e informações acadêmicas do(a) aluno(a)
- ORCID do autor: https://orcid.org/0000-0003-0334-1065
- Currículo Lattes do autor: http://lattes.cnpq.br/6661003490402429

COMISSÃO EXAMINADORA DA DEFESA DE DOUTORADO

CARLOS FERNANDO ODIR RODRIGUES MELO

ORIENTADOR: PROF. DR. RODRIGO RAMOS CATHARINO

MEMBROS:

1. PROF. DR. RODRIGO RAMOS CATHARINO

2. PROFA. DRA. KARINA COGO MÜLLER

3. PROF. DR. DANIEL FABIO KAWANO

4. PROFA. DRA. DAISY MACHADO

5. PROFA. DRA. REJANE MARIA TOMMASINI GROTT

Programa de Pós-Graduação em Fisiopatologia Médica da Faculdade de Ciências Médicas da Universidade Estadual de Campinas.

A ata de defesa com as respectivas assinaturas dos membros encontra-se no SIGA/Sistema de Fluxo de Dissertação/Tese e na Secretaria do Programa da FCM.

Data de Defesa: 23/09/2019

Dedico este trabalho aos meus pais que sempre se esforçaram em buscar e prover os melhores meios para a minha educação.

Ao apoio incondicional da minha amiga, parceira e esposa: Tatiane, que me apoiou, me incentivou e acompanhou durante todo o doutorado; apoio este fundamental para que eu mantivesse o foco.

Dedico também à sociedade e espero que os resultados alcançados colaborem no combate a essas duas doenças tão presentes na vida dos brasileiros, mostrando e evidenciando a necessidade de se financiar e investir em pesquisa, e na universidade pública, como forma de prover uma vida melhor à sociedade e para que seja possível nos tornarmos cada vez mais autossuficientes e independentes da tecnologia e soluções externas.

AGRADECIMENTOS

Ao Prof. Dr. Rodrigo pela oportunidade de fazer parte deste grupo de pesquisa incrível que visa sempre a ciência aplicada à sociedade e metodologias disruptivas; uma pessoa sempre disposta a ajudar e a conversar sobre e o que preciso fosse.

Aos amigos de bancada Tatiane, Diogo, Cibele, Estela, Jeany e Mohamad que sempre me auxiliaram dando ideias, nas revisões dos manuscritos, com o preparo de amostras, auxiliando na análise e interpretação dos resultados. Acredito que os resultados aqui encontrados só foram possíveis em razão do trabalho em equipe que é característico do Laboratório Innovare de Biomarcadores e sempre incentivado pelo Prof. Dr. Rodrigo.

Aos pesquisadores externos ao Innovare que colaboraram em muito com os resultados aqui alcançados por meio da colaboração para a obtenção de amostras, colaboração na análise e discussão dos dados e resultados e colaboração no delineamento de experimentos: Prof. Dr. Maurício Lacerda Nogueira (FAMERP), Prof. Dr. Jayme de Souza Neto (Unesp-Botucatu), Prof. Dra. Maria Luiza Moretti (FCM-Unicamp) e Prof. Dr. Anderson de Rezende Rocha (IC – Unicamp).

Ao *Full Professor* Liang Li, por ter me recebido de portas abertas em seu grupo de pesquisa (Prof. Li's Group), e oferecer a oportunidade de conhecer e utilizar as instalações do *The Metabolomics Innovation Centre* durante o período de estágio na Universidade de Alberta, Canada.

Quero agradecer também as agências de fomento, sem as quais este trabalho não seria possível, e que apoiaram financeiramente este projeto: Coordenação de Aperfeiçoamento de Pessoal de Nível Superior - Brasil (CAPES) - PROEX 1645986 e a Fundação de Amparo à Pesquisa do Estado de São Paulo (FAPESP) processos nº 2016/17066-2 e nº 2018/03321-6.

RESUMO

O vírus da Zika (ZIKV) é um arbovírus que apresenta um papel importante no aumento de nascimentos de bebês microcefálicos e em adultos tem sido associado à síndrome de Guillain–Barré, tendo se mostrado como de grande preocupação para a saúde pública. O vírus da Dengue (DENV) se apresenta endêmico no Brasil, se caracterizando, assim como o ZIKV, por provocar infecções autolimitada na grande maioria dos pacientes, sendo de grande importância na saúde pública pelas perdas econômicas em razão da diminuição da produtividade nas populações atingidas e, sobretudo na forma hemorrágica da doença que pode levar à morte. Esses dois arbovírus se adaptaram a mosquitos urbanos facilitando a ocorrência de graves epidemias de Dengue e Zika uma vez que o *A. aegypti* (principal vetor) apresenta discordância gonotrófica, o que o torna um excelente vetor. De uma forma geral as doenças transmitidas por mosquitos têm uma tradição de serem negligenciadas, existindo lacunas de informações biomédicas importantes como, o mecanismo de infecção no mosquito, mecanismo de infecção viral no homem e o diagnostico laboratorial. Em paralelo, a metabolômica e a lipidômica são metodologias de estudo estratégicas e revolucionárias que auxiliam na determinação de biomarcadores importantes no controle de infecções e dada a emergência global para a saúde pública e o potencial revolucionário das novas "ômicas"; que nos permite estudar mecanismos da infecção na forma adulta dos vetores, no homem e se mostra muito importante no diagnóstico. Dado em contexto em tela, este projeto visou estudar as duas arboviroses mais importantes atualmente no Brasil: o ZIKV, propondo busca por biomarcadores para identificar e entender o mecanismo da infecção no mosquito (Objetivo 1) e no Homem (Objetivo 2) para seu melhor controle e desenvolvimento de um método diagnóstico para o ZIKV através de plataformas "ômicas" (Objetivo 3). Para o DENV o objetivo proposto foi a busca de biomarcadores para as alterações provocadas pelo DENV em pacientes que apresentaram a Dengue hemorrágica (Objetivo 4).

Palavras-chave: Zika vírus; Vírus da Dengue; Dengue Hemorrágica; *Aedes aegypti*; Espectrometria de Massas; Metabolômica.

ABSTRACT

Zika virus (ZIKV) is an arbovirus that plays an important role in increasing births of microcephalic babies and in adults and has been associated with Guillain-Barré syndrome and it has been of major public health concern. Dengue virus (DENV) is endemic in Brazil and, like ZIKV, is characterized by causing self-limiting infections in the vast majority of patients, being of great importance in public health due to economic losses due to decreased productivity in affected populations and above all in the hemorrhagic form of the disease that can lead to death. These two arboviruses have adapted to urban mosquitoes facilitating the occurrence of severe epidemics of Dengue and Zika since the *A. aegypti* (main vector) presents with gonotrophic discordance, which makes it an excellent vector. In general, mosquito-borne diseases have a tradition of being neglected, and there are gaps in important biomedical information such as mosquito infection mechanism, viral infection mechanism in man, and laboratory diagnosis. In parallel, metabolomics and lipidomics are strategic and revolutionary study methodologies that aid in the determination of important biomarkers in infection control and the global emergence of public health and the revolutionary potential of the new "omics"; which allows us to study mechanisms of infection in the adult form of the vectors in humans and is very important in the diagnosis. Given in context on screen, this project aimed to study the two most important arboviruses currently in Brazil: the ZIKV, proposing a search for biomarkers to identify and understand the mechanism of infection in the mosquito (Goal 1) and human (Goal 2) for its better disease control and development of a diagnostic method for ZIKV through "omic" platforms (Goal 3). For DENV the proposed goal was to search for biomarkers for DENV alterations in patients presenting with hemorrhagic Dengue (Goal 4).

Keywords: Zika virus; Dengue virus; Hemorrhagic Dengue Ferver; *Aedes aegypti*; Mass Spectrometry; Metabolomic.

LISTA DE ABREVIATURAS E SIGLAS

°C	Escala Celsius
A. aegypti	*Aedes aegypti*
A. albopictus	*Aedes albopictus*
ANG	Angiotensina
APCI	Ionização Química em Pressão Atmosférica
C	Capsídeo Viral
CAISM	Centro de Atenção Integral à Saúde da Mulher
CCD	Cromatografia em Camada Delgada
cDNA	DNA complementar
CG	Cromatografia Gasosa
CHIV	Vírus Chikungunya
CL	Cromatografia Líquida
CLAE	Cromatografia Liquida de Alta Eficiência
COL	Colesterol
DENV	Vírus da Dengue
DIAC	Diacilgliceróis
DNA	Ácido Desoxirribonucleico
E	Envelope Viral
ECA	Enzima Conversora de Angiotensina
EFS	Extração em Fase Sólida
EM	Espectrometria de Massas
EMAR	Espectrometria de Massas de Alta Resolução
ESF	Esfingolípido
ESI	Ionização por Spray de Elétrons
FAMERP	Faculdade de Medicina de São José do Rio Preto
FWHM	Largura à Meia Altura
GANG	Gangliosídeo

HMDB	Base de Dados do Metaboloma Humano
IgM	Imunoglobulina M
KEGG	Enciclopédia de Kyoto de Genes e Genomas
m/z	Relação Massa/Carga
MAC-ELISA	Ensaio de Imunoabsorção Enzimática por Captura de Imunoglobulina M
MALDI	Ionização/Dessorção a Laser Assistida por Matriz
mRNA	RNA mensageiro
NS	Proteina Não Estrutural
NS1 Ag	Antígeno NS1
OROV	Vírus Oropouche
PAF	Fator de Ativação Plaquetária
PC	Fosfatidilcolinas
PCA	Análise de Componentes Principais
PIP	Fosfatidilinositol Fosfato
PLS	Mínimos Quadrados Parciais
PLS-DA	Análise Discriminante Parcial dos Mínimos Quadrados
ppm	Partes por milhão
prM	Pré-Membrana
PVDF	Fluoreto de Polivinilideno
RNA	Ácido Ribonucleico
rpm	Rotações Por Minuto
RT-qPCR	Reação em Cadeia da Polimerase Quantitativo em Tempo Real
SRA	Sistema Renina Angiotensina
ssRNA	Ácido Ribonucleico Positivo de Cadeia Única
TG	Triglicerídeos
UNESP	Universidade Estadual Paulista Júlio de Mesquita Filho
Unicamp	Universidade Estadual de Campinas
VIP	Importância Variável na Projeção
ZIKV	Vírus da Zika

SUMÁRIO

1. INTRODUÇÃO

1.1. Vírus da Zika

O vírus da Zika (ZIKV) é um arbovírus da família *Flaviviridae* isolado pela primeira vez em macacos da floresta de Zika, em Uganda, no continente Africano[1], e tem como vetor o mosquito *Aedes africanus*[2]. A despeito de o macaco ser seu reservatório natural, a infecção de humanos com o vírus também foi verificada[3] e desde então sempre houve relatos de surtos urbanos de infecção por ZIKV. Esses relatos tinham como característica serem casos isolados e extremantes pontuais em uma determinada localidade geográfica, como locais na Nigéria[4] e Indonésia[5]. Recentemente, mais especificamente de 2013 em diante, o ZIKV tem preocupado as autoridades sanitárias por estar se disseminando rapidamente e por ser confirmado em 33 países do continente americano, sobretudo nos países localizados na região equatorial[3], além de estar presente em grande parte dos países do sudeste asiático[6].

A hipótese que explica como o vírus que originariamente se caracterizava como uma zoonose restrita ao continente africano, e que hoje está sendo cada vez mais encontrado em humanos, se relacionada com as alterações climáticas, o aumento do perímetro urbano sobre áreas até então silvestres e o rápido tráfego de pessoas pelo mundo através dos atuais meios de transporte. O vírus, que até então permanecia restrito a uma região e a um vetor específico, conseguiu chegar a outras localidades e se adaptou ao homem como hospedeiro assim como se adaptou a novos vetores urbanos como o *A. aegypti* e *A. albopictus* [7]. Desta forma, estabeleceu- se um novo ciclo, não mais animal-artrópode-homem, mas homem-artrópode-homem. Estes novos vetores encontrados pelo ZIKV se caracterizam por possuir alta capacidade vetorial, ou seja, apresentam alta capacidade de transmitir um agente patogênico num determinado local e há um tempo específico. O *A. aegypti*, considerado atualmente o mais importante vetor urbano do ZIKV, tem como característica as fêmeas se alimentarem, principalmente, de sangue de seres humanos e frequentemente conseguem picar vários indivíduos em um único período de alimentação, adicionalmente este mosquito tem uma picada quase imperceptível e vive em estreita associação com a habitação humana. Assim, o

ZIKV ao estabelecer-se em um novo vetor, fez com que o número de casos aumentasse exponencialmente [3], passando também a ser um vírus urbano, não mais restrito apenas a algumas áreas de risco.

As manifestações clínicas da infecção por ZIKV não são específicas, sendo os sintomas mais frequentes o exantema macular ou papular, febre, artrite ou artralgia, conjuntivite não purulenta, mialgia, cefaléia, febre, dor retro-orbital, edema e vômitos [8] fazendo o diagnóstico clínico ser de difícil conclusão e confundido com infecções virais como por vírus da dengue (DENV), vírus Chikungunya (CHIV) e até mesmo com o vírus Oropouche (OROV), este último especialmente na região norte do Brasil, onde é endêmico. Os diagnósticos laboratoriais existentes também apresentam dificuldades em produzir um laudo conclusivo uma vez que o exame sorológico, que visa a detecção de anticorpos Imunoglobulina M (IgM) por meio do Ensaio de Imunoabsorção Enzimática por Captura de Imunoglobulina M (do inglês *"*Immunoglobulin M Capture Enzyme-Linked Immunosorbent Assays*"* - MAC-ELISA) apresenta reação cruzada com outros tipos de Flavivírus como o DENV [9]; já ao exame virológico, que é considerado padrão ouro para o diagnóstico, feito por meio de Reação em Cadeia da Polimerase da Transcrição Reversa em Tempo Real (do inglês "Reverse transcription polymerase chain reaction quantitative real time*"* - RT-qPCR) é possível fazer apenas na fase aguda da doença uma vez que a viremia do ZIKV é baixa, tornando o isolamento do vírus a partir de amostras clínicas extremante difícil [10]; assim , se preconiza fazer o exame exatamente uma semana após o início das manifestações clínicas [10].

A preocupação em se fazer um diagnóstico rápido e assertivo do ZIKV e para reduzir a disseminação do vírus e também ao fato de que tem-se verificado um aumento na síndrome de Guillain–Barré associado à infecção por ZIKV (síndrome que se caracteriza como uma doença autoimune que causa paralisia flácida aguda ou subaguda) e também ao aumento no nascimento de bebês microcefálicos a partir de mães infectadas com ZIKV [11] , sendo esta última uma condição neurológica onde a cabeça e o cérebro da criança são significativamente menores do que os de outras da mesma idade e sexo em razão do anormal

desenvolvimento neurológio durante a gestação ou após o nascimento [12]. Estas associações foram estabelecidas a partir de estudos epidemiológicos, entretanto ainda se faz necessários estudos adicionais, com os pacientes sendo efetivamente diagnósticos com ZIKV para corroborar ou não a associação hoje existente.

1.2. Vírus da Dengue

Os vírus da Dengue (DENV) são arbovírus transmitidos por mosquitos do gênero *Aedes*, como *Aedes aegypti* e *Aedes albopictus*, associados a epidemias explosivas de doenças febris nas regiões geográfica compreendida nos trópicos em todo o mundo [13]. O grande número de pacientes infectados por DENV a cada ano (estimado pela Organização Mundial de Saúde em 390 milhões de infecções por dengue por ano) faz do DENV o arbovírus de maior importância epidemiológica mundialmente.

Os vírus DENV se caracterizam por serem envelopados e pertencentes à família *Flaviviridae*, gênero *Flavivirus*, classificados em quatro sorotipos (DENV-1, DENV-2, DENV-3, DENV-4 e DENV-5) intimamente relacionados, mas antigenicamente distintos. Como outros flavivírus, o genoma DENV é composto por um RNA (do inglês "ribonucleic acid*")* positivo de cadeia única (do inglês "positive-sense single-stranded RNA" – (+)ssRNA) de quase 11 kb, que codifica uma poliproteína que é clivada em três proteínas estruturais, o capsídeo viral (C), a pré-membrana (prM) e o envelope viral (E) e sete proteínas não estruturais (do inglês *"*Non-Structural Protein" – NS*)*, denominadas NS1, NS2A, NS2B, NS3, NS4A, NS4B e NS5 [14].

Embora o espectro do quadro clínico após a infecção por DENV possa variar de subclínica para morte, a maioria dos pacientes sintomáticos desenvolve uma doença febril aguda autolimitada com duração de aproximadamente 4-7 dias, caracterizada pelos seguintes sintomas e características: febre, calafrios, retro-cefaleia orbital, mialgia, mal-estar, leucopenia, trombocitopenia (por vezes grave) e níveis elevados de transaminases hepáticas [15]. Neste contexto, uma pequena porcentagem de pacientes infectados, geralmente crianças ou adultos durante uma segunda infecção com um sorotipo diferente de DENV, podem desenvolver

Dengue em sua forma grave, com sangramento espontâneo, vazamento de plasma, falência de órgãos e choque [15].

O conhecimento disponível sugere que o resultado da infecção por DENV depende de vários fatores produzidos durante o início da infecção viral, como carga viral, presença de anticorpos neutralizantes, recrutamento de células imunes e produção de mediadores imunológicos [14] . Esses fatores criam um ambiente favorável e ao mesmo tempo desfavorável, proporcionando controle da infecção viral e uma reação inflamatória prejudicial associada à permeabilidade vascular. Neste sentido, a falta de marcadores imunológicos confiáveis ou outros marcadores metabólicos para respostas protetoras ou patológicas ainda é uma lacuna importante para o desenvolvimento de novos testes diagnósticos, testes prognósticos ou marcadores candidatos à fabricação de vacinas eficientes [16,17].

1.3. *Aedes Aegypti*

O *Aedes aegypti* é um mosquito originário do Egito. Esse vetor foi descrito cientificamente pela primeira vez em 1762, sendo inicialmente denominado *Cúlex aegypti* (“cúlex” significa mosquito e “aegypti”, egípcio). Com a descrição do gênero *Aedes* em 1818, verificou-se que a espécie *aegypti*, apresentava características morfológicas e biológicas semelhantes às de espécies do gênero *Aedes* fato que alterou a classificação de *Cúlex* para *Aedes*, sendo então estabelecido *Aedes aegypti* [18,19]. Este mosquito teve sua dispersão pelo mundo a partir dos navios negreiros que faziam tráfico de escravos da África para Europa e América [20–22].

A razão pela qual os mosquitos sugam o sangue de animais, em realidade apenas a fêmea, é que estas necessitam de sangue para a maturação dos ovos e neste processo, ao picar o homem, se o mosquito estiver infectado com o ZIKV ou DENV, ele pode infectar o indivíduo que está sendo picado. Os mosquitos urbanos têm por hábito sugar o sangue de uma só pessoa a cada ovo postura, entretanto o *A. aegypti* é capaz de picar mais de uma pessoa a cada ovo postura, característica chamada de discordância gonotrófica, tornando-o um excelente vetor para doenças, devido ao grande número de pessoas diferentes que ele é

capaz de picar e consequentemente transmitir o vírus, quando infectado [22]. A maneira como o mosquito combate ao vírus, do ponto de vista imunológico, ainda é muito pouco explorada; sendo normalmente abordados em modelos de estudo já estabelecido como a *Drosófila melanogáster* [23], adicionalmente os estudos focam genômica e proteômica [23–27] não tendo estudos que analisam o fenótipo metabolômico relacionado à infecção viral no mosquito, abordagem que este trabalho tem como foco; de verificar as alterações ocorridas em mosquitos infectados.

1.4. Metabolômica

Hoje o grande desafio dos pesquisadores não é mais desvendar as sequências de pares de bases nitrogenadas que compõe o RNA de um vírus ou o DNA (Ácido Desoxirribonucleicodo - inglês “Deoxyribonucleic Acid”) de um ser vivo, o que faz com que tenhamos hoje uma grande quantidade de genomas disponíveis em domínio público [28]. O desafio hoje é conectar os genes com suas funções, relacionar o genótipo com o fenótipo. O impulso para entender a função dos genes descobertos recentemente alavancou a análise sistemática dos níveis de expressão de componentes de um sistema biológico, tais como mRNA (RNA mensageiro - do inglês “Messenger RNA”), proteínas e metabólitos, e a catalogação global destes componentes tem dado origem a vários “OMAs” (o genoma, o proteoma, o metaboloma). Entender a rede de componentes e como eles interagem é a base do acesso aos sistemas biológicos [29].

A metabolômica é o estudo sistemático e completo da série de intermediários de baixo peso molecular, não protéicos, sintetizados endogenamente (o metaboloma) e que esteja contido em uma célula representando o produto final da expressão gênica. Dentre esses estão os aminoácidos, ácidos nucléicos, açúcares e lipídeos. Assim, a metabolômica é responsável por estudar outras subáreas como glicômica (açúcares), a lipidômica (lipídios) e pepdidômica (peptídeos não proteicos) [29,30]. A Figura 1 mostra como a lipidômica, por meio da metabolômica, representa o ponto final da cascata “ÔMICA” e consequentemente o ponto mais próximo ao fenótipo. Assim a

lipidômica, como a metabolômica, se desenvolve como uma ferramenta funcional da genômica. Combinando a genômica, transcriptômica, proteômica e a metabolômica (lipidômica), essas podem fornecer uma poderosa série de ferramentas para examinar mudanças fenotípicas [30].

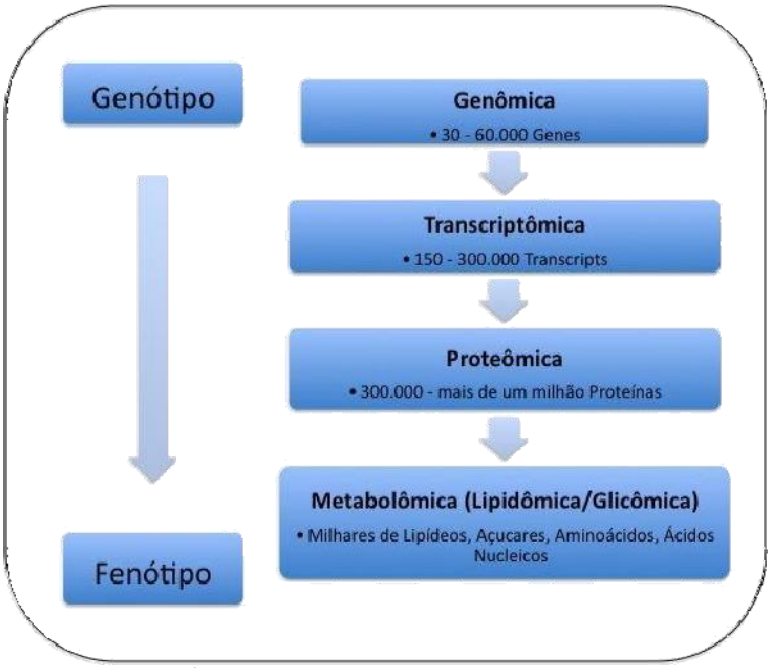

Figura 1: Diferentes níveis das "ÔMICAS" demonstrados como uma cascata que relaciona o genótipo com o fenótipo [35].

Uma vez que o vírus depende exclusivamente do metabolismo celular da célula hospedeira para sua replicação, no processo de infecção celular; ele altera a metabolômica celular a fim que a célula produza os metabólitos necessários para sua infecção e replicação [31–33]. A partir das alterações fenotípicas apresentadas pelas células infectadas é possível verificar quais vias metabólicas estão ativas ou têm sua atividade aumentada ou diminuída, ajudando a entender como ocorre o processo de infecção celular pelo vírus [31,34–36].

1.5. Lipídeos e Lipidômica

Lipídeos podem ser definidos, de uma maneira geral, como pequenas moléculas hidrofóbicas ou anfifílicas que podem se originar parcial ou inteiramente pela condensação de subunidades de cetoacil e isoprenos, oleosos ao toque, e que, juntamente com carboidratos e proteínas, constituem o principal material

estrutural para a vida celular [29,30,37–39], mas que têm sua função no processo de infecção viral, bem como sua função estrutural nos vírus ainda muito pouco explorada sendo uma área quase que desconhecida embora já se tenha demonstrado de extrema importância no processo de infecção viral e de manutenção da replicação viral [32,34,40].

A maioria dos lipídeos que ocorrem biologicamente são combinações lineares de cadeias alifáticas e grupos com cabeças polares ligados ao glicerol ou esfingolipídios, assim como cadeias alifáticas covalentes ligadas ao colesterol. A grande variabilidade de lipídeos ocorre devido à grande variabilidade estrutural que pode ocorrer nas combinações dos seus constituintes como: natureza dos grupos da cabeça (definindo classes lipídicas); tamanho das cadeias alifáticas; número, posição e estereoquímica de duplas ligações; grupos hidroxil e outras funções nas cadeias alifáticas; a natureza das ligações covalentes do grupo da cabeça (éter, éster, vinil éster) [30,41].

Os lipídeos apresentam ampla função dentro das células, incluindo constituinte de membranas, manutenção de gradientes eletroquímicos, primeiros e segundos mensageiros na sinalização celular, estoque de energia, transporte de proteínas e ancoragem destas em membranas [30,37–39,42].Desta forma , uma vez que o vírus se utiliza da maquinaria celular no processo de replicação e infecção, alguns desses lipídios são cruciais também para o vírus [43,44].

A lipidômica, uma subclasse da metabolômica, pode ser definida como a determinação molecular, quantitativa e completa, de moléculas de lipídeos isolados a partir de células, tecidos e fluidos biológicos, em várias condições fisiológicas e patológicas[29,30,37,45]. Existem duas maneiras de se fazer estudos em lipidômica: com alvo (do inglês “Target Lipidomic”) e sem alvo (do inglês “Untarget Lipidomic”). Na lipidômica com alvo, os lipídeos caracterizados e quantificados já são conhecidos antes do início da análise e são utilizados protocolos de análise específicos para cada uma destas classes de lipídeos. E na lipidômica sem alvo se faz um levantamento exploratório e qualitativo do conjunto de lipídeos da amostra, sendo útil para descoberta de novos lipídeos e criação de bibliotecas de lipídeos [29,46].

A partir desses estudos, a lipidômica está se desenvolvendo rapidamente e emergindo como uma disciplina independente de interface entre biologia lipídica, tecnologia e medicina. A diversidade e complexidade dos lipidomas biológicos requerem inovações técnicas e melhoramento para suprir a necessidade dos vários estudos biomédicos desenvolvidos. A recente onda de expansão no campo da lipidômica pode ser atribuída aos avanços na tecnologia analítica, em particular, o desenvolvimento de novas ferramentas de cromatografia, espectrometria de massas e bioinformática para quantificação e caracterização da grande série de lipídeos presentes em um lipidoma [37,47].

1.6. Análise de Lipídeos e Espectrometria de Massas (EM)

Estratégias tradicionais de análise de lipídeos usualmente pré-fracionam os lipídeos em classes por Cromatografia em Camada Delgada (CCD), Cromatografia Líquida (CL), Extração em Fase Sólida (EFS), e depois separam as classes particulares de lipídeos em moléculas individuais por Cromatografia Liquida de Alta Eficiência (CLAE) acoplada a diferentes detectores. Com estes métodos tradicionais as moléculas individuais de muitas classes de lipídeos podem ser analisadas, porém estes apresentam baixa sensibilidade, resolução limitada, necessitam de grande quantidade de amostra e muitas vezes são necessários vários passos para sua preparação. Mas ainda são utilizados, pois são relativamente fáceis e apresentam baixo custo experimental [38,47] .

Com o desenvolvimento da CL e da Cromatografia Gasosa (CG), a separação de muitos lipídeos de misturas complexas se tornou possível; no entanto a identificação e quantificação de lipídeos em misturas complexas, tais como extratos brutos de lipídeos, ainda permanecia desafiador e muitos procedimentos demorados, como hidrólise e derivatização, são necessários nestes tipos de análise cromatográficas. O campo teve grande avanço quando o CG foi acoplado a EM [38,41,45] e com o desenvolvimento da tecnologia da ionização suave tais como Ionização/Dessorção a Laser Assistida por Matriz (do inglês “Matrix-Assisted Laser Desorption Ionization” – MALDI), Ionização por Spray de Elétrons (do inglês “Eletronspray Ionization” - ESI) e Ionização Química por

Pressão Atmosférica (do inglês “Atmospheric Pressure Chemical Ionization” – APCI); e possibilidade de acoplar algumas dessas fintes à CL, tornou possível em uma única análise à avaliação rápida e sensível da maioria, ou fração substancial, dos lipídeos presentes em uma determinada amostra/matriz de interesse [29,41,45].

Comumente os lipídeos são extraídos antes de serem submetidos à análise por EM por diferentes métodos de extração tais como Bligh Dyer [48], Folch [49]; e então , a amostra lipídica é injetada no EM, ionizada e vaporizada, resultando em íons que são separados de acordo com sua relação massa/carga (*m/z*) no analisador de massas[38].

Existem duas ferramentas fundamentais para identificação e quantificação de lipídeos por EM [42]. A primeira, e mais tradicional, é a Análise Lipidômica Abrangente por Simplificação de Separação (CLASS do inglês “Comprehensive Lipidomics Analisys by Separation Simplification”), baseada na separação de diferentes categorias de lipídeos utilizando extração e separação cromatográfica antes da análise por EM, e por fim otimizar o espectrômetro de massas para analisar classes específicas de lipídeos [30,42].

A segunda ferramenta, também chamada de “Shotgun Lipidomics”, omite a separação cromatográfica e analisa essencialmente todas as classes de lipídeos, por injeção direta no espectrômetro de massas enquanto emprega diferentes fontes de polaridade de íons (para formar íons positivos e negativos) e, ao adicionar soluções ionizantes, favorece a análise de classes específicas de lipídeos [29,30,42].

1.7. Lipidômica e diagnóstico

Os lipídeos atuam na composição de membrana, fontes de energia e transdução de sinal e por isso podem realizar papel importante como em doença de Alzheimer, doenças cardiovasculares e infecções por vírus e bactérias. Assim sendo, é extremamente importante caracterizar os lipídeos envolvidos nestes processos e há diversas inciativas com o intuito de mapear os metabólitos envolvidos nos mais diversos processos fisiológicos ou patofisiológicos, tais como consórcio “Lipid MAPS” (http://www.lipidmaps.org) [50,51] o consorcio do “Human

Metabolome Database" (HMDB-http://www.hmdb.ca/) [52] e o consorcio Metlin (https://metlin.scripps.edu) [53].

Neste contexto, muitos esforços para catalogar o lipidoma de células infectadas por vírus têm sido realizados como para o vírus da Hepatite C [44], o vírus da Dengue [54], vírus Ebola [43] e outros [39,55]; estes estudos têm apontado que os lipídios têm grande importância no processo de infecção da célula pelo vírus [44,54–56] . Os diferentes lipídeos presentes em cada um dos processos infecciosos dos diferentes patógenos abrem novos campos de investigação para a lipidômica. Uma investigação sistemática dos lipídeos particulares do processo de infecção e que identifiquem os diferentes patógenos de espécies relacionadas podem fornecer informações sobre biomarcadores para aplicação em diagnósticos e/ou terapia [44,47,57].

O diagnóstico por espectrometria de massas já é uma realidade para uma série de doenças como, por exemplo, diversos tipos de cânceres, infecções bacterianas com a identificação taxonômica do agente infeccioso e análise de DNA para busca de alterações características de determinadas doenças [58–62]. Devido a isso, a inclusão do ZIKV e DENV no portfólio de doenças diagnosticadas por espectrometria de massas visando um laboratório que já possui este equipamento, implicaria na redução do custo unitário do exame para apenas US$ 0,65, em comparação com o método diagnóstico padrão ouro hoje utilizado (RT-qPCR). Além disso, outro benefício seria a facilidade que um laboratório central conseguiria fazer este tipo de diagnóstico, a qualquer tempo e com qualquer número de amostras, uma vez que a técnica aqui apresentada é passível de automação e independe da compra de sondas ou "kits", o que extinguiria problemas como o controle do estoque de materiais e prazos de validade, além da flutuação cambial destes insumos.

2. OBJETIVOS

2.1. Objetivo geral

Estudo metabolômico e lipidômico para um melhor entendimento da relação parasito-hospedeiro e determinação de potenciais biomarcadores para o

diagnóstico e prognostico das infecções causadas pelos arbovírus Zika e Dengue.

2.1.1. Objetivos Específicos

- Identificar marcadores que se apresentem alterados a partir de amostras de mosquitos infectados com ZIKV para um melhor entendimento do processo de infecção/replicação viral neste organismo.
- Identificar marcadores que se apresentem alterados a partir de amostras de soro sanguíneo de pacientes infectados com ZIKV visando um melhor entendimento da patogenesia da doença.
- Desenvolver uma metodologia diagnostica rápida a partir de amostras de soro sanguíneo e urina de pacientes infectados com ZIKV.
- Identificar marcadores que se apresentem alterados em pacientes infectados com DENV e que manifestam a forma Hemorrágica da doença a partir de amostras de soro sanguíneo de pacientes infectados, permitindo um melhor entendimento da patogenesia da doença e prognostico.

3. METODOLOGIA

As metodologias específicas para cada uma das frentes estudadas nesta tese serão abordadas em detalhes nos artigos apresentados na seção 4. Resultados

3.1. Amostras:

3.1.1. Amostras biológicos:

3.1.1.1. Fluidos biológicos de pacientes

3.1.1.1.1. ZIKV

Amostras de fluidos biológicos (urina e soro) de pacientes infectados e controles foram coletadas a partir de pacientes pelo Centro de Atenção Integral à Saúde da Mulher (CAISM) da Unicamp, todos na fase aguda da infecção.

Todas as 69 amostras utilizadas no estudo, foram analisadas por RT-qPCR para o diagnóstico do ZIKA na amostra. Esta análise foi realizada no Instituto de Biologia da Unicamp, no departamento de Genética, Evolução e Bioagentes no laboratório coordenado pela Profa. Dra. Clarice Weis Arns.

3.1.1.1.2. DENV

Todas as 20 amostras foram obtidas do Laboratório de Pesquisa em Virologia da Faculdade de Medicina de São José do Rio Preto (FAMERP), cidade localizada na região noroeste do Estado de São Paulo, Brasil. Todas as amostras foram obtidas de pacientes febris atendidos em centros de saúde de São José do Rio Preto durante o ano de 2014, quando o ZIKV e o CHIKV não foram detectados no Estado de São Paulo e na fase aguda da infecção.

Todas as amostras clínicas de DENV usadas neste estudo foram positivas para o antígeno DENV-NS1 usando o “kit” de teste rápido para antígeno NS1 (NS1 Ag) de acordo com as instruções do fabricante. Além disso, todas as amostras foram positivas para DENV-4 por RT-Multiplex-Nested-PCR específica realizada após extração de RNA de 140 µL de soro com o mini “kit” QIAamp Viral RNA (QIAGEN), de acordo com o protocolo do fabricante. A Multiplex-Nested-PCR para DENV 1-4 foi realizada segundo Colombo et al., (2016) [63].

3.1.1.2. Amostras do mosquito:

As fêmeas do mosquito *Aedes aegypti*, infectadas por Zika vírus, foram fornecidas pelo Laboratório de Genômica e Microbiologia Funcional de Vetores do Instituto de Biotecnologia da UNESP que é coordenado pelo Prof. Dr. Jayme Augusto de Souza-Neto.

Os 72 mosquitos foram divididos em dois grupos: 36 alimentados com sangue infectado pelo ZIKV e 36 alimentados com sangue não contaminado para o grupo de controle. Esses 36 indivíduos de cada grupo foram posteriormente separados e analisados em três etapas: 1, 6 e 12 horas, com 6 sujeitos por grupo. Indivíduos de ambos os grupos foram expostos a uma refeição de sangue artificial contendo 800 µL de sangue de ovelha comercial. Para o grupo de mosquitos

infectados, a alimentação com sangue foi composta de 400 µL de sangue com 400 µl de ZIKV derivado do sobrenadante de cultura de células da linha de células C6/36 de *Aedes albopictus*. O suprimento de sangue durou aproximadamente 45 minutos e, após a alimentação, os mosquitos foram desinfetados externamente em álcool a 70% e posteriormente armazenados em metanol.

A confirmação da presença do ZIKV foi realizada pela metodologia de quantificação absoluta em RT-qPCR, convertendo os valores de Limiar do Ciclo (do inglês “Cycle threshold” - Ct) em concentração viral Unidade Formadora de Colônia (UFC) por mL com o auxílio de uma curva padrão. A partir de uma alíquota pré-titulada, $4{,}4.10^{7}$ UFC/mL foram preparados três repetições de diluição seriada (10^{-1} a 10^{-4}), procedendo-se à extração de RNA (Trizol® Reagent-Life Technologies) e síntese de DNA complementar (cDNA) (RevertAid First Strand cDNA Synthesis-Thermo Scientific) para cada diluição. Posteriormente, o cDNA das amostras foi quantificado, e o valor de *Ct* correspondeu a uma diluição. Assim, após a formação da curva padrão, a amostra utilizada para o suprimento sanguíneo foi quantificada, e o *Ct* adquirido correspondente foi o de $1{,}37.10^{6}$ UFC/mL.

3.2. Acondicionamento das amostras

As amostras foram acondicionadas em tubos de 1,5 mL, 25mL e 50mL, de acordo com a necessidade. Todas as amostras foram transportadas em gelo seco (-20 ^{o}C) e armazenadas em freezer -80 ^{o}C até o momento da análise.

3.3. Análise das amostras

3.3.1. Preparo das amostras para análise por Espectrometria de Massas de Alta Resolução (EMAR)

3.3.1.1. Amostras de soro de pacientes controle, soro de pacientes infectados por ZIKV, soro de pacientes infectados por DENV e urina de pacientes infectados por ZIKV.

Para a preparação das amostras, 20 µL de cada amostra biológica (soro sanguíneo) foram diluídos em 200 µL de tetrahidrofurano e homogeneizados em vortex por 30 s; o volume foi então completado para 1 mL com metanol, com posterior homogeneização. A solução obtida foi centrifugada por 5 min a 3.200 rpm. Uma fração de 20 µL do sobrenadante foram então coletados e diluídos em 980 µL de metanol, resultando na solução final, que foi dividida em duas porções de 500 µL para análise nos modos de íons positivos e negativos após a adição de 0,1% de ácido fórmico e hidróxido de amônio, respectivamente.

3.3.1.2. Amostras dos mosquitos íntegros infectados e não infectados com ZIKV.

Para a preparação das amostras, cada indivíduo (mosquito) foi colocado em metanol dentro de um eppendorf® de 2 mL e sonicado em banho de gelo (± 4°C) por 10 minutos, a seguir cada amostra foi vortexada por 30 segundos, centrifugada a 10.000 Rotações Por Minuto (RPM) por 10 minutos (4°C) e 400 µL do sobrenadante foi retirado e filtrado com filtro de fluoreto de polivinilideno (PVDF) de 0,22 µm para outro eppendorf® de 2 mL. A este filtrado foi adicionado 600 µL de metanol, completando uma solução de 1 mL, em que foi adicionado 0,1% de ácido fórmico.

3.3.2. Análise por EMAR

Todas as amostras foram diretamente injetadas para análise do “full scan” em um instrumento ESI-LTQ-XL Orbitrap Discovery (Thermo Scientific, Bremen, Alemanha) com resolução nominal de 30.000 (Largura à Meia Altura – FWHM do inglês “full width at half maximum”), sob os seguintes parâmetros: vazão de 10 $\mu L.min^{-1}$ temperatura do capilar de 280 ^{o}C, 5 kV de voltagem no pulverizador e gás de arraste á 10 unidades arbitrarias. As análises de EMAR foram realizadas em triplicatas ou quintuplicata para cada amostra, usando a faixa de massa de 50 a

2000 *m/z* nos modos de íon positivo e negativo. No item **4. Resultados**, constam as descrições exatas utilizadas para cada experimento.

3.3.3. Análise estatística

As análises estatísticas para escolha dos marcadores químicos foram realizadas por métodos de análise multivariada, sendo quatro as ferramentas utilizadas neste projeto:

- Análise de Componentes Principais (do inglês “Principal Components Analysis” - PCA) que reduz o conjunto original de recursos para um novo conjunto de características (os componentes principais atuais), que representam as informações importantes extraídas do conjunto de dados inicial, como pares linearmente independentes. A redução dos dados de dimensão auxilia encontrar os dados mais representativos em cada amostra, comparável a partir de combinações lineares do recurso original, que é o que permite a escolha do(s) marcadores(s) distintivo(s) de cada amostra.
- Análise Discriminante por Mínimos Quadrados Parciais (do inglês “Partial Least Squares Discriminant Analysis” - PLS-DA) foi usada como método de escolha para avaliar a associação entre os grupos; este método supervisionado usa técnicas de regressão multivariada para extrair, através da combinação linear das variáveis originais, as características que podem evidenciar essa associação. A significância estatística do modelo obtido foi avaliada por meio de dois testes de permutação: pré-visualização de precisão durante a modelagem e distância de separação; 2000 permutações foram usadas em ambos os testes. A seleção dos lipídeos característicos de cada amostra foi realizada considerando o impacto que cada metabólito teve na análise através dos “escores” (pontuações) da “VIP” (Importância Variável na Projeção), que consiste na média ponderada dos quadrados das cargas do PLS, e leva em consideração a quantidade de variância explicada em cada dimensão usada no modelo.
- Análise Discriminante dos Mínimos Quadrados Parciais Ortogonais (do inglês “Orthogonal Partial Least Squares Discriminant Analysis” - OPLS-DA). Sendo uma variação da análise discriminante de mínimos quadrados parciais (PLS-DA),

OPLS-DA é um método de regressão multivariada supervisionado que realiza a combinação linear das variáveis originais, extraindo de dados de espectrometria de massa bruta, características responsáveis pelo seu agrupamento. A principal diferença do OPLS-DA do PLS-DA é que ele usa correção de sinal ortogonal para maximizar a covariância explicada entre os componentes do modelo. Para esta análise, o intervalo interquartil foi usado como método de filtragem de dados, com normalização quantílica e escala de alcance.

3.4. Elucidação de marcadores

Para elucidação estrutural dos marcadores foram utilizados os valores de massa em alta resolução, a distribuição do padrão isotópico, os padrões de quebra molecular MS2 e MS3. Essas informações foram verificadas em banco de dados disponíveis on-line como Lipids MAPS (Universidade da Califórnia, San Diego, CA) [51], HMDB (Banco de Dados do Metaboloma Humano) versão 3.6[64] e METLIN (Centro Scripps de Metabolômica, La Jolla, CA)[65]. O erro máximo de precisão de massa adotada foi 2 ppm.

3.5. Elucidação das vias metabólicas envolvidas

A elucidação das vias metabólicas foi feita por meio da busca das vias metabólicas na Enciclopédia de Kyoto de Genes e Genomas (KEGG) [do inglês *Kyoto Encyclopedia of Genes and Genomes – KEGG*] [28,66]. A busca foi realizada para cada um dos marcadores que tiveram a sua estrutura elucidada (Item 3.4).

4. RESULTADOS

A seguir estão apresentados os trabalhos desenvolvidos durante este doutorado, demonstrando a execução e discussões de cada umas das frentes anteriormente apresentadas:

4.1. Artigos

4.1.1. Artigo I

SNS1 SYNTHESIS ANALYSIS IN MOSQUITOES INFECTED WITH ZIKV - A LIPIDOMIC APPROACH

Carlos Fernando Odir Rodrigues Melo[1,2], Tatiane Melina Guerreiro[1], Jeany Delafiori[1], Diogo Noin de Oliveira[1], Letícia Tiemi Egami Oda[3], Letícia Tsiemi Gushi[3], Jayme A. Souza-Neto[3,4], Rodrigo Ramos Catharino[1]

[1]Innovare Biomarkers Laboratory, School of Pharmaceutical Sciences, University of Campinas, Campinas, 13083-877, Brazil
[2]Superintendência da Polícia Técnico-Científica, São Paulo, SP 05507-060, Brazil
[3]São Paulo State University (UNESP), School of Agricultural Sciences, Department of Bioprocesses and Biotechnology, Botucatu, 18610-034, Brazil
[4]São Paulo State University (UNESP), Institute of Biotechnology, Botucatu, 18607-440, Brazil

* Corresponding author: Rodrigo Ramos Catharino [e-mail: rrcatharino@gmail.br]

ABSTRACT

Zika virus (ZIKV) is an arbovirus responsible for the Zika Fever disease with which several outbreaks have been reported in the South Pacific and Latin America since 2007. The most recent cases since 2016 drew extra attention because patients infected with ZIKV started presenting severe neurological complications that were previously unknown or had not been identified as a clinical condition connected to this infection, such as Guillain-Barré syndrome and microcephaly in children of ZIKV-infected pregnant women. As an arbovirus, the most transmission to humans is through the bite of a previously infected mosquito. In this context, one method to interrupt the Zika viral infection circle is to stop its replication in the mosquito before it can be passed to a human host. ZIKV is a single chain, enveloped RNA virus whose 10.7 kb genome encodes seven non-structural proteins (NS1, NS2a, NS2b, NS3, NS4a, NS4b and NS5) and three structural proteins (C, capsid; M, membrane; E, envelope). The functions of most non-structural proteins are well defined in the

literature, being NS2a, NS2b, NS4a and NS4b transmembrane proteins that anchor the replication complex catalytic proteins formed in the endoplasmic reticulum. On the other hand, NS3 and NS5 proteins have well-defined roles in viral genome duplication and protein translation. In this collaboration, we studied the NS1, since this protein participates in a significant number of activities; However, the function it plays in the pathogenesis of Flavivirus viral infection is still not entirely clear, especially when explicitly addressing the Zika virus vector, the *Aedes Aegypt* mosquito. In order to elucidate the relevance of the NS1 protein activity during the Zika viral replication process under these circumstances, this collaboration used a lipidomic approach to investigate the mechanisms of infection in its vector. The choice of the lipidomic approach is due to the NS1 itself be a lipoprotein and therefore involved in the process of a series of lipids synthesis in favour of viral infection. In this way, the objective of this work was to study the changes in lipidoma of mosquitoes in the first 12 hours after the ingestion of ZIKV-contaminated blood in comparison with mosquitoes that were fed with regular blood using high resolution mass spectrometry. It was possible to determined lipids markers in ZIKV, such as cholesterol ester, sphingolipid, di and triacylglycerol, as well as lipids involved in the process of the hexamer soluble lipoprotein formation NS1 in mosquito cells.

Introduction

The Zika virus (ZIKV) was first isolated in 1947 in East Africa[1]. It is an arbovirus since its transmission occurs through arthropods, and specifically to the ZIKV, mosquitoes of the genus Aedes [2]. Until 2007, this arbovirus remained restricted to Africa and Asia with rare cases presenting in humans in these regions[1]. Initially, ZIKV infection in humans was not characterized by its severity since it was asymptomatic in the vast majority of infected patients. When there were symptoms, which appeared in about 20% of infected people, these were both non-specific and self-limiting symptoms to headaches, fever, body pain, and others; Those that could be, and have been, medically mistaken for other arboviruses such as Dengue Fever, Chicungunha Fever or the common flu[3].

Since 2007, ZIKV outbreaks have been reported in the South Pacific and Latin America. These new cases identified outside the Asian continent drew attention once new evidence pointed to the infection being connected with severe clinical neurological complications such as Guillain-Barré syndrome[4] and microcephaly in children of women infected with ZIKV [5]. The neurological alterations presenting as a result of the ZIKV infection were crucial to making this arbovirus important in the global public health scenario[3].

Similar to other Flaviviruses such as Dengue virus (DENV), West Nile Fever virus (WNF) or Japanese Encephalitis virus (JEV); ZIKV is a single chain, enveloped RNA virus whose 10.7 kb genome encodes seven non-structural proteins (NS1, NS2a, NS2b, NS3, NS4a, NS4b and NS5) and three structural proteins (C, capsid; M, membrane; E, envelope) [6]. The functions of most non-structural proteins are well defined in the literature, being NS2a, NS2b, NS4a and NS4b transmembrane proteins that anchor the replication complex catalytic proteins formed in the endoplasmic reticulum. In addition, NS3 and NS5 proteins have well-defined roles in viral genome duplication and protein translation [7,8].

Under these circumstances, the function of the NS1 protein is still not very clear, but it is widely accepted that it could participate in many steps in the viral replication process. In addition, NS1 can assume different conformations, being able to be associated with membranes (mNS1) or in its soluble form (sNS1) [9]. Some functions already described for the mNS1 show that it is associated with the replication complex at the membrane of the endoplasmic reticulum (ER) on the luminal side [10]. For sNS1, it was verified that in patients infected with ZIKV, this plays an immunomodulatory role [11], interacting with complement proteins [12]. Also, sNS1 is directly related to the severity of DENV infection [13–16] as confirmed by previous research. Furthermore, NS1 is shown to be a strong biomarker candidate in human yellow fever virus (YFV) and DENV infections [17,18]; and also in mosquitoes infected by DENV [19]. Therefore it is a therapeutic target for DENV therapy [20] and a potential epitope for the development of DENV vaccines [13].

Despite the enormous potential that this NS1 non-structural protein shows in the control, treatment, diagnosis and infections symptoms of Flavivirus

diseases [13,17–20], there is much to discover about the role of NS1 in the pathogenesis of the Flavivirus viral infection. For example, confirmation of its presence on the external surface of the plasma membrane of infected mosquito cells [21] is required to establish the function of NS1 and its association with the outer surface of the plasma membrane of infected mammalian cells. [22] This confirmation would also verify that mosquito cells are capable of actively secreting sNS1 [23]. Since the in vitro study by Mason *et. al.* (1989) using JEV-infected Vero and C6/36 cells, it was believed that only infected mammalian cells were able to secrete NS1 during the viral infection process and that the insect cells were not [24]. Thus, the finding of the presence of NS1 in the culture supernatant of cells from infected mosquitoes was attributed to cell lysis and not due to active secretion from the infected cells[25]. In contrast, Alcalá *et al.* (2016) recently revealed that infected mosquito cells are capable of secreting NS1 [21].

Due to the many outstanding issues about NS1 and its essential role in the replication of Flavivirus, this study focused on a lipidomic approach. In turn, this is the subfield of metabolomics that studies aspects of the lipid molecules individually, including its structure, function and connection with other cellular constituents, like proteins, other lipids and metabolites. Because of this, lipidomic has gained increasing prominence in approaches that investigate mechanisms of infectious diseases [26–29]. The current methodology for the study of profile lipids in the pathogenesis of infectious diseases are due to the fact that there has been significant progress in analytical techniques such as chromatographic and high-resolution mass spectrometry[30] in recent years; These techniques allow **broader** approaches with considerable sensitivity and specificity [31]. The lipidomics studies applied to both ZIKV and DENV infections process have shown that lipid changes during viral infection are crucial in the immune response [27,32], viral replication [28,33] and virulence of infectious agents [34,35]. Therefore, the understanding of lipid alterations is opening up a better understanding of the clinical signs and symptoms presented by infected patients[27,36,37]. The lipidomic approach is further justified, in this particular collaboration, by the fact that NS1 in its soluble form presents itself as a lipoprotein, further involving the process of lipid synthesis in favour of viral infection

[27,28,38]. This work aimed to study the changes in the lipidome of mosquitoes in the first 12 hours after the ingestion of ZIKV-contaminated blood using high-resolution mass spectrometry.

Results

The score plot graph analysis (Figure 1) generated from the study of the full scan data of the respective stages (1, 6 and 12 hours) shows a clear difference between both groups: control and ZIKV infected mosquitoes. This difference is present in the analysis of the graph where the clusters are formed by the samples of the control groups (red, green and blue) are clustered together. Furthermore, it is evident that there are no differences between the groups that ingested regular blood 1-hour before analysis and the group that ingested regular blood 6-hour before analysis. This proximity between these two groups is probably due to the fact that they were fed just before being analyzed, being that the blood ingested is responsible for the ionized molecules found in their full scan spectra. Thus, there was no statistically significant difference between the metabolites of either group, as illustrated with the overlapping that occurs between clusters of their confidence intervals (Figure 1).

On the other hand, when analyzing the clusters formed for the groups that ingested ZIKV infected blood, we can see that the group analyzed 1-hour after the blood intake already presented a significant statistical difference in comparison with its corresponding control group. Likewise, it is possible to see a clear and independent clustering between the ZIKV-infected groups. Through the analysis of the graph, it is also possible to verify some intrinsic characteristics of the viral infection kinetics for each individual (mosquito) over time with the ZIKV-infected groups making increasingly dispersed clusters. Even though they contain similarities regarding the metabolites responsible for characterizing each group, the amount present of these metabolites in each individual, due to the infection, is responsible for the unique dispersion that is observed. This phenomenon can be explained because samples from the ZIKV-infected group present different viral infection kinetics among their individuals. These differences could mean that the metabolic

pool resulting from viral infection occurs at different times, whether derived from mechanisms to thrive during viral installation or resulting from a possible immune response by the host due to the virus. This causes the distances between points of the same cluster to increase in the ZIKV-infected group according to the passage of time while remaining practically constant in the control group. The validation of the generated models was evaluated by a permutation test where both presented values lower than $p < 5.10^{-4}$.

The ions that have been identified by statistical analysis as features (mass value) of importance for the formation of each ZIKV-infected group clusters, the top 12 primary markers were selected given their statistical relevance for the model (Figure 2). From these 12 mass values (markers), it was possible to identify 10 molecules (Table 1), 3 triglycerides, 1 sphingolipid, 3 cholesterols, 2 diacylglycerols and 1 ganglioside.

Discussion

The main objective of the study was to determine the profile of lipid changes that occur in the early stages of infection, as the virus controls the lipid synthesis processes in cells [39]. A few hours after receiving ZIKV-infected blood, the most discriminating molecules were the lipid molecules (Table 1) which involve the non-structural protein NS1 [38] and are also participates in the formation of "lipid rafts" (LR). LR is a lipid framework where non-structural proteins are allocated and characterized as subunits of the cell membrane; Furthermore, they are formed by large concentrations of cholesterol, sphingomyelins and gangliosides (Figure 3) [40,41]. These subunits are essential to the mechanism that allows the virus replicates in the host cell, through a process of replication, assembly and finally viral budding [41].

The NS1 nonstructural protein is characterized by being highly conserved in Flaviviruses that use arthropods as vectors [9,42–44], and it participates in three functional structures during the process of infection by Flavivirus [10,45,46]. In its preliminary function, NS1 presents as an intracellular dimer present in membranes of the endoplasmic reticulum and acts on the formation of LR in the virus replication complex of the infected cell (Figure 3) [10] . In its another role, it appears on the outer

surface of the plasma membrane of the infected cells, however, there is no in-depth knowledge about its function [47]. Finally, NS1 is found in the viral infection process taking the form of soluble hexamer (sNS1) and being secreted by the infected cells [46]; However, in spite of these three macro functions already described for NS1 that have been studied for a long time [48,49], not much is known about the full role that it plays during the Flavivirus infection [9,50], in particular, it's relation to ZIKV [22,51].

So far, it has been found that the function of NS1 depends on the body where the infection is being established [23]. Alcalá *et al*. (2016) showed that in mosquito cells infected with DENV, there is no presence of NS1 on the external surface of the plasma membrane of the infected cells [21]. In contrast, the presence of NS1 on the outer surface of the plasma membrane in Flavivirus infections of mammalian cells is in order to promote the evasion of the immune system, specifically during the acute phase of infection [12]. Therefore, acting mainly on the inhibition of the complement system, as demonstrated in WNF infections, where NS1 inhibits C3b deposition and the C5b-9 membrane attack complex [52]. This same behaviour has been demonstrated for DENV and YFV [53]. The reason for the absence of NS1 on the cell surface of infected mosquito cells may be due to the need to avoid evasion of the immune system by acting as the complement system, though this fact needs further research as the complement system is conserved in invertebrates and vertebrates [54].

The lipidomic approach performed in this work was an attempt to better understand the functions of NS1 or more specifically sNS1, the hexameric form, which is known to be secreted by Flavivirus infected mammalian cells [24]. The results showed that the lipids forming the sNS1 lipoprotein are synthesized in the first few hours of infection. This result corroborates findings by Alcalá *et al.* (2016)[21], contrary to previous beliefs that sNS1 was only secreted by Flavivirus-infected mammalian cells [23–25]. Research by Alcalá et *al*. (2016) demonstrates that DENV-infected mosquito cells actively secrete NS1 through their studies with cultured C6/36 cells infected with DENV [55] or WNV [56]. The presence of NS1 in the culture medium supernatant has always been associated with viral lysis caused by a viral infection.

Thus, the presence of NS1 in the supernatant of these cultures was not attributed due to the active secretion of NS1 by the infected living cell. [25].

When we verified the presence of diacylglycerol, triacylglycerol, sphingolipid, ganglioside and especially cholesterol esters as lipid markers (Table 1) for the ZIKV-infected group during the initial hours of infection, it became entirely plausible to assume that these lipids were shown as discriminants due to the sNS1 formation (Figure 3). The release kinetics of sNS1 are variable for different Flaviviruses, as demonstrated for JEV and YFV, where the release may take up to 2 hours, and for TBEV, where it occurs within 45 min of the establishment of the infection [24,57]. In the study by Alcalá *et al*. (2016), it was found that C6/36 cells released sNS1 within the first 3 hours of infection [21]. These results are in agreement with the data presented in this work since the lipids that form the sNS1 lipoprotein were already indicated as markers within the first 6 hours of viral infection. The dispersion between individuals (Figure 1) illustrates that these lipids are being actively secreted by mosquitoes, otherwise the dispersion between the treated and control groups would be similar (low).

Further evidence of secretion of sNS1 by infected mosquito cells was performed by Thiemmeca *et al.* (2016). They that found that sNS1 may be present in the saliva of mosquitoes infected by DENV, mediating immune system evasion early in the viral infection process, i.e. when the mosquito bites a mammal [58]. Thus, it is possible to say that the markers found (Table 1) corroborate the secretion of sNS1 by infected cells since it is characterized as a high-density lipoprotein composed of triacylglycerol, diacylglycerol, cholesterol ester and phospholipids [38], the same lipids indicated in this study as markers for the first 6 and 12 hours of infection.

In addition to the functions of the lipids already described above, there is an another function developed by them besides the composition of the sNS1 [38]. Since secretion of sNS1 is performed via a non-classical pathway dependent on caveolin-1 (CAV-1) [59], sphingolipids, ganglioside and cholesterol, found here as markers for the infected group, are precisely the lipids responsible for organizing the LR [60,61]; They are a requirement for allocation of the CAV-1 protein, which is an

essential protein for the formation of caveolae [62] (Figure 3). Diwaker *et al*. (2015) showed that in the first 6 hours of DENV infection an increase in LR occurs, allowing a series of membrane proteins required in the viral replication process, such as non-structural proteins of the virus, to be allocated in these regions [63] (Figure 3). Still analyzing the lipid alterations of cell membranes, the large number of cholesterols molecules found are due to the fact that cholesterol promotes the grouping of the subdomains of LR, functioning as a spacer between the hydrocarbon chains of the sphingolipids and a dynamic glue; while also maintaining the conformation of the functional LR [64]. In addition, cholesterol is also one of the major molecular class that form the high-density lipoprotein sNS1, along with the hexamer of NS1.

With the presence of lipids that make up the soluble lipoprotein formed by a hexamer of NS1 plus cholesterol ester, sphingolipid, di and triacylglycerol as biomarkers, it is possible to verify that the lipid pool found in the first hours of infection corroborates with the new studies that point to Flavivirus-infected mosquito cells as being able to secrete sNS1 [23,58,59]. These three classes of lipids have also been found to be responsible for the formation of the lipid subunit where the ZIKV viral replication machinery is installed: the lipid raft [39], which also participates in the pathway through which sNS1 is secreted by the cell [59].

Methodology

- Mosquitoes

Aedes aegypti mosquitoes, originally from the PAEA strain of French Polynesia and isolated at the laboratory since 1994, were used in this experiment [65]. The 72 mosquitoes were divided into two groups: 36 fed with ZIKV infected blood and 36 fed with un-contaminated blood to form a control group. These 36 individuals from each group were further separated and analyzed in three stages: 1, 6 and 12 hours, with 6 subjects per group. Individuals from both groups were exposed to an artificial blood meal containing 800 µL of commercial sheep blood. For the infected mosquitoes group, the blood meal was composed of 400 µL of blood with 400 µl of ZIKV derived from cell culture supernatant from cells line C6/36 of *Aedes albopictus*. The blood supply lasted approximately 45 minutes, and after feeding, the

mosquitoes were disinfected externally in 70% alcohol then subsequently stored in methanol (JT Baker, Xalostoc, Mexico).

-Confirmation of ZIKV in blood ingested by mosquitoes

Confirmation of the ZIKV presence was performed by the absolute quantification methodology in RT-PCR, converting the Ct values into viral concentration PFU (Plaque Forming Unit)/ml with the aid of a standard curve. From a pre-titered aliquot, $4{,}4.10^{7}$ PFU/mL were prepared in three replicates of serial dilution (10^{-1} to 10^{-4}), proceeding with the extraction of RNA (Trizol® Reagent-Life Technologies) and cDNA synthesis (RevertAid First Strand cDNA Synthesis-Thermo Scientific) for each dilution. Subsequently, the cDNA of the samples was quantified, and the value of Ct corresponded to a dilution. Thus, after the formation of the standard curve, the sample used for the blood supply was quantified, and the corresponding acquired Ct was that of $1{,}37.10^{6}$ PFU/mL.

-Sample preparation for HRMS analysis

The mosquitoes were placed intact in a 1.5 mL vial (Eppendorf, Hamburg, Germany) containing methanol (they were submerged). The samples were sonicated in an ice bath (± 4 °C) for 10 minutes. After sonication, the samples were vortexed for 30 seconds and then centrifuged at 10,000 rpm for 10 minutes at 4 °C. An aliquot of 400 µL of supernatant was filtered using membrane filter units of PVDF - Polyvinylidene Fluoride (0.22 µm) (Jet Biofil, Guangzhou, China) and were added to 600 µL of methanol (JT Baker, Xalostoc, Mexico). Then 1 % formic acid was added to the final solution of 1 mL. (JT Baker, Xalostoc, Mexico).

-HRMS Analysis

All samples were directly injected for survey scan analysis in an ESI-LTQ-XL Orbitrap Discovery instrument (Thermo Scientific, San Jose, California) with nominal resolution of 30,000 (FWHM), under the following parameters: flow rate of 10 µL.min-1, capillary temperature of 280 °C, 5 kV as spray voltage and sheath gas at 10 arbitrary units. HRMS analyses were performed in technical quintuplicates for

each sample using the mass range of 500–2000 m/z in the positive ion mode. Spectra were analyzed using XCalibur™ software (v. 2.4, Thermo Scientific, San Jose, CA)

-Statistical Analysis

Statistical analysis was performed using the Partial Least Squares Discriminant Analysis (PLS-DA) with the list of markers by the importance of the variable in the projection (VIP score). This data analysis technique is dedicated to studying the identification of metabolites of interest through metabolic profiling analysis using a non-targeting approach [66]. This analysis is possible since the PLS-DA is a supervised multivariate method that uses regression techniques to extract, by linear combination of the original variables, characteristics that can indicate the association with a particular class; Therefore, providing low-dimensional representations of data sets of interest using graphs to visually interpret scores (Figure 1) from a set of complex data [67]. The statistical significance of the generated model was evaluated by two permutation tests: prediction accuracy during modelling and separation distance. In both trials, the number of permutations, 2000, was established (*Supplementary Material 1 and 2*). The selection of the lipid characteristics from each sample was performed by the impact of each metabolite in the analysis using the VIP score, which consists of the weighted sum of squares of PLS loads. This methodology takes into account the amount of variation explained in each dimension used in the model. As a cut-off point, we analyzed only those markers with a VIP score greater than 1.5. Prior to PLS-DA analyses, the interquartile range was used as a data filtering method, with quantile normalization and autoscaling. A heatmap of the features selected by the PLS-DA analyses was built using the Pearson's distance measurement and Ward's clustering algorithm. All statistical analyses were performed using the online platform MetaboAnalyst 4.0 [68].

Structure determination of markers

METLIN (Scripps Center for Metabolomics, La Jolla, CA) was consulted to elect the most suitable markers based on the exact mass of each species. A maximum error of 2 ppm was established for mass accuracy, from the experimental exact mass obtained in the study and positive adducts available on the platform [69].

Acknowledgements

CFORM would like to thank the São Paulo Research Foundation for the grant (2016/17066-2 and 2018/03321-6). We also thank the Coordination for the Improvement of Higher Level Personnel (CAPES) for the fellowships , TMG (PROEX: 1489740) and JD. DNO would like to thank the Brazilian Ministry of Health (Plano Nacional de Enfrentamento ao Aedes aegypti e à Microcefalia [Brazilian Plan for Fighting Aedes aegypti and Microcephaly]) for the fellowship under process No. 88887.137889/2017-00. RRC thanks MCTIC-CNPq/MEC-CAPES/MS-Decit/FNDCT No. 14/2016 for the grant. JASN would like to thank the São Paulo Research Foundation for the Young Investigator grant (013/11343-6). Finally, RRC would like to thank the São Paulo Research Foundation for the grant (FAPESP, Process Nos. 11/50400-0 and 15/06809-1).

Author contributions

CFORM performed experiments, data collection, analyzed data and wrote the manuscript. TMG and JD performed data collection, analyzed data and wrote the manuscript; DNO reviewed the manuscript; LTEO and LTG raised and took care of the mosquitoes, fed them with ZIKV blood contaminated and collected them. JASN and RRC coordinated the team, revised the manuscript and planned all experiments.

Competing interests

The authors declare no competing interests of any nature.

Manuscript Comment

The figure 3 was created drowned by CFORM and JD.

References

1. Chang, C., Ortiz, K., Ansari, A. & Gershwin, M. E. The Zika outbreak of the 21st century. *J. Autoimmun.* **68**, 1–13 (2016).

2. Faria, N. R. *et al.* Zika virus in the Americas: Early epidemiological and genetic findings. *Science (80-.).* **352**, 345–349 (2016).

3. Petersen, L. R., Jamieson, D. J., Powers, A. M. & Honein, M. A. Zika Virus. *New Engl J Med* (2016). doi:10.1056/NEJMra1602113

4. Cao-Lormeau, V.-M. *et al.* Guillain-Barre; Syndrome outbreak associated with Zika virus infection in French Polynesia: a case-control study. *Lancet* **387**, 1531–1539 (2016).

5. Brasil, P. *et al.* Zika Virus Infection in Pregnant Women in Rio de Janeiro — Preliminary Report. *N. Engl. J. Med.* NEJMoa1602412 (2016). doi:10.1056/NEJMoa1602412

6. Lindenbach, B. D. & Rice, C. M. Molecular Biology of Flavivirus. *Adv. Virus Res.* **59**, 23–62 (2003).

7. Moradpour, D. & Penin, F. *Hepatitis C Virus: From Structure to Function*. *Current topics in microbiology and immunology* **369**, (2013).

8. Bollati, M. *et al.* Structure and functionality in flavivirus NS-proteins: Perspectives for drug design. *Antiviral Research* **87**, 125–148 (2010).

9. Rastogi, M., Sharma, N. & Singh, S. K. Flavivirus NS1: A multifaceted enigmatic viral protein. *Virology Journal* **13**, (2016).

10. Noisakran, S. *et al.* Association of dengue virus NS1 protein with lipid rafts. *J. Gen. Virol.* **89**, 2492–2500 (2008).

11. Asif, A. *et al.* Zika Virus: Immune Evasion Mechanisms, Currently Available Therapeutic Regimens, and Vaccines. *Viral Immunol.* vim.2017.0046 (2017). doi:10.1089/vim.2017.0046

12. Conde, J. N., Silva, E. M., Barbosa, A. S. & Mohana-Borges, R. The complement system in flavivirus infections. *Frontiers in Microbiology* **8**, (2017).

13. Beatty, P. R. *et al.* Dengue virus NS1 triggers endothelial permeability and vascular leak that is prevented by NS1 vaccination. *Sci. Transl. Med.* **7**, (2015).

14. Mackenzie, J. M., Jones, M. K. & Young, P. R. Immunolocalization of the

Dengue virus nonstructural glycoprotein NS1 suggests a role in viral RNA replication. *Virology* (1996). doi:10.1006/viro.1996.0307

15. Young, P. R., Hilditch, P. A., Bletchly, C. & Halloran, W. An antigen capture enzyme-linked immunosorbent assay reveals high levels of the dengue virus protein NS1 in the sera of infected patients. *J. Clin. Microbiol.* (2000). doi:10.1002/anie.201411533

16. Muller, D. A., Corrie, S. R., Coffey, J., Young, P. R. & Kendall, M. A. Surface modified microprojection arrays for the selective extraction of the dengue virus NS1 protein as a marker for disease. *Anal. Chem.* (2012). doi:10.1021/ac2034387

17. Ricciardi-Jorge, T. *et al.* Development of a quantitative NS1-capture enzyme-linked immunosorbent assay for early detection of yellow fever virus infection. *Sci. Rep.* **7**, (2017).

18. Lim, J. M. *et al.* An electrochemical peptide sensor for detection of dengue fever biomarker NS1. *Anal. Chim. Acta* **1026**, 109–116 (2018).

19. Wasik, D., Mulchandani, A. & Yates, M. V. Point-of-Use Nanobiosensor for Detection of Dengue Virus NS1 Antigen in Adult Aedes aegypti: A Potential Tool for Improved Dengue Surveillance. *Anal. Chem.* **90**, 679–684 (2018).

20. Xie, Q. *et al.* Structure and Function of the Non-Structural Protein of Dengue Virus and its Applications in Antiviral Therapy. *Curr. Top. Med. Chem.* **17**, 371–380 (2017).

21. Alcalá, A. C. *et al.* The dengue virus non-structural protein 1 (NS1) is secreted efficiently from infected mosquito cells. *Virology* **488**, 278–287 (2016).

22. Brown, W. C. *et al.* Extended surface for membrane association in Zika virus NS1 structure. *Nat. Struct. Mol. Biol.* **23**, 865–867 (2016).

23. Accepted, J. V. I., Posted, M., Society, A. & Reserved, A. R. Secretion of the non-structural protein 1 of dengue virus from infected mosquito cells: facts and speculations. *J. Virol.* 1–18 (2018). doi:10.1128/JVI.00275-18

24. Mason, P. W. Maturation of Japanese encephalitis virus glycoproteins produced by infected mammalian and mosquito cells. *Virology* **169**, 354–364 (1989).

25. Muller, D. A. & Young, P. R. The flavivirus NS1 protein: Molecular and structural biology, immunology, role inpathogenesis and application asadiagnostic

biomarker. *Antiviral Research* **98**, 192–208 (2013).

26. Koriem, K. M. M. A lipidomic concept in infectious diseases. *Asian Pacific Journal of Tropical Biomedicine* **7**, 265–274 (2017).

27. Melo, C. F. O. R. *et al.* The role of lipids in the inception, maintenance and complications of dengue virus infection. *Sci. Rep.* **8**, (2018).

28. Melo, C. F. O. R. *et al.* A lipidomics approach in the characterization of zika-infected mosquito cells: Potential targets for breaking the transmission cycle. *PLoS One* **11**, (2016).

29. Melo, C. F. O. R. *et al.* Serum Metabolic Alterations upon Zika Infection. *Front. Microbiol.* **8**, (2017).

30. Niu, Z., Zhang, W., Yu, C., Zhang, J. & Wen, Y. Recent advances in biological sample preparation methods coupled with chromatography, spectrometry and electrochemistry analysis techniques. *TrAC - Trends in Analytical Chemistry* **102**, 123–146 (2018).

31. Nagana Gowda, G. A. & Djukovic, D. Overview of mass spectrometry-based metabolomics: Opportunities and challenges. *Methods Mol. Biol.* **1198**, 3–12 (2014).

32. Tisoncik-Go, J. *et al.* Integrated Omics Analysis of Pathogenic Host Responses during Pandemic H1N1 Influenza Virus Infection: The Crucial Role of Lipid Metabolism. *Cell Host Microbe* **19**, 254–266 (2016).

33. Hofmann, S. *et al.* Complex lipid metabolic remodeling is required for efficient hepatitis C virus replication. *Biochim. Biophys. Acta (BBA)-Molecular Cell Biol. Lipids* (2018).

34. Madigan, C. A. *et al.* Lipidomic Analysis Links Mycobactin Synthase K to Iron Uptake and Virulence in M. tuberculosis. *PLoS Pathog.* **11**, 1–21 (2015).

35. Gao, Q. *et al.* Phospholipid homeostasis maintains cell polarity, development and virulence in Metarhizium robertsii. *Environ. Microbiol.* **18**, 3976–3990 (2016).

36. Dabaja, M. Z. *et al.* Metabolic alterations induced by attenuated Zika virus in glioblastoma cells. *Cell Biosci.* **8**, (2018).

37. Lima, E. O. *et al.* MALDI imaging detects endogenous digoxin in glioblastoma cells infected by Zika virus—Would it be the oncolytic key? *J. Mass Spectrom.* **53**, (2018).

38. Gutsche, I. *et al.* Secreted dengue virus nonstructural protein NS1 is an atypical barrel-shaped high-density lipoprotein. *Proc. Natl. Acad. Sci.* **108**, 8003–8008 (2011).

39. Martï¿½n-Acebes, M. A., Vï¿½zquez-Calvo, ï¿½ngela & Saiz, J. C. Lipids and flaviviruses, present and future perspectives for the control of dengue, Zika, and West Nile viruses. *Progress in Lipid Research* **64**, 123–137 (2016).

40. Pike, L. J. Lipid rafts: bringing order to chaos. *J. Lipid Res.* **44**, 655–67 (2003).

41. Takahashi, T., Suzuki, T., Takahashi, T. & Suzuki, T. Function of Membrane Rafts in Viral Lifecycles and Host Cellular Response, Function of Membrane Rafts in Viral Lifecycles and Host Cellular Response. *Biochem. Res. Int. Biochem. Res. Int.* **2011**, **2011**, e245090 (2011).

42. Edeling, M. A., Diamond, M. S. & Fremont, D. H. Structural basis of Flavivirus NS1 assembly and antibody recognition. *Proc. Natl. Acad. Sci.* **111**, 4285–4290 (2014).

43. Akey, D. L. *et al.* Flavivirus NS1 structures reveal surfaces for associations with membranes and the immune system. *Science (80-.).* **343**, 881–885 (2014).

44. Xu, X. *et al.* Contribution of intertwined loop to membrane association revealed by Zika virus full-length NS1 structure. *EMBO J.* **35**, 2170–2178 (2016).

45. Avirutnan, P. *et al.* Binding of Flavivirus Nonstructural Protein NS1 to C4b Binding Protein Modulates Complement Activation. *J. Immunol.* **187**, 424–433 (2011).

46. Watterson, D., Modhiran, N. & Young, P. R. The many faces of the flavivirus NS1 protein offer a multitude of options for inhibitor design. *Antiviral Research* **130**, 7–18 (2016).

47. Akey, D. L., Brown, W. C., Jose, J., Kuhn, R. J. & Smith, J. L. Structure-guided insights on the role of NS1 in flavivirus infection. *BioEssays* **37**, 489–494 (2015).

48. Falconar, A. K. I. & Young, P. R. Immunoaffinity purification of native dimer forms of the flavivirus non-structural glycoprotein, NS1. *J. Virol. Methods* **30**, 323–332 (1990).

49. Gibson, C. A., Schlesinger, J. J. & Barrett, A. D. Prospects for a virus non-

structural protein as a subunit vaccine. *Vaccine* **6**, 7–9 (1988).

50. Shi, P. Y. Unraveling a flavivirus enigma. *Science* **343**, 849–850 (2014).

51. Xia, H. *et al.* An evolutionary NS1 mutation enhances Zika virus evasion of host interferon induction. *Nat. Commun.* **9**, (2018).

52. Chung, K. M. *et al.* West Nile virus nonstructural protein NS1 inhibits complement activation by binding the regulatory protein factor H. *Proc. Natl. Acad. Sci. U. S. A.* **103**, 19111–6 (2006).

53. Avirutnan, P. *et al.* Antagonism of the complement component C4 by flavivirus nonstructural protein NS1. *J. Exp. Med.* **207**, 793–806 (2010).

54. Levashina, E. A. *et al.* Conserved role of a complement-like protein in phagocytosis revealed by dsRNA knockout in cultured cells of the mosquito, Anopheles gambiae. *Cell* **104**, 709–718 (2001).

55. Juárez-Martínez, A. B. *et al.* Detection and sequencing of defective viral genomes in C6/36 cells persistently infected with dengue virus 2. *Arch. Virol.* **158**, 583–599 (2013).

56. Youn, S., Cho, H., Fremont, D. H. & Diamond, M. S. A Short N-Terminal Peptide Motif on Flavivirus Nonstructural Protein NS1 Modulates Cellular Targeting and Immune Recognition. *J. Virol.* **84**, 9516–9532 (2010).

57. Lee, J. M., Crooks, A. J. & Stephenson, J. R. The synthesis and maturation of a non-structural extracellular antigen from Tick-borne encephalitis virus and its relationship to the intracellular NS1 protein. *J. Gen. Virol.* **70**, 335–343 (1989).

58. Thiemmeca, S. *et al.* Secreted NS1 Protects Dengue Virus from Mannose-Binding Lectin–Mediated Neutralization. *J. Immunol.* **197**, 4053–4065 (2016).

59. Alcalá, A. C. *et al.* The dengue virus non-structural protein 1 (NS1) is secreted from infected mosquito cells via a non-classical caveolin-1- dependent pathway. *J. Gen. Virol.* **98**, 2088–2099 (2017).

60. Pietiäinen, V. M., Marjomäki, V., Heino, J. & Hyypiä, T. Viral entry, lipid rafts and caveosomes. *Annals of Medicine* **37**, 394–403 (2005).

61. Obayashi, T. K., Akahashi, M. T., Agatsuka, Y. N. & Irabayashi, Y. H. Lipid Dynamics and Pathobiology in Membrane Lipid Rafts Lipid Rafts. *Biol Pharm Bill* **29**, 1526–1531 (2006).

62. Huang, J. H. *et al.* Identification of the HIV-1 gp41 core-binding motif in the scaffolding domain of caveolin-1. *J. Biol. Chem.* **282**, 6143–6152 (2007).

63. Diwaker, D., Mishra, K. P., Ganju, L. & Singh, S. B. Protein Disulfide Isomerase Mediates Dengue Virus Entry in Association with Lipid Rafts. *Viral Immunol.* **28**, 153–160 (2015).

64. Simons, K. & Toomre, D. Lipid rafts and signal transduction. *Nat. Rev. Mol. Cell Biol.* **1**, 31–39 (2000).

65. Vazeille, M., Gaborit, P., Mousson, L., Girod, R. & Failloux, A. B. Competitive advantage of a dengue 4 virus when co-infecting the mosquito Aedes aegypti with a dengue 1 virus. *BMC Infect. Dis.* (2016). doi:10.1186/s12879-016-1666-0

66. Worley, B., Halouska, S. & Powers, R. Utilities for quantifying separation in PCA/PLS-DA scores plots. *Anal. Biochem.* **433**, 102–104 (2013).

67. Kalivodová, A. *et al.* PLS-DA for compositional data with application to metabolomics. *J. Chemom.* **29**, 21–28 (2015).

68. Chong, J. *et al.* MetaboAnalyst 4.0 : towards more transparent and integrative metabolomics analysis. *Nucleic Acids Res.* 1–9 (2018). doi:10.1093/nar/gky310

69. Guijas, C. *et al.* METLIN: A Technology Platform for Identifying Knowns and Unknowns. *Anal. Chem.* acs.analchem.7b04424 (2018). doi:10.1021/acs.analchem.7b04424

Figure's Description

Figure 1: The score plots of Partial Least Squares Discriminant Analysis (PLS-DA) analysis among the 6 different groups: 1, 6 and 12 hours for both infected and control mosquitoes groups.

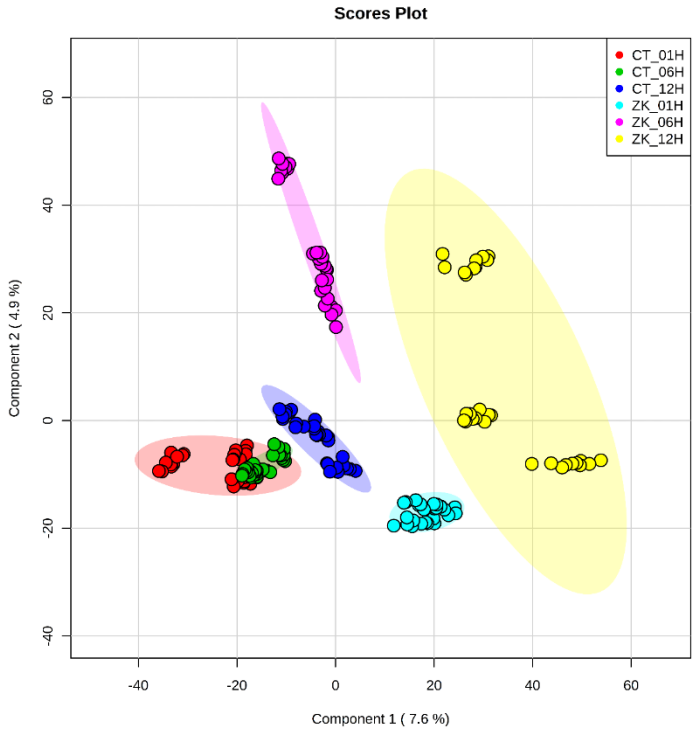

Figure 2: Clustering result for the 12 top features selected by Partial Least Squares Discriminant Analysis (PLS-DA) shown as a heatmap (distance measured by Pearson's distance measurement and Ward's clustering algorithm). The color-

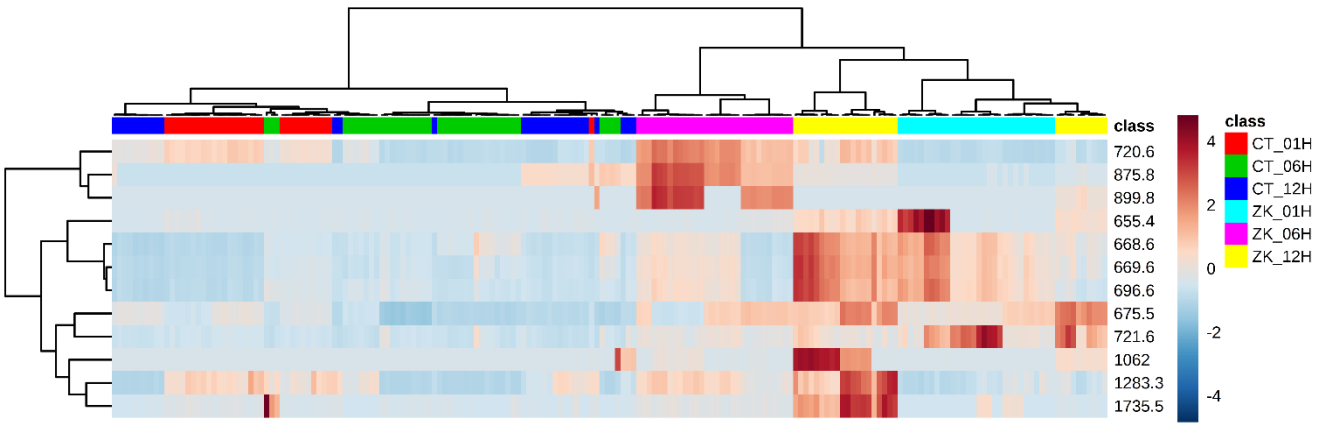

coded thermometer (bottom) indicates the relative presence of metabolites among the groups.

Figure 3: 1) The NS1 monomer is synthesized in the viral replication complex. 2) The dimeric NS1 (mNS1) has a hydrophobic character, which causes it to associate with the membrane. 3) Part of the synthesized mNS1 acquires GPI in the ER and is associated with lipid rafts (highlights of the yellow membrane). 4) The dimeric units of mNS1 associate, three by three, to form soluble hexameric units. 5) Secreted sNS1 will be dependent on Caveolin-1, a protein that is organized in the lipid raft zones. 6) Secretion of sNS1.

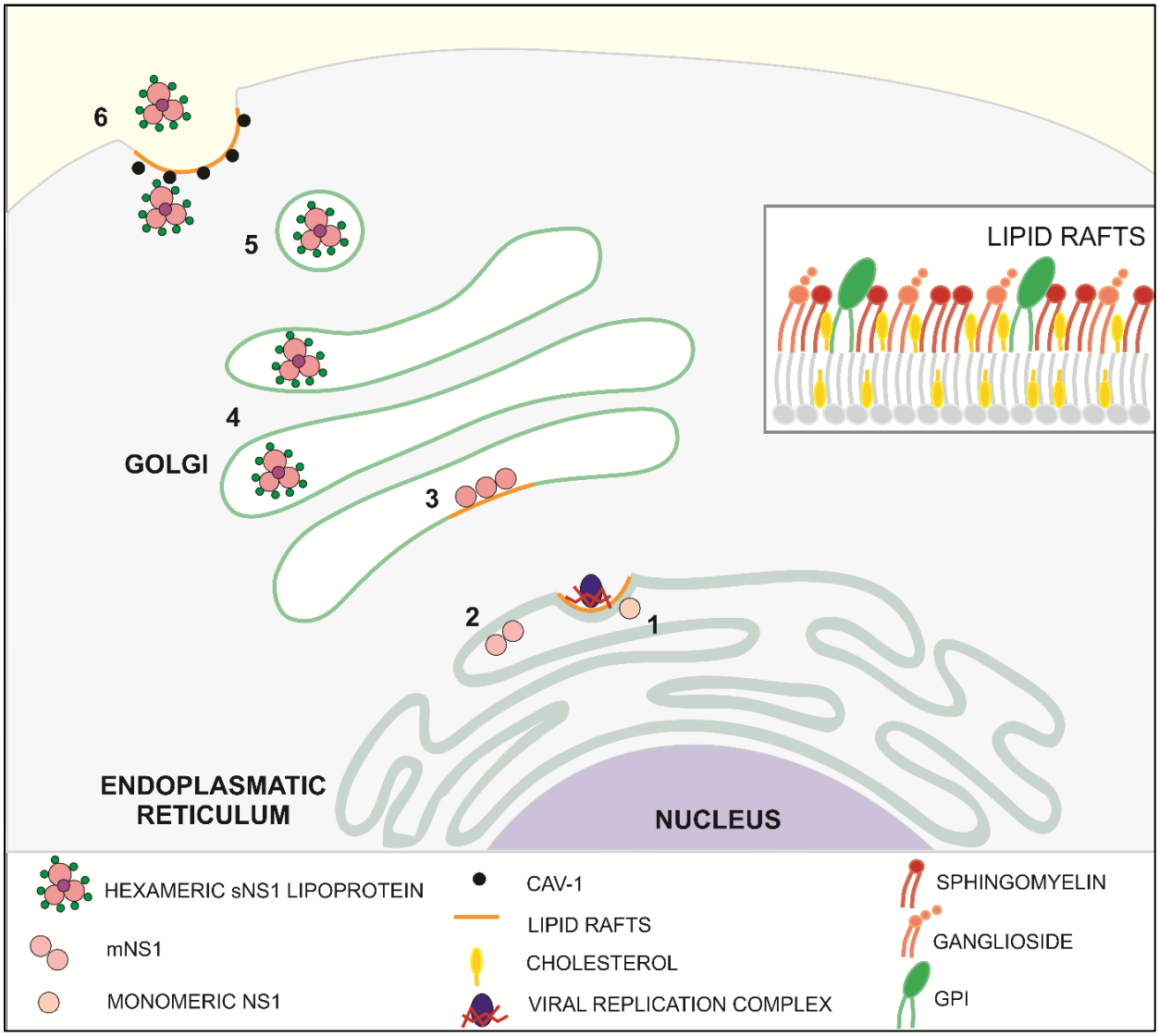

Table's Description

Table 1: Lipid markers elected by Partial Least Squares Discriminant Analysis (PLS-DA) from the ZIKV-infected mosquitoes (ZIKV group). Characterization was performed with the assistance of METLIN database[69].

Experimental Mass	Theoretical Mass	Error (ppm)	Molecules	Adduct	Database ID*
720.6002	720.6014	1.67	SM(d34:1)	$[M+NH4]^+$	41586 83744 83743
875.8047	875.8062	1.71	TG (53:1)	$[M+H]^+$	4814.0
899.8044	899.8062	2.00	TG(55:3)	$[M+H]^+$	101359 101465 101377
655.4461	655.4474	1.98	DG(36:7)	$[M+2Na-H]^+$	58860 59224
668.6198	668.6187	1.65	DG(38:1)	$[M+NH4]^+$	59280 59252 59095
669.6331	669.6344	1.94	22:2 Cholesteryl ester	$[M+H-2H2O]^+$	41712
696.6560	696.6547	1.87	Ganglioside GT1b (d18:1/12:0) Ganglioside GT1c (d18:1/12:0)	$[M+2Na+H]^{3+}$	62679 62709
675.5490	675.5477	1.92	17:1 Cholesteryl ester	$[M+K]^+$	41718
721.5908	721.5894	1.94	22:5 Cholesteryl ester	$[M+NH4]^+$	57687
1062.0025	1062.0046	1.98	TG(64:1)	$[M+CH3OH+H]^+$	38544 38539 38799

* METLIN: A Technology Platform for Identifying Knowns and Unknowns

Supplementary Information #1

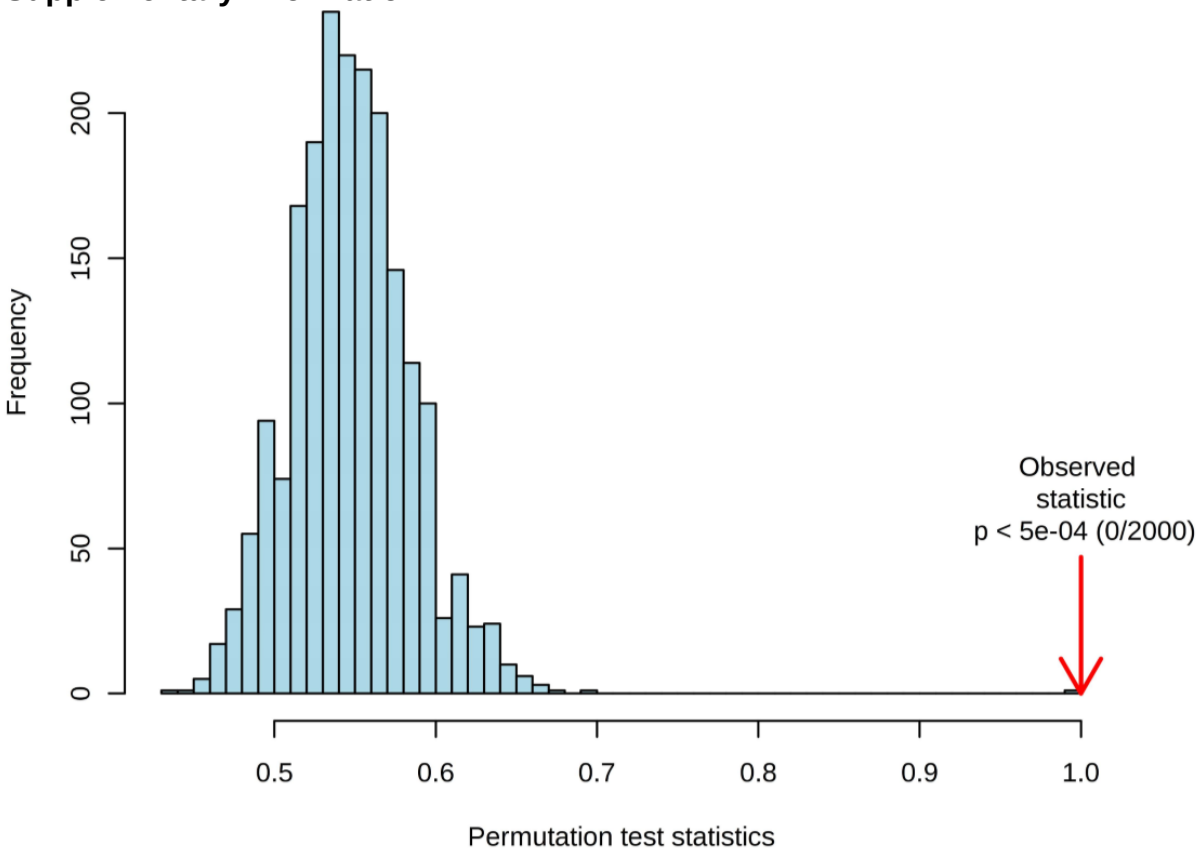

Supplementary Information #2

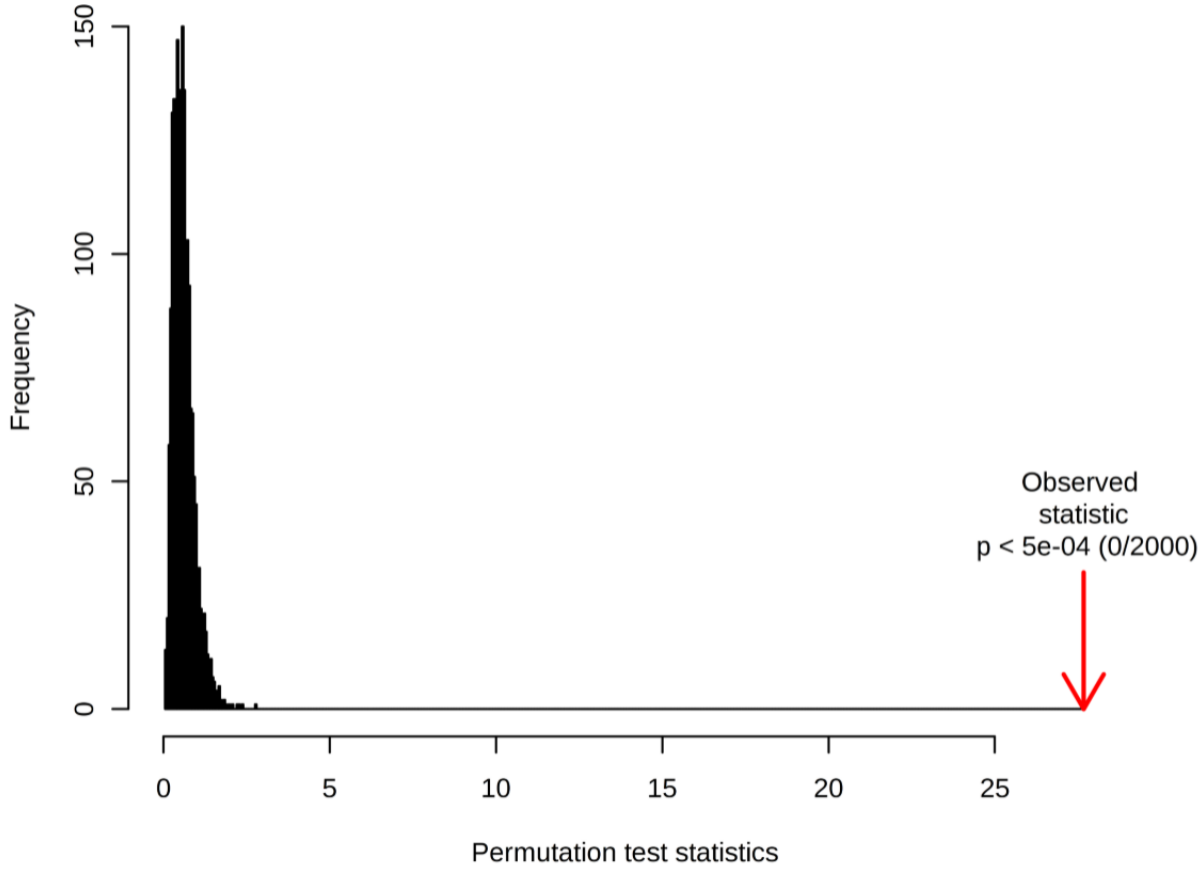

4.1.2. Artigo II

Serum metabolic alterations upon Zika infection[29]

Carlos Fernando O. R. Melo[1], Jeany Delafiori[1], Diogo N. de Oliveira[1], Tatiane M. Guerreiro[1], Cibele Z. Esteves[1], Estela de O. Lima[1], Victoria Pando-Robles[2], Rodrigo R. Catharino[1]*, and the Zika-Unicamp Network‡

‡**Zika-Unicamp Network:** Guilherme P. Milanez[3], Gabriela M. do Nascimento[3], André R. R. Freitas[4,12], Rodrigo Angerami[5], Fábio T. Maranhão Costa[3], Clarice W. Arns[3], Mariangela R. Resende[5], Eliana Amaral[6], Renato P. Junior[6], Carolina C. Ribeiro-do-Valle[6], Helaine Milanez[6], Maria L. Moretti[5], Jose L. Proenca-Modena[3], Glaucia M. Pastore[7], Kleber Y. Fertrin[5], Márcia T. Garcia[5], Roseli Calil[7], João R. B. Júnior[6], Giuliane J. Lajos[6], Maria L. Costa[6], Marcos T. N. da Silva[8], Albina Altemani[9]; Ana C. Coan[10]; Maria F. Colella-Santos[11]; Andrea P. B. von Zuben[4]; Marco A. R. Vinolo[3], Rosemeire F. de O. de Paula[3]; Carla C. Judice[3], Juliana A. Leite[3], Leonardo C. Caserta[3], Ana P. de Moraes[3], Ana C. S. Barnabé[3]; Ana L. R. da Soledade[3], Daniel A. T. Teixeira[3], Évellyn R. de Morais[3], Felipe R. Santos[3]

Affiliation: .[1]INNOVARE Biomarkers Laboratory, School of Pharmaceutical Sciences, University of Campinas, Brazil (Unicamp); [2]Instituto Nacional de Salud Publica (INSP), Cuernavaca, Mexico; [3]Department of Genetic, Evolution and Bioagents (Unicamp); [4]Campinas Department of Public Health Surveillance; [5]Clinical Pathology Department, Faculty of Medical Sciences (Unicamp); [6]Obstetrics and Gynecology Department, School of Medical Sciences (Unicamp); [7]Faculty of Food Engineering (Unicamp); [8]Pediatric Immunology, Center for Investigation in Pediatrics, Faculty of Medical Sciences (Unicamp); [9]Pathology Department, Faculty of Medical Sciences (Unicamp); [10]Neurology Department, Faculty of Medical Sciences (Unicamp); [11]Department of Human Development and Rehabilitation, Faculty of Medical Sciences (Unicamp); [12]São Leopoldo Mandic Institute and Research Center, Campinas.

*** Corresponding author:** Rodrigo Ramos Catharino

Keywords: Zika virus, mass spectrometry, metabolomics, viromics.

https://doi.org/10.3389/fmicb.2017.01954

Abstract

Zika virus (ZIKV) infection has recently emerged as a major concern worldwide due to its strong association with nervous system malformation (microcephaly) of fetuses in pregnant women infected by the virus. Signs and symptoms of ZIKV infection are often mistaken with other common viral infections. Since transmission may occur through biological fluids exchange and coitus, in addition to mosquito bite, this condition is an important infectious disease. Thus, understanding the mechanism of viral infection has become an important research focus, as well as providing potential targets for assertive clinical diagnosis and quality screening for hemoderivatives. Within this context, the present work analyzed blood plasma from 79 subjects, divided as a control group and a ZIKV-infected group. Samples underwent direct-infusion mass spectrometry and statistical analysis, where eight markers related to the pathophysiological process of ZIKV infection were elected and characterized. Among these, Angiotensin (1-7) and Angiotensin I were upregulated under infection, showing an attempt to induce autophagy of the infected cells. However, this finding is concerning about hypertensive individuals under treatment with inhibitors of the Renin-Angiotensin System (RAS), which could reduce this response against the virus and exacerbate the symptoms of the infection. Moreover, one of the most abundant glycosphingolipids in the nervous tissue, Ganglioside GM2, was also elected in the present study as an infection biomarker. Considered an important pathogen receptor at membrane's outer layer, this finding represents the importance of gangliosides for ZIKV infection and its association with brain tropism. Furthermore, a series of phosphatidylinositols were also identified as biomarkers, implying a significant role of the PI3K-AKT-mTOR Pathway in this mechanism. Finally, these pathways may also be understood as potential targets to be considered in pharmacological intervention studies on ZIKV infection management.

Introduction

Zika virus (ZIKV) was isolated for the first time in 1947 in the Zika forest, Uganda; a member of the Flaviviridae family, it is the etiologic agent of a disease with the same name, which is characterized as a self-limited infection where over 80% of the infected patients do not present any signs or symptoms (Duffy et al., 2009;Petersen et al., 2016). Individuals who present clinical manifestations of the disease usually develop unspecific symptoms such as fever, conjunctivitis, skin rashes, arthralgia, macular rash, myalgia, migraine, and retro-orbital pain, among other symptoms that may be clinically associated with the common influenza virus, as well as other arboviruses such as dengue (DENV), oropouche (OROV) or chikungunya (CHIKV) (Duffy et al., 2009;Daumas et al., 2013;Pabbaraju et al., 2016;Paniz-Mondolfi et al., 2016).

Because it was considered a relatively harmless infection up to 2014, ZIKV was not remarkably relevant in public health worldwide, remaining relatively unknown among people and even physicians. However, in view of the growing cases of microcephaly in newborns from ZIKV-infected mothers, a close relationship between the infection and problems during neural development has been established (Petersen et al., 2016). The result is a clinical condition characterized by abnormal brain development and decreased head diameter compared to individuals born from non ZIKV-infected mothers. Additionally, patients suffering from this condition present impaired neurological functions, as well as delayed development of motor, speech and cognitive functions (Woods et al., 2005). ZIKV has also been associated with an increased number of Guillain-Barre syndrome (GBS), an autoimmune disorder where the immune system attacks parts of the nervous system, resulting in acute (or subacute) flaccid paralysis due to nerve inflammation (Cao-Lormeau et al., 2016). Because of the severity of these events associated with ZIKV infection, the control of its main vector, mosquitoes from the *Aedes* genus (Petersen et al., 2016), has emerged as an important public health issue, given the difficulty in controlling its proliferation, especially in developing countries (Morrison et al., 2008;Bhatt et al., 2013;Boeuf et al., 2016). Moreover, the recent possibility of ZIKV transmission sexually and via hemoderivatives (Musso et

al., 2015;Fréour et al., 2016;Katz and Rossmann, 2016;Research, 2016;Russell et al., 2016) has created a context in which understanding the pathophysiological mechanism of infection became vitally relevant to pave the way towards the development of effective therapies, and to prevent associated aggravations.

For all these reasons, better understanding the pathophysiological mechanism of diseases is critical for delivering improved patient care. Recent advances in analytical approaches and metabolomics studies have been growing in the last few years and expanded the knowledge physiological and pathological alterations in living organisms (Dunn et al., 2013;Junot et al., 2014;Melo et al., 2016b). In line with this trend, this contribution focuses in understanding metabolomic alterations caused by ZIKV infection in serum samples from patients infected with ZIKV.

Recent literature states that there are important alterations in human cell metabolome (lipidome) caused by flaviviruses (Martín-Acebes et al., 2016). Such as alterations in the biosynthesis of steroid hormones and fatty acids, catabolism of phospholipids, and β-oxidation (Cui et al., 2013). In DENV-infected mosquitoes, for example, alterations of circa 15% on cell lipidome are observed when compared to uninfected cells. These alterations happen mostly on cell membranes, and correspond to up to 85% of the existing lipid species (Perera et al., 2012), and the nature of these alterations was corroborated by a previous contribution from our group in ZIKV-infected mosquito cells (Melo et al., 2016a). Thus, lipid metabolites have become a promising molecular class, still little explored in the pathophysiological mechanisms of disease and infection, where they have shown capabilities of associating prognostic and diagnostic of infections (van Gorp et al., 2002;Durán et al., 2015;Lima et al., 2015). This report ultimately aims at verifying serum lipid metabolites alterations in ZIKV-infected patients using direct infusion high-resolution mass spectrometry.

Materials and Methods

Ethics Statement

This study was conducted according to the principles expressed in the Declaration of Helsinki and was approved by the Ethics Committee of Unicamp (CEP-Unicamp: Comitê de Ética em Pesquisa da Unicamp - Campus Campinas), number 053407/2016. A written informed consent was obtained from all patients prior to enrollment. All samples were obtained from the Clinical Hospital of the University of Campinas.

Research participants

-*Study design and rationale*

This study included 79 subjects, regardless of age and gender, divided into a control group and a ZIKV group. The ZIKV group was composed of individuals that were positive after testing with the gold standard methodology for detecting ZIKV infection: real-time reverse transcription polymerase chain reaction (RT-PCR) (Lanciotti et al., 2008). According to the results obtained from RT-PCR, samples were treated as either RT-PCR(+) or RT-PCR(-) for ZIKV; all positive samples for ZIKV were also screened for other arboviruses to ensure the absence of cross-infections. On the other hand, for the control group to be considered heterogeneous and faithful to a “real-world” condition, in addition to including healthy individuals and symptomatic patients that were negative for ZIKV according to RT-PCR, we also did not perform testing for any other pathogens. This was to ensure that any biomarkers elected further in the study would pertain to ZIKV infection only, thus providing an unbiased metabolomic result. A summary of subject selection with the three subgroups rendered can be found below:

-ZIKV-infected patients – RT-PCR(+), ZIKV group

The group of symptomatic patients, whose RT-PCR test was positive for ZIKV infection; it corresponded to 35 adult patients, which also presented clinical features compatible with ZIKV infection (i.e. fever, joint pain, conjunctivitis and rash).

-Symptomatic patients – RT-PCR(-), Control group

A group of symptomatic patients, whose RT-PCR test for ZIKV was negative; it corresponded to 34 patients, which presented the same clinical features described above for ZIKV the group.

-Healthy individuals – RT-PCR(-), Control group

The control group was composed by 10 healthy adults, i.e. asymptomatic individuals who did not present any signs of infection within 30 days prior to sample collection and, therefore, presented a negative result in RT-PCR for ZIKV.

The collected specimens from all participants of the present study consisted of blood (serum) samples. Table 1 organizes the structure of sample collection and provides a view of the total number of analyzed specimens, according to type and group. All RT-PCR were performed using RNA extracted from the serum of the analyzed subjects.

PCR diagnosis

In order to confirm ZIKV infection, the viral stock and sample suspects of ZIKV-infected were assayed by real time RT-qPCR (Lanciotti et al., 2008). Briefly, the viral RNA was isolated by a commercial kit following the manufacturer's instruction (RNeasy Mini Kit, Qiagen, Hilden, Germany). One-step RT-PCR amplification of viral RNA (Taqman RNA to-CT, Applied Biosystems) was performed with following primers and probes: ZIKV-F: 5'- CCGCTGCCCAACACAAG-3'; ZIKV-R: 5'- CCACTAACGTTCTTTTGCAGACAT -3'; ZIKV-P: 5'-/FAM/AGCCTACCTTGACAAGCAGTCAGACACTCAA/-3'. All reactions were assembled in a final volume of 12.5 µL with 300 ng of RNA, 1× PrimeTime mix (Integrated DNA Technologies) containing both primers and probe, and 6.25 µL of TaqMan master mix (Applied Biosystems) by using the following cycling algorithm: 48°C for 30 min, 95°C for 10 min, followed by 45 cycles of 95°C for 15 s and 60°C for 1 min.

Sample preparation for HRMS

For sample preparation, 20 microliters of each biological sample (blood serum) were diluted in 200 µL of tetrahydrofuran and homogenized under vortex for 30 seconds; the volume was then completed to 1 mL with methanol, with further homogenization. The obtained solution was centrifuged for 5 minutes under 3200 rpm. 20 µL of the supernatant was then collected and diluted in 980 µL of methanol, resulting in the final solution, which was divided in two 500-µL portions for analysis in positive and negative ion modes after the addition of 0.1% of formic acid and ammonium hydroxide, respectively.

HRMS analyses

All samples were directly infused into an ESI-LTQ-XL Orbitrap Discovery (Thermo Scientific, Bremen, Germany) with a nominal resolution of 30,000 (FWHM). Data were acquired in the survey scan mode, according to the following parameters: flow rate at 10 $\mu L.min^{-1}$, capillary temperature at 280°C, spray current at 5 kV, and sheath gas at 5 arbitrary units. Each sample was analyzed in quintuplicate. The utilized mass range for analysis was 700-1800 *m/z*.

Statistical analyses and structural proposals

Biomarkers choice was guided by using the orthogonal partial least squares discriminant analysis (OPLS-DA). Being a variation of the partial least squares discriminant analysis (PLS-DA), OPLS-DA is a supervised multivariate regression method that performs the linear combination of the original variables, thereby extracting, from raw mass spectrometry data, features that are responsible for sample grouping. The main difference of OPLS-DA from PLS-DA is that it uses orthogonal signal correction in order to maximize the explained covariance among the components of the model. For this analysis, interquartile range was used as data filtering method, with quantile normalization and range scaling. All analyses were performed using the online platform MetaboAnalyst 3.0 (Xia and Wishart, 2011;2016).

After careful selection of the candidate markers using the statistical model, the significance of each ion was assessed by comparing signal intensities in

the raw data matrix to ensure that all elected candidates (i) were above the signal-to-noise ratio and (ii) were not significantly present in the control group (intensities below the signal-to-noise ratio). For characterization, HMDB version 3.6 (Human Metabolome database—www.hmdb.ca), METLIN (Scripps Center for Metabolomics, La Jolla, CA), as well as Lipid MAPS online database (University of California, San Diego, CA—www.lipidmaps.org) were consulted to elect the most suitable marker. Mass accuracy was the method of choice for database research, with a maximum adopted mass error of 2 ppm.

Results

Statistical analysis was performed by using OPLS-DA, based on mass spectral data obtained by the direct infusion of serum, using the results from RT-PCR (absence or confirmation of ZIKV) to provide guidance and support in the establishment of the two studied groups. A detailed description with individuals' demographics and clinical conditions from each group is provided in Table 1. The rationale of mixing symptomatic patients and healthy individuals in the control group was a key feature of this study, as it is an ideal representation of the heterogeneity found in any given population in terms of clinical status. The absence of ZIKV infection in the symptomatic individuals of the control group, as determined by RT-PCR, increases the level of confidence in the biomarkers that were elected by the statistical modeling, thereby providing another level of assurance that such molecules are indeed related to ZIKV and no other related viral infection. This was ultimately corroborated when the OPLS-DA graph was plotted and the two groups remained isolated. In this sense, RT-PCR results were validated by OPLS-DA and vice-versa, as presented in Figure 1. The two-dimensional plot evidenced two very clear clusters, regardless of the ion mode analyzed in HRMS, grouping samples with similar ion content; the green cluster represents patients with RT-PCR-positive ZIKV infection, while the red cluster represents all other individuals that were negative for ZIKV after RT-PCR assessment.

The loadings plot from the statistical model formed by features selected by OPLS-DA assisted in obtaining a list of ions (i.e. the candidate biomarkers) that

were specific for the ZIKV group, according to the presented clustering model. Fifty major features were pointed out as the markers that described the ZIKV group in each ion mode on mass spectrometry (positive and negative), rendering one-hundred features in total. After crosschecking data from literature and metabolomics databases, three biomarkers were characterized for the positive mode: a phosphatidylinositol bisphosphate (PIP2), Angiotensin I, and Ganglioside GM2; for the negative mode, five biomarkers were identified and characterized: Angiotensin (1-7), and four phosphatidylinositol phosphates (PIP). A thorough description of all identified biomarkers is given in Table 2. It is important to remark that not only are the main selected ions supported by the statistical model, but also they are in line with the spectral data in each ion mode (Figures 2 and 3).

Finally, supported by literature information, we were able to provide the significance and the roles that all selected biomarkers play in a very particular metabolic pathway, the PI3K-AKT-mTOR. As displayed in Figure 4, these molecules were selected probably due to their accumulation after cell response to the blockade of AKT by viral proteins, thereby inhibiting relevant mTOR-related mechanisms such as autophagy and neurogenesis, and providing evidence that ZIKV infection has a very close relationship with the renin-angiotensin system (RAS).

Discussion

Biomarker elucidation has revealed the presence of Angiotensin (1-7) (Ang (1-7)) [*m/z* 933.4355] in the negative ion mode (Figure 2), and Angiotensin I (Ang I) [*m/z* 1296.6848] in the positive ion mode (Figure 3). These two metabolites are part of the RAS, which is directly involved in the uptake and excretion of sodium and potassium; these two ions promote vasoconstriction and blood pressure regulation, respectively (Tikellis et al., 2011) (Passos-Silva et al., 2013). RAS has always been studied with focus on its role in metabolic syndromes such as obesity and hypertension (van Vark et al., 2012;Santos et al., 2013;Cabandugama et al., 2017); however, its importance in the viral infection process has only recently been observed, as demonstrated by a study in which DENV-infected rats were treated with either losartan or enalapril. In this case, the treatment decreased DENV

absorption by macrophages, showing that the RAS may be associated with infection severity (Hernández-Fonseca et al., 2015). In an experiment carried out with knockout rats for the angiotensin II converting enzyme (ACE2) and wild-type rats, both infected by the respiratory syncytial virus (RSV), knockout rats presented a 5-fold higher viral titer than wild-type rats, in addition to increased pulmonary injury, mortality and angiotensin II (Ang II) plasma concentrations (Gu et al., 2016). In another study, also carried out with knockout rats for ACE2, this time assessing the infection by H5N1 virus (avian flu), has also demonstrated that knockouts presented a more severe infection, as well as higher mortality compared to wild-type animals. This result was, therefore, associated with increased plasma levels of Ang II, which presented close relationship with the severity and lethality of the avian flu (Zou et al., 2014). This was also observed for the H7N9 virus infection, where knockout rats for ACE2 presented increased plasma levels of angiotensin II, also with increased infection severity. The lack of ACE2 results in deficiency of Ang (1-7), a cleavage product of either angiotensin I or angiotensin II that is highly dependent on ACE2 activity to be formed (Lumbers and Pringle, 2014). Since Ang (1-7) has been associated with infection mitigation, its absence in knockout animals for ACE2 may be directly related to the severity of viral infection (Ferrario and Iyer, 1998).

Given that Ang (1-7) diminishes the severity of pathogen infections due to alterations in the cell machinery, thereby breaking its life cycle (Saraiva et al., 2011;Fedson, 2016), the biomarkers elucidated in our study reveal that these species may also be linked to the control of the immune response to ZIKV infection. One of the most primordial forms of innate immune defense may be autophagy, which has been described as a mechanism involved with antigen presentation, microbe elimination and secretion of immune mediators (Tallóczy et al., 2006;Deretic et al., 2013). The Ang (1-7) signaling pathway, for instance, is also related to the process of autophagy, a process that causes infected cells to die, thus decreasing viral replication rate in the organism (Saraiva et al., 2011;Petersen et al., 2016). Electing both Ang I and Ang (1-7) as ZIKV group biomarkers, therefore, allow us to infer that the RAS is part of the immune response process against ZIKV in humans.

The other four markers that were found for ZIKV-infected patients are phosphatidylinositol phosphates (Table 2); these help corroborate the role of Ang (1-7) in the immune response upon infection, since this peptide is responsible for activating the PI3K-AKT-mTOR pathway (Giani et al., 2007;Sampaio et al., 2007). This process initiates a series of lipid phosphorylations upon binding to the MAS receptor, which modulates the activation of PI3K and leads to the activation of the phosphatidylinositol signaling system (PSS). The activation of PSS is also part of the cell signaling system for autophagy, hence the importance of PIPs on immune response during the infection. Although both the RAS activation and autophagy process contribute with higher biomarkers concentrations, an additional factor seem to cause the increase of the elected markers in the viral infection process of ZIKV. As demonstrated in the metabolic scheme presented in Figure 4, two non-structural ZIKV proteins, NS4A and NS4B, inhibit the AKT-mTOR signaling pathway (Liang et al., 2016). Such inhibition leads to the accumulation of intermediate metabolites and precursors involved in the PI3K-AKT-mTOR pathway signaling. As the virus inhibits AKT and the signaling through the RAS (Ang (1-7)) persists due to viral infection, the positive modulation over PI3K is maintained. Therefore, ZIKV infection has induced alterations in different signaling pathways, which have culminated with the overexpression of some metabolites, amongst them the above-reported lipids.

This is the first time that lipids for ZIKV infection are described, whereas the great majority of previous contributions deal with general immune response species such as proteins, as well as with molecules potentially linked with microcephaly (Petersen et al., 2016). Taking into account that neurologic malformations such as microcephaly are associated with alterations in PI3K-AKT-mTOR pathway, the lipid markers elected, consequently, are part of this process during embryogenesis, as the mTOR signaling pathway is active in both neurogenesis and autophagy signaling processes (Figure 4). The latter is triggered as protection against infections, as discussed before, and, during a neurogenesis process, autophagy activation may lead to neurologic malformations, as in the case of pregnant women infected by ZIKV.

The last marker described in this contribution for understanding the metabolomics of ZIKV infection is a ganglioside, GM2 [*m/z* 1323.7423], which belongs to the class of sphingolipids. These lipids are known for their relation with the identification and inclusion of several types of viruses into the cells, as soon as the infection process begins, as in the case of polyomavirus and HIV (Mazzon and Mercer, 2014). Gangliosides are located in the external side of the plasma membrane and regulate cell development processes (Coskun et al., 2011); additionally, as they are part of the membrane's outer layer, these molecules are explored by pathogens, functioning as binders in the process of cell recognition and supporting endocytosis of microbes (Eidels et al., 1983;Tsai et al., 2003). These lipids are also fundamental for viral genome replication, where they compose the viral replication complex (VRC) in conjunction with NS4A (Wang et al., 2016), as demonstrated in a study with DENV, where NS4A, is responsible for anchoring the VRC in the endoplasmic reticulum. Thus, together, gangliosides and NS4A are essential molecules for viral replication. In addition, gangliosides are further associated with an important complication attributed to infections: the Guillain-Barre Syndrome (GBS), an autoimmune condition where the host's immune system attacks the gangliosides of neurons. This clinical picture has been described in a series of infections (Cao-Lormeau et al., 2016), including ZIKV (Kuwabara and Yuki, 2013). Our results, therefore, suggest that the elected ganglioside is related to GBS, as these molecules are related with the formation of viral replication vacuoles from plasma membrane invaginations in the infected cells (Wang et al., 2016); because of its location in the plasma membrane, this lipid is subject to recognition by the immune system and works as a marker for infected cells. However, as neurons effectively present this molecule under normal circumstances, the immune system attacks not only the infected cells, but the whole environment, due to cross-identification (Kuwabara and Yuki, 2013;Liang et al., 2016;van Doorn and Jacobs, 2016).

Our results suggest, ultimately, that it is possible to perform a viral infection mechanism study through the direct analysis of the serum from infected patients. All biomarkers were elected and validated by statistical analysis, and are

in consonance with previous studies that were focused on proteins (kinases and phosphorylases) involved in the infection process, whilst the biomarkers presented herein are substrates/products of these enzymes. Studies on viral infections, such as DENV and H5N1 have explored the inhibition of ACE (Tikellis et al., 2011;Zou et al., 2014;Hernández-Fonseca et al., 2015;Gu et al., 2016) and kinases involved in the PI3K-AKT-mTOR pathway (Easton et al., 2005;Tokuda et al., 2010;Liang et al., 2016); seven out of the eight biomarkers reported in this contribution are directly related to these enzymes, corroborating the relevance of these molecules and providing the targets in which substrate they work. Therefore, the metabolomic insight on human infection by ZIKV provided by this contribution broadens the knowledge of the pathophysiological aspects of the disease by elucidating molecular targets of the cell immune response facing viral infection and replication; this also provides grounds for further developments within the field of pharmacology for differential therapies, interventions and insights in ZIKV infection management.

Conflict of interests

The authors declare no conflict of interests of any nature.

Authors and contributions

CFORM and JD performed sample collection, experiments and wrote the manuscript. DNO, TMG, CZE, EOL and VPR performed data analysis, and performed manuscript review. RRC idealized all experiments and managed the research group. The Zika Unicamp Network is mentioned as an initiative from the University of Campinas of mutual collaboration in the Brazilian Plan for Fighting Zika Virus.

Funding

The authors would like to thank the São Paulo Research Foundation (FAPESP) for the fellowships of CFORM (16/17066-2) and CZE (14/00302-0), and the grants for RRC (11/50400-0 and 15/06809-1). We also acknowledge CAPES for the scholarships for EOL (PNPD 1578388) and TMG (PROEX 1489740). DNO

acknowledges the *Plano Nacional de Enfrentamento ao* Aedes aegypti *e Microcefalia* from the Brazilian Ministry of Health for the fellowship (88887.137889/2017-00).

Acknowledgements

The authors acknowledge the Zika Unicamp Network for the support during the conceptual development of the initiative.

References

Bhatt, S., Gething, P.W., Brady, O.J., Messina, J.P., Farlow, A.W., Moyes, C.L., Drake, J.M., Brownstein, J.S., Hoen, A.G., and Sankoh, O. (2013). The global distribution and burden of dengue. *Nature* 496**,** 504-507.

Boeuf, P., Drummer, H.E., Richards, J.S., Scoullar, M.J., and Beeson, J.G. (2016). The global threat of Zika virus to pregnancy: epidemiology, clinical perspectives, mechanisms, and impact. *BMC medicine* 14**,** 112.

Cabandugama, P.K., Gardner, M.J., and Sowers, J.R. (2017). The Renin Angiotensin Aldosterone System in Obesity and Hypertension: Roles in the Cardiorenal Metabolic Syndrome. *Medical Clinics of North America* 101**,** 129-137.

Cao-Lormeau, V.-M., Blake, A., Mons, S., Lastère, S., Roche, C., Vanhomwegen, J., Dub, T., Baudouin, L., Teissier, A., and Larre, P. (2016). Guillain-Barré Syndrome outbreak associated with Zika virus infection in French Polynesia: a case-control study. *The Lancet* 387**,** 1531-1539.

Coskun, Ü., Grzybek, M., Drechsel, D., and Simons, K. (2011). Regulation of human EGF receptor by lipids. *Proceedings of the National Academy of Sciences* 108**,** 9044-9048.

Cui, L., Lee, Y.H., Kumar, Y., Xu, F., Lu, K., Ooi, E.E., Tannenbaum, S.R., and Ong, C.N. (2013). Serum metabolome and lipidome changes in adult patients with primary dengue infection. *PLoS Negl Trop Dis* 7**,** e2373.

Daumas, R.P., Passos, S.R., Oliveira, R.V., Nogueira, R.M., Georg, I., Marzochi, K.B., and Brasil, P. (2013). Clinical and laboratory features that discriminate dengue from other febrile illnesses: a diagnostic accuracy study in Rio de Janeiro, Brazil. *BMC infectious diseases* 13**,** 1.

Deretic, V., Saitoh, T., and Akira, S. (2013). Autophagy in infection, inflammation and immunity. *Nature Reviews Immunology* 13**,** 722-737.

Duffy, M.R., Chen, T.-H., Hancock, W.T., Powers, A.M., Kool, J.L., Lanciotti, R.S., Pretrick, M., Marfel, M., Holzbauer, S., and Dubray, C. (2009). Zika virus outbreak on Yap Island, federated states of Micronesia. *New England Journal of Medicine* 360**,** 2536-2543.

Dunn, W.B., Erban, A., Weber, R.J., Creek, D.J., Brown, M., Breitling, R., Hankemeier, T., Goodacre, R., Neumann, S., and Kopka, J. (2013). Mass

appeal: metabolite identification in mass spectrometry-focused untargeted metabolomics. *Metabolomics* 9**,** 44-66.

Durán, A., Carrero, R., Parra, B., González, A., Delgado, L., Mosquera, J., and Valero, N. (2015). Association of lipid profile alterations with severe forms of dengue in humans. *Archives of virology* 160**,** 1687-1692.

Easton, R.M., Cho, H., Roovers, K., Shineman, D.W., Mizrahi, M., Forman, M.S., Lee, V.M.-Y., Szabolcs, M., De Jong, R., and Oltersdorf, T. (2005). Role for Akt3/protein kinase Bγ in attainment of normal brain size. *Molecular and cellular biology* 25**,** 1869-1878.

Eidels, L., Proia, R., and Hart, D. (1983). Membrane receptors for bacterial toxins. *Microbiological reviews* 47**,** 596.

Fedson, D.S. (2016). Treating the host response to emerging virus diseases: lessons learned from sepsis, pneumonia, influenza and Ebola. *Annals of Translational Medicine* 4.

Ferrario, C.M., and Iyer, S.N. (1998). Angiotensin-(1–7): a bioactive fragment of the renin–angiotensin system. *Regulatory peptides* 78**,** 13-18.

Fréour, T., Mirallié, S., Hubert, B., Splingart, C., Barrière, P., Maquart, M., and Leparc-Goffart, I. (2016). Sexual transmission of Zika virus in an entirely asymptomatic couple returning from a Zika epidemic area, France, April 2016. *Eurosurveillance* 21.

Giani, J.F., Gironacci, M.M., Munoz, M.C., Pena, C., Turyn, D., and Dominici, F.P. (2007). Angiotensin-(1–7) stimulates the phosphorylation of JAK2, IRS-1 and Akt in rat heart in vivo: role of the AT1 and Mas receptors. *American Journal of Physiology-Heart and Circulatory Physiology* 293**,** H1154-H1163.

Gu, H., Xie, Z., Li, T., Zhang, S., Lai, C., Zhu, P., Wang, K., Han, L., Duan, Y., and Zhao, Z. (2016). Angiotensin-converting enzyme 2 inhibits lung injury induced by respiratory syncytial virus. *Scientific reports* 6.

Hernández-Fonseca, J.P., Durán, A., Valero, N., and Mosquera, J. (2015). Losartan and enalapril decrease viral absorption and interleukin 1 beta production by macrophages in an experimental dengue virus infection. *Archives of virology* 160**,** 2861-2865.

Junot, C., Fenaille, F., Colsch, B., and Bécher, F. (2014). High resolution mass spectrometry based techniques at the crossroads of metabolic pathways. *Mass spectrometry reviews* 33**,** 471-500.

Katz, L.M., and Rossmann, S.N. (2016). Zika and the Blood Supply: A Work in Progress. *Archives of Pathology & Laboratory Medicine*.

Kuwabara, S., and Yuki, N. (2013). Axonal Guillain-Barré syndrome: concepts and controversies. *The Lancet Neurology* 12**,** 1180-1188.

Lanciotti, R.S., Kosoy, O.L., Laven, J.J., Velez, J.O., Lambert, A.J., Johnson, A.J., Stanfield, S.M., and Duffy, M.R. (2008). Genetic and serologic properties of Zika virus associated with an epidemic, Yap State, Micronesia, 2007. *Emerg Infect Dis* 14**,** 1232-1239.

Liang, Q., Luo, Z., Zeng, J., Chen, W., Foo, S.-S., Lee, S.-A., Ge, J., Wang, S., Goldman, S.A., and Zlokovic, B.V. (2016). Zika virus NS4A and NS4B proteins deregulate Akt-mTOR signaling in human fetal neural stem cells to inhibit neurogenesis and induce autophagy. *Cell Stem Cell* 19**,** 663-671.

Lima, E.D.O., De Macedo, C.S., Esteves, C.Z., De Oliveira, D.N., Pessolani, M.C.V., Nery, J.a.D.C., Sarno, E.N., and Catharino, R.R. (2015). Skin imprinting in silica plates: a potential diagnostic methodology for leprosy using high-resolution mass spectrometry. *Analytical chemistry* 87**,** 3585-3592.

Lumbers, E.R., and Pringle, K.G. (2014). Roles of the circulating renin-angiotensin-aldosterone system in human pregnancy. *American Journal of Physiology-Regulatory, Integrative and Comparative Physiology* 306**,** R91-R101.

Martín-Acebes, M.A., Vázquez-Calvo, Á., and Saiz, J.-C. (2016). Lipids and flaviviruses, present and future perspectives for the control of dengue, Zika, and West Nile viruses. *Progress in Lipid Research* 64**,** 123-137.

Mazzon, M., and Mercer, J. (2014). Lipid interactions during virus entry and infection. *Cellular microbiology* 16**,** 1493-1502.

Melo, C.F.O.R., De Oliveira, D.N., De Oliveira Lima, E., Guerreiro, T.M., Esteves, C.Z., Beck, R.M., Padilla, M.A., Milanez, G.P., Arns, C.W., and Proença-Modena, J.L. (2016a). A Lipidomics Approach in the Characterization of Zika-Infected Mosquito Cells: Potential Targets for Breaking the Transmission Cycle. *PloS one* 11**,** e0164377.

Melo, C.F.O.R., Esteves, C.Z., De Oliveira, R.N., Guerreiro, T.M., De Oliveira, D.N., De Oliveira Lima, E., Miné, J.C., Allegretti, S.M., and Catharino, R.R. (2016b). Early developmental stages of Ascaris lumbricoides featured by high-resolution mass spectrometry. *Parasitology research* 115**,** 4107-4114.

Morrison, A.C., Zielinski-Gutierrez, E., Scott, T.W., and Rosenberg, R. (2008). Defining challenges and proposing solutions for control of the virus vector Aedes aegypti. *PLoS Med* 5**,** e68.

Musso, D., Roche, C., Robin, E., Nhan, T., Teissier, A., and Cao-Lormeau, V.-M. (2015). Potential sexual transmission of Zika virus. *Emerg Infect Dis* 21**,** 359-361.

Pabbaraju, K., Wong, S., Gill, K., Fonseca, K., Tipples, G.A., and Tellier, R. (2016). Simultaneous detection of Zika, Chikungunya and Dengue viruses by a multiplex real-time RT-PCR assay. *Journal of Clinical Virology* 83**,** 66-71.

Paniz-Mondolfi, A.E., Rodriguez-Morales, A.J., Blohm, G., Marquez, M., and Villamil-Gomez, W.E. (2016). ChikDenMaZika Syndrome: the challenge of diagnosing arboviral infections in the midst of concurrent epidemics. *Annals of Clinical Microbiology and Antimicrobials* 15**,** 42.

Passos-Silva, D.G., Verano-Braga, T., and Santos, R.A. (2013). Angiotensin-(1–7): beyond the cardio-renal actions. *Clinical Science* 124**,** 443-456.

Perera, R., Riley, C., Isaac, G., Hopf-Jannasch, A.S., Moore, R.J., Weitz, K.W., Pasa-Tolic, L., Metz, T.O., Adamec, J., and Kuhn, R.J. (2012). Dengue virus infection perturbs lipid homeostasis in infected mosquito cells. *PLoS Pathog* 8**,** e1002584.

Petersen, L.R., Jamieson, D.J., Powers, A.M., and Honein, M.A. (2016). Zika virus. *New England Journal of Medicine* 374**,** 1552-1563.

Research, C.F.B.E.A. (2016). "Donor Screening Recommendations to Reduce the Risk of Transmission of Zika Virus by Human Cells, Tissues, and Cellular and Tissue-Based Products", (ed.) F.a.D. Administration. (United States).

Russell, K., Hills, S.L., Oster, A.M., Porse, C.C., Danyluk, G., Cone, M., Brooks, R., Scotland, S., Schiffman, E., and Fredette, C. (2016). Male-to-Female Sexual

Transmission of Zika Virus—United States, January–April 2016. *Clinical infectious diseases*, ciw692.

Sampaio, W.O., Dos Santos, R.a.S., Faria-Silva, R., Da Mata Machado, L.T., Schiffrin, E.L., and Touyz, R.M. (2007). Angiotensin-(1-7) through receptor Mas mediates endothelial nitric oxide synthase activation via Akt-dependent pathways. *Hypertension* 49**,** 185-192.

Santos, R.A., Ferreira, A.J., Verano-Braga, T., and Bader, M. (2013). Angiotensin-converting enzyme 2, angiotensin-(1–7) and Mas: new players of the renin–angiotensin system. *Journal of Endocrinology* 216**,** R1-R17.

Saraiva, V.B., De Souza Silva, L., Ferreira-Dasilva, C.T., Da Silva-Filho, J.L., Teixeira-Ferreira, A., Perales, J., Souza, M.C., Das Graças Henriques, M., Caruso-Neves, C., and De Sá Pinheiro, A.A. (2011). Impairment of the Plasmodium falciparum erythrocytic cycle induced by angiotensin peptides. *PloS one* 6**,** e17174.

Tallóczy, Z., Virgin, I., Herbert, and Levine, B. (2006). PKR-dependent xenophagic degradation of herpes simplex virus type 1. *Autophagy* 2**,** 24-29.

Tikellis, C., Bernardi, S., and Burns, W.C. (2011). Angiotensin-converting enzyme 2 is a key modulator of the renin–angiotensin system in cardiovascular and renal disease. *Current opinion in nephrology and hypertension* 20**,** 62-68.

Tokuda, S., Mahaffey, C.L., Monks, B., Faulkner, C.R., Birnbaum, M.J., Danzer, S.C., and Frankel, W.N. (2010). A novel Akt3 mutation associated with enhanced kinase activity and seizure susceptibility in mice. *Human molecular genetics*, ddq544.

Tsai, B., Gilbert, J.M., Stehle, T., Lencer, W., Benjamin, T.L., and Rapoport, T.A. (2003). Gangliosides are receptors for murine polyoma virus and SV40. *The EMBO Journal* 22**,** 4346-4355.

Van Doorn, P.A., and Jacobs, B.C. (2016). Neuronal endocytosis of anti-ganglioside antibodies: implications for Guillain-Barré syndrome. *Brain* 139**,** 1622-1625.

Van Gorp, E.C., Suharti, C., Mairuhu, A.T., Dolmans, W.M., Van Der Ven, J., Demacker, P.N., and Van Der Meer, J.W. (2002). Changes in the plasma lipid profile as a potential predictor of clinical outcome in dengue hemorrhagic fever. *Clinical infectious diseases* 34**,** 1150-1153.

Van Vark, L.C., Bertrand, M., Akkerhuis, K.M., Brugts, J.J., Fox, K., Mourad, J.-J., and Boersma, E. (2012). Angiotensin-converting enzyme inhibitors reduce mortality in hypertension: a meta-analysis of randomized clinical trials of renin–angiotensin–aldosterone system inhibitors involving 158 998 patients. *European heart journal* 33**,** 2088-2097.

Wang, K., Wang, J., Sun, T., Bian, G., Pan, W., Feng, T., Wang, P., Li, Y., and Dai, J. (2016). Glycosphingolipid GM3 is Indispensable for Dengue Virus Genome Replication. *International Journal of Biological Sciences* 12**,** 872-883.

Woods, C.G., Bond, J., and Enard, W. (2005). Autosomal recessive primary microcephaly (MCPH): a review of clinical, molecular, and evolutionary findings. *The American Journal of Human Genetics* 76**,** 717-728.

Xia, J., and Wishart, D.S. (2011). Web-based inference of biological patterns, functions and pathways from metabolomic data using MetaboAnalyst. *Nature protocols* 6**,** 743-760.

Xia, J., and Wishart, D.S. (2016). Using MetaboAnalyst 3.0 for Comprehensive Metabolomics Data Analysis. *Current Protocols in Bioinformatics*, 14.10. 11-14.10. 91.

Zou, Z., Yan, Y., Shu, Y., Gao, R., Sun, Y., Li, X., Ju, X., Liang, Z., Liu, Q., and Zhao, Y. (2014). Angiotensin-converting enzyme 2 protects from lethal avian influenza A H5N1 infections. *Nature communications* 5.

Figure captions

Figure 1. Establishment of the OPLS-DA model. The figure illustrates the score plot of OPLS-DA modeling for serum metabolomic data on positive and negative mode. The non-infected serum group clustered to the left region and the infected serum group clustered to the right area in the both positive and negative modes. The shaded area shows represents the confidence interval of 95% from OPLS-DA models; the T score [1] shows the relevance of the predictive component [1] in explaining the clustering model.

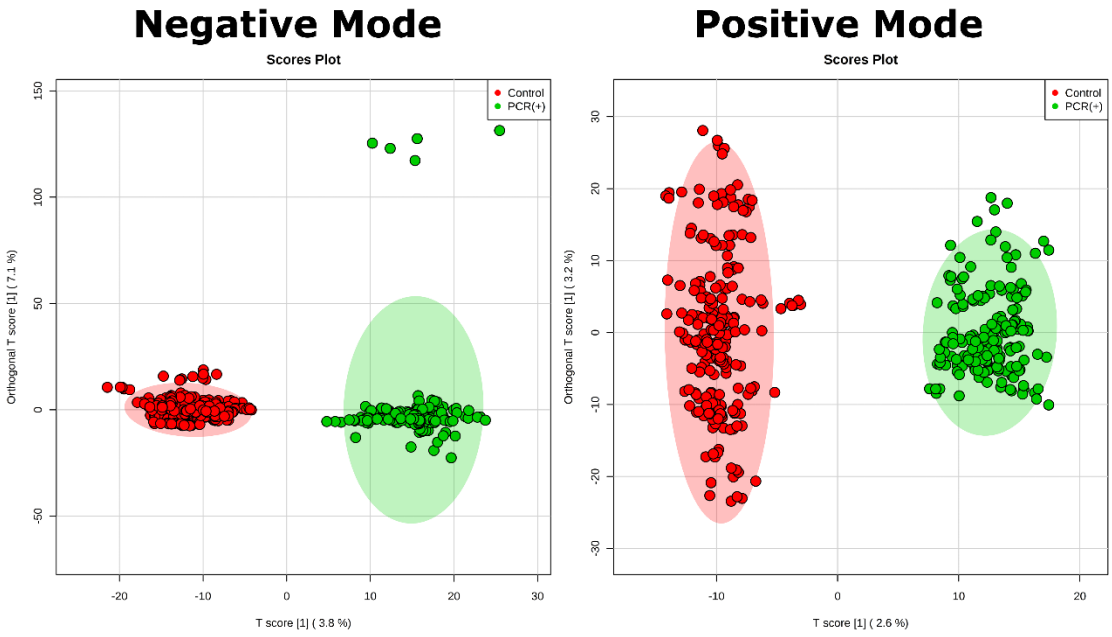

Figure 2. High-resolution mass spectrum of patients' serums on the negative ion mode: asymptomatic individuals with negative PCR results, patients with clinical manifestations of Zika virus infection and negative diagnosis by PCR, and patients with clinical manifestations of Zika virus infection and diagnosis Positive by PCR.

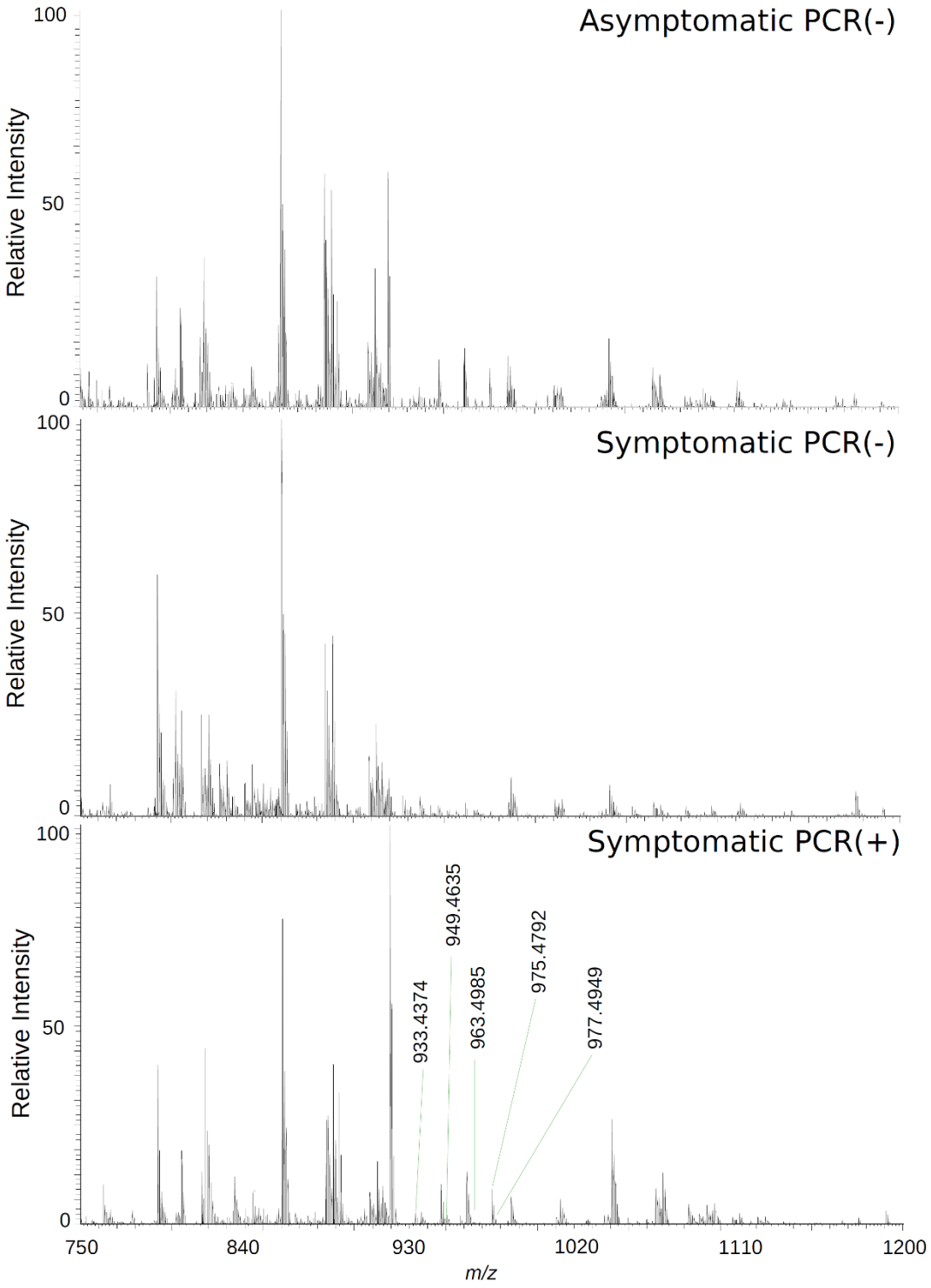

Figure 3. High-resolution mass spectrum of the serum patients on the positive mode: asymptomatic individuals with negative PCR results, patients with clinical manifestations of Zika virus infection and negative diagnosis by PCR, and patients with clinical manifestations of Zika virus infection and diagnosis Positive by PCR.

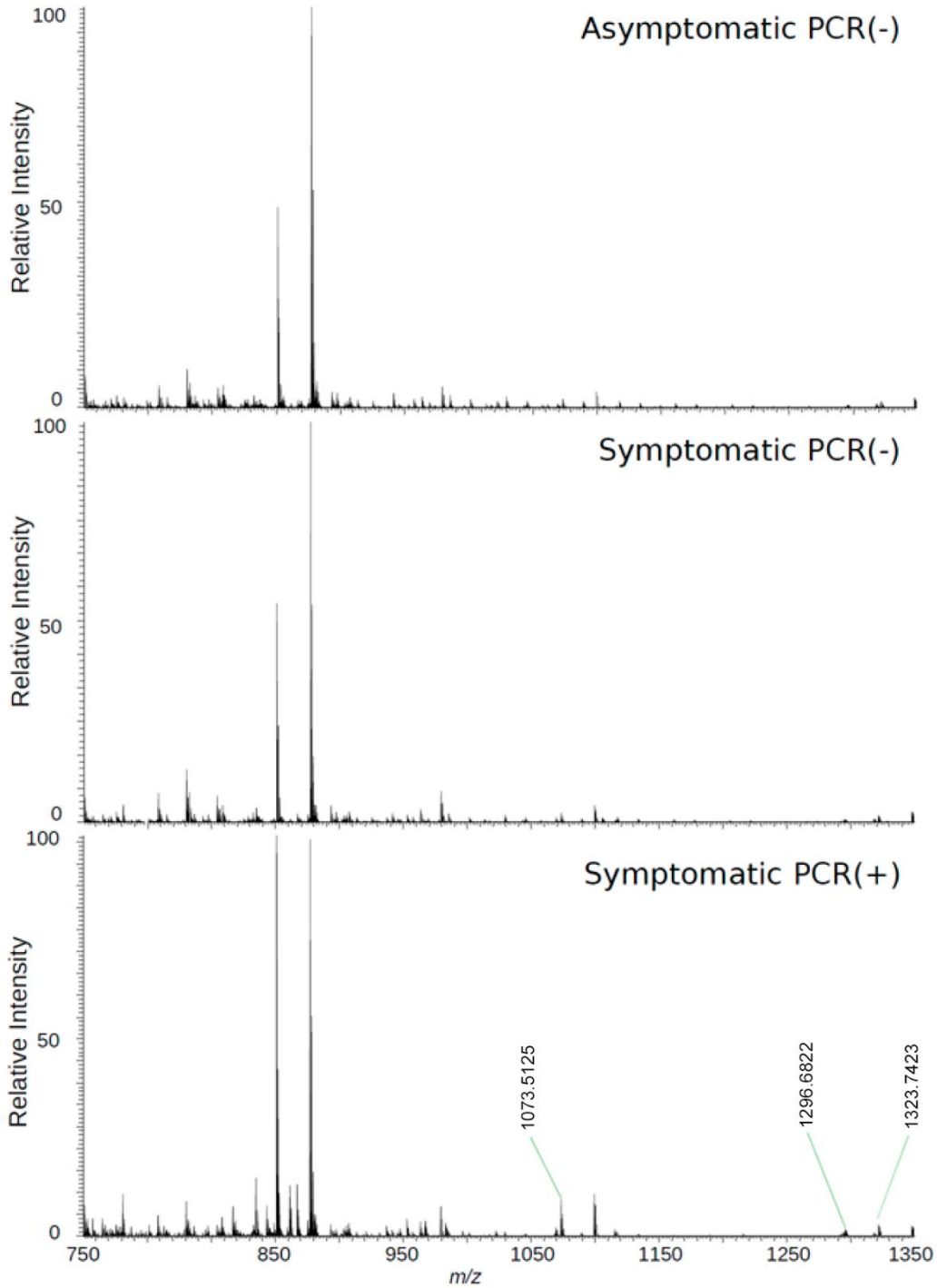

Figure 4. Cell signaling pathway scheme of metabolic alterations due to Zika virus infection. The scheme shows the cell response, attempting to control the viral infection, with Ang I or II, Ang 1-9 and Ang 1-7 signaling to activate autophagy process, which would lead to cell death and, consequently, decreased viral replication. It is also possible to see the close participation of lipids PI, PIP2 and PIP3 as key players in this process, all of which were elected biomarkers. The scheme also shows the inhibition of AKT by the viral proteins of ZIKV (solid and dashed red lines), which culminates in the inhibition of autophagy, so that replication can occur. In a parallel mechanism, it is possible to see that the same pathway is responsible for the inhibition of neurogenesis. Captions: Ang I / II: Angiotensin I / II; Ang 1-9: Angiotensin 1-9; Ang 1-7: Angiotensin 1-7; MAS1: MAS receptor; PI: 1-Phosphatidyl-D-myo-inositol; PIP: Phosphatidylinositol 5-phosphate; PIP2: Phosphatidylinositol-4,5-bisphosphate; PIP3: Phosphatidylinositol-3,4,5-trisphosphate; PDK1: 3-phosphoinositide-dependent protein kinase 1; AKT: AKT serine/threonine kinase 3; mTOR: mechanistic target of rapamycin (atypical serine/threonine kinase); PIKFYVE: 1-phosphatidylinositol-3-phosphate 5-kinase; PIP4K: phosphatidylinositol-5-phosphate 4-kinase type 2 alpha; PIK3C: phosphoinositide-3-kinase regulatory subunit 5; PIK3: phosphoinositide-3-kinase regulatory; ACE2: angiotensin-converting enzyme 2; CTSA: carboxypeptidase C; CPA3: carboxypeptidase A3; ACE: angiotensin-converting enzyme; MME: Neprilysin.

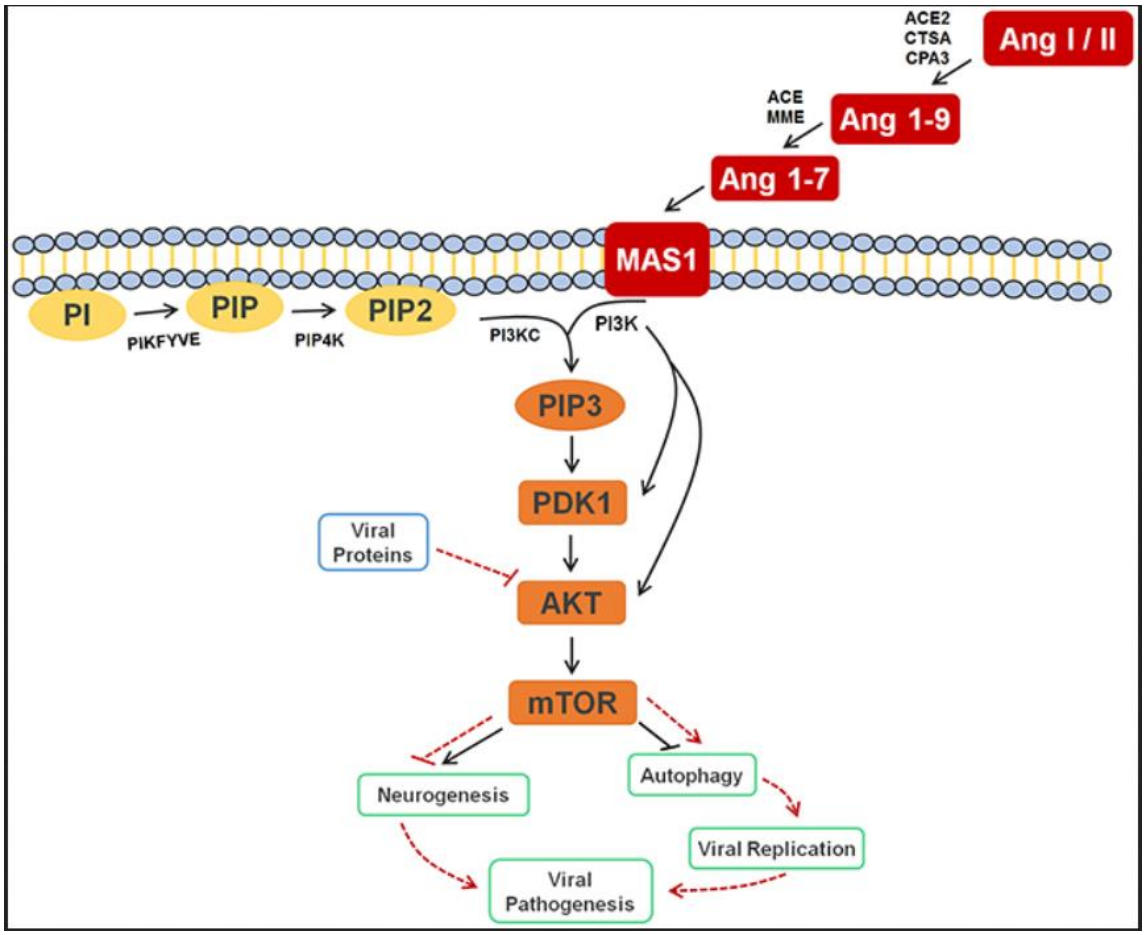

Table 1. Demographics and clinical conditions of all recruited and included individuals in the study.

Parameters	Groups		
	Control		ZIKV
RT-PCR exam	Negative	Negative	Positive
Symptomatic?	No	Yes	Yes
Demographics			
Male	6	25	27
Female	4	9	8
Mean age (median)	32.76 (30)	31.67 (30)	35.45 (35)
Symptoms			
Fever (%)	NA[a]	17.14	29.40
Rash (%)	NA[a]	20.00	41.18
Joint pain (%)	NA[a]	2.86	11.76
Retro-orbital pain (%)	NA[a]	5.71	5.88
Migraine (%)	NA[a]	8.57	17.60
Conjunctivitis (%)	NA[a]	14.29	17.60
Neurological syndrome (%)	NA[a]	17.14	8.80

[a] NA: Not Applicable

Table 2. Lipid markers elected by OPLS-DA from serum analysis of patients infected with Zika Virus (ZIKV group).

Exact Mass	Theoretical Mass	Error (ppm)	Adduct	ID[1]	Molecule
NEGATIVE MODE					
977.4949	977.4929	2.04	$[M+Cl]^-$	61356 61365 61384	PIP(18:1/18:1) and/or PIP(18:2/18:0) and/or PIP(20:2/16:0)
933.4374	933.4355	2.03	$[M+Cl]^-$	71112	Angiotensin (1-7)
963.4985	963.5005	-2.07	$[M-H]^-$	61399 61395 61403 61319 61405	PIP(20:4/18:1) and/or PIP(20:3/18:2) and/or PIP(20:4/18:1) and/or PIP(16:0/22:5) and/or PIP(22:3/16:2)
949.4635	949.4616	2.00	$[M+Cl]^-$	61326 61323 61364	PIP(16:2/18:0) and/or PIP(16:1/18:1) and/or PIP(18:2/16:0)
975.4792	975.4772	2.05	$[M+Cl]^-$	61366 61374 61386	PIP(18:2/18:1) and/or PIP(18:3/18:0) and/or PIP(20:3/16:0)
POSITIVE MODE					
1073.5125	1073.5103	2.04	$[M+Na]^+$	61492 61495 61498 61423	PIP2(20:0/18:2) and/or PIP2(20:1/18:1) and/or PIP2(20:2/18:0) and/or PIP2(16:0/22:2)
1296.6822	1296.6848	-2.01	$[M+H]^+$	65540	Angiotensin I
1323.7423	1323.7395	2.11	$[M+Na]^+$	62596	Ganglioside GM2 (d18:0/12:0)

[1]METLIN ID

4.1.3. Artigo III

A machine learning application based in random forest for integrating mass spectrometry-based metabolomic data: a simple screening method for patients with zika virus[36]

Carlos Fernando Odir Rodrigues Melo[1], Luiz Claudio Navarro[2], Diogo Noin de Oliveira[1], Tatiane Melina Guerreiro[1], Estela de Oliveira Lima[1], Jeany Delafiori[1],

Mohamed Ziad Dabaja[1], Marta Ribeiro[1], Maico de Menezes[1], Rafael Gustavo Martins Rodrigues[1], Karen Noda Morishita[1], Cibele Zanardi Esteves[1], Aline Lopes Lucas de Amorim[1], Caroline Tiemi Aoyagui[1], Pierina Lorencini Parise[3], Guilherme Paier Milanez[3], Gabriela Monsano do Nascimento[3], André Ricardo Ribas Freitas[4,12], Rodrigo Angerami[5], Fábio Trindade Maranhão Costa[3], Clarice Weis Arns[3], Mariangela Ribeiro Resende[5], Eliana Amaral[6], Renato Passini Junior[6], Carolina C. Ribeiro-do-Valle[6], Helaine Milanez[6], Maria Luiza Moretti[5], Jose Luiz Proenca-Modena[3], Sandra Eliza Fontes de Ávila[2], Anderson de Rezende Rocha[2] and Rodrigo Ramos Catharino[1], on behalf of the Zika-Unicamp Network*

* The Zika-Unicamp Network: Glaucia Maria Pastore[7], Kleber Yotsumoto Fertrin[5], Márcia Teixeira Garcia[5], Roseli Calil[7], João Renato Bennini Júnior[6], Giuliane Jesus Lajos[6], Maria Laura Costa[6], Marcos Tadeu Nolasco da Silva[8], Albina Altemani[9]; Ana Carolina Coan[10]; Maria Francisca Colella-Santos[11]; Andrea Paula Bruno von Zuben[4]; Marco Aurélio Ramirez Vinolo[3], Rosemeire Florênça de Oliveira de Paula[3]; Carla Cristina Judice[3], Juliana Almeida Leite[3], Leonardo Cardia Caserta[3], Ana Paula de Moraes[3], Ana Caroline de Souza Barnabé[3]; Ana Lucia Rodrigues da Soledade[3], Daniel Augusto de Toledo Teixeira[3], Évellyn Ribeiro de Morais[3], Felipe Rebelo Santos[3]

[1]Innovare Biomarkers Laboratory, School of Pharmaceutical Sciences (FCF), University of Campinas, Brazil.

[2]RECOD Lab., Institute of Computing (IC), University of Campinas, Brazil.

[3]Department of Genetics, Evolution and Bioagents, Biology Institute, University of Campinas, Brazil.

[4]Campinas Department of Public Health Surveillance, Campinas, Brazil.

[5]Clinical Pathology Department, School of Medical Sciences, University of Campinas, Brazil.

[6]Obstetrics and Gynecology Department, School of Medical Sciences, University of Campinas, Brazil.

[7]Faculty of Food Engineering, University of Campinas, Brazil.

[8]Pediatric Immunology, Center for Investigation in Pediatrics, School of Medical Sciences, University of Campinas, Brazil.;

[9]Pathology Department, School of Medical Sciences, University of Campinas, Brazil.

[10]Neurology Department, School of Medical Sciences, University of Campinas, Brazil.

[11]Department of Human Development and Rehabilitation, School of Medical Sciences, University of Campinas, Brazil.

[12]São Leopoldo Mandic Institute and Research Center, Campinas, Brazil.

*Correspondence: Prof. Dr. Rodrigo Ramos Catharino (rrc@g.unicamp.br)

DOI:10.3389/fbioe.2018.00031

Abstract

Recent Zika outbreaks in South America, accompanied by unexpectedly severe clinical complications have brought much interest in fast and reliable screening methods for ZIKV (Zika virus) identification. Reverse-transcriptase polymerase chain reaction (RT-PCR) is currently the method of choice to detect ZIKV in biological samples. This approach, nonetheless, demands a considerable amount of time and resources such as kits and reagents that, in endemic areas, may result in a substantial financial burden over affected individuals and health services veering away from RT-PCR analysis. This study presents a powerful combination of high-resolution mass spectrometry and a machine-learning prediction model for data analysis to assess the existence of ZIKV infection across a series of patients that bear similar symptomatic conditions, but not necessarily are infected with the disease. By using mass spectrometric data that are inputted into the developed decision-making algorithm, we were able to provide a set of features that work as a “fingerprint” for this specific pathophysiological condition, even after the acute phase of infection. Since both mass spectrometry and machine learning approaches are well-established and largely utilized tools within their respective fields, this combination of methods emerges as a distinct alternative for clinical applications, providing a diagnostic screening --- faster and more accurate --- with improved cost-effectiveness when compared to existing technologies.

Keywords: Zika virus; Zika diagnosis; diseases diagnosis; high resolution mass spectrometry; machine learning; random forest; feature importance; diagnosis classifier.

Introduction

Zika virus (ZIKV) is an emerging pathogen that belongs to the Flaviviridae family and, as with other members, ZIKV is classified as an arthropod-borne RNA virus (arbovirus). The association between ZIKV and microcephaly in newborns from the recent outbreak of this viral infection in South America has raised much concern in the medical community, especially for the significant amount of cases of microcephaly in potentially endemic areas (Enfissi, et al. 2016), (Schuler-Faccini, et al. 2016), as well as for the demonstrated tropism of ZIKV for neural cells medical community, especially for the significant amount of cases of microcephaly in potentially endemic areas (Enfissi, et al. 2016), (Attar 2016), (Cao-Lormeau, et al. 2016). Furthermore, increasing evidence on the potential of ZIKV transmissions through contaminated blood products for transfusion shines an entirely different light over infection routes, broadening transmission sources beyond the mosquito bite (Motta, et al. 2016), (Musso, et al. 2014).

These cases reinforce the importance of accurate ZIKV identification in a broad scope, ranging from newborn screening to the control of hemoderivatives. Additionally, since ZIKV can easily be clinically mistaken by other infections of similar symptomatic profile (To, et al. 2015), bioanalytical approaches that accurately differentiate these conditions are vitally important.

Current laboratory diagnostic tests are still limited in accuracy, either because of cross-reactivity, as in the case of serological tests (Fauci and Morens 2016), (Morizono 2014), (Steinhagen, et al. 2016), or because of the current lack of standardization/validation and sensitivity/specificity data, as is the case of reverse-transcriptase polymerase chain reaction (RT-PCR) (Eltzov, et al. 2010). Furthermore, current analysis techniques demand a substantial amount of time to produce results (Pardee, et al. 2016), and costs associated with kits, reagents and specialized personnel per sample run are considerably high (Rouet, et al. 2005), especially considering that endemic areas are located in regions of low-income and/or poor healthcare support (Fauci and Morens 2016). Thus, there is great interest in providing an expeditious approach that can produce accurate results in a timely fashion and with a cost-effective workflow.

Mass spectrometry-based metabolomics has been widely utilized as a relevant alternative for diagnostic purposes in biological samples (Deng, et al. 2017), (Kind, et al. 2016), (Takayama, et al. 2016), and data processing tools and spectral databases are key players in the success of these approaches (Gromski, et al. 2015), (Vinaixa, et al. 2016), since the mass spectra of a given set of complex matrices reveals a multitude of chemical entities/molecules. This richness of information is the starting point for many comparative studies, for example, in the analysis of biological samples from individuals with a pathophysiological condition versus a control group with healthy individuals (Melo, et al. 2017). By using data processing tools to drive this comparison, it is possible to establish which is the specific spectral signature for that particular condition based on their intrinsic differences, even if very subtle (Eiras, et al. 2014). Such differences allow us to infer that spectral data of that particular sample group will behave, therefore, as a “fingerprint”, where feature by feature will compose a unique model of pattern recognition (Lima, et al. 2015).

Given the large amount of spectral data generated, and the requirement of always providing a comparison to obtain spectral signatures of the condition under study, bioinformatics approaches have been built to solve these problems, so that the classification/taxonomy of sample groups may be achieved (Johnson, et al. 2015). In turn, Machine Learning (ML) approaches have allowed the comparison between spectral data of a large number of samples and sample groups (N), as opposed to a limited amount of data as in the case of multivariate data analysis (Zheng, Yoon and Lam 2014). Since ML models can be continuously fed with more information, it allows the user to focus only on the chemical species that provide actual discrimination between samples/sample groups (Acharjee, et al. 2016), (Smith, et al. 2014).

The main objective of using Machine Learning in the method presented in this paper is to generate a classifier based on mass spectral input data from blood serum to predict, with high accuracy and precision, whether a patient is positive or negative for a disease, in this case, for the ZIKV infection. The mass spectral data

of each sample (*m/z* value × intensity) is used as the input for all analyses and predictions performed herein.

For this purpose, we selected the Random Forest supervised machine learning algorithm (Breiman, Random Forests 2001), which is nd used in many applications, e.g. image analysis (Shotton, et al. 2013), cancer diagnosis (Suna, et al. 2017), and genetic assignment (Sylvester, et al. 2017). Random Forest is based on decision trees (Criminisi, Shotton and Konukoglu 2012), (Caruana and Niculescu-Mizil 2006) and a probabilistic interpretation of its principles can be found in (Murphy 2012). This machine learning algorithm has the following advantages when processing the data we have at hand:

High-classification performance: Random forest is one of the best classifiers for different problems (Fernández-Delgado, et al. 2014).

No need of kernel and complex parametrization adjustments: Random forest is known as a non-parametrized method, which means it does not require a complex search of parameters, kernel transformation, neither is it sensitive to normalization of input data. Only two parameters are subject to adjust for performance tuning: number of feature randomly selected in each tree building cycle, which is commonly set to the root square of the number of input variables, and the number of trees in the forest, which is usually subject to simple grid search approach.

Execution performance: A trained random forest classifier is a set of binary trees, which can be seen as a sequence of “if then else” statements being extremely fast at prediction time.

Feature importance: Decision tree classifiers provide information about the relevance of each feature in the decision trees by evaluating how a change or omission of one feature impacts classification results. This is referred to as out of bag (OOB) evaluation concept used as a performance measurement in (Breiman, Out-of-bag estimation 1996) and further applied to Random Forest feature importance determination by the mean decrease of accuracy of OOB samples with features randomly permuted (Breiman, Random Forests 2001), (Altmann, et al. 2010), (Louppe, et al. 2013). Importance assessment is a key property of the

classification algorithm to provide explainability and accountability of results achieved by the classifier.

In this work, we rely upon feature importance analysis to rank and to isolate the most discriminant features generating a high-performance classifier, which identifies the presence (or not) of signatures of ZIKV in the patient's mass spectral sample. Those ranked most discriminant features can also be used to single out some physical molecules, which are part of the signature and can be found with high presence in the serum positive patient's blood in contrast with negative ones. This fact corroborates with physical evidence the power of the method, which is in line with a new frontier in machine learning techniques called accountable or interpretable machine learning (Diakopoulos, et al. 2017).

In summary, we propose an innovative methodology based on high-resolution mass spectrometry (HRMS), combined with the Random Forest algorithm (Breiman, Random Forests 2001), to provide an accurate prediction model for discriminating serum samples of individuals with ZIKV. Since supervised methods such as Random Forest induce classifiers (i.e. a set of features that provide a "fingerprint" for the viral infection), this model is intended to be employed as a fast and accurate test for ZIKV infection in healthcare institutions. With specificity and sensitivity over 95%, in addition to the relatively low cost per sample run, this novel platform shows potential for forming a large integrated database for further epidemiological studies in infections by ZIKV.

Methods

Ethics Statement

This study was conducted according to the principles expressed in the Declaration of Helsinki and was approved by the Research Ethics Committee of the University of Campinas, under the number 053407/2016. A written informed consent was obtained from all patients prior to enrollment. All samples were obtained from the Clinical Hospital of the University of Campinas.

Research Participants and Specimen Collection

In total, 203 patients were included in this study, regardless of age and gender, in two main groups: ZIKV and control. Group division considered patients' retrospective laboratory results, obtained after testing with RT-PCR (**Table 2**).

The *ZIKV group* consists of 82 patients split into: (a) 43 adults with acute ZIKV infection (i.e. within the high-viremia period) confirmed by positive RT-PCR test, in association with clinical presentation (symptoms) compatible with ZIKV infection (i.e. fever, joint pain, conjunctivitis and rash); and (b) 39 patients after 30 days of confirmed ZIKV infection by positive RT-PCR test (i.e. after the acute phase).

The *control group* contains the remaining 121 patients in which a) 64 presented the same clinical symptoms as described above for ZIKV infection, but with a negative result for real-time RT-PCR test for ZIKV, b) 46 patients with Dengue virus infection confirmed by positive immunosorbent (ELISA) test, and c) 11 healthy adults, i.e. asymptomatic individuals who did not present any signs of infection within 30 days prior to sample collection which, therefore, also presented a negative result in RT-PCR for ZIKV.

All RT-PCR were performed using RNA extracted from the serum of the analyzed patients.

Serum of patients was obtained from 10 mL of peripheral blood collected in dry tube after peripheral venipuncture. All samples were transported on ice within less than six hours to the Laboratory for Study of Emerging Viruses at the Biology Institute of the University of Campinas, where they were processed and tested for ZIKV on real-time RT-PCR. Aliquots of serum were kept at -80°C until HRMS analysis.

ZIKV Detection by Real-time RT-PCR

RNA samples were extracted from 140 µL of serum and urine using the QIAamp Viral RNA Mini Kit (Qiagen, Hilden, Germany) following manufacturer's instructions. Samples were tested by One-step TaqMan real-time RT-PCR (Taqman RNA to-CT, Applied Biosystems) for the presence of ZIKV genomes.

ZIKV detection was performed with primers and probes adapted from the original described by (Lanciotti, et al. 2008) (*ZIKV-F: 5'- CCGCTGCCCAACACAAG-3'; ZIKV-R: 5'- CCACTAACGTTCTTTTGCAGACAT -3'; ZIKV-P: 5' FAM - AGCCTACCTTGACAAGCAGTCAGACACTCAA - BHQ1-3'*). Briefly, all reactions were performed in a final volume of 12.5 µL with 50 ng of RNA, 10 mM forward and reverse primers, 5 mM probe, and 6.25 µL of TaqMan master mix (Applied Biosystems, Foster City, CA, USA), using the following cycling algorithm: 48°C for 30 min, 95°C for 10min, followed by 45 cycles of 95°C for 15 s and 60°C for 1 min. All real-time RT-PCR were performed in duplicate.

HRMS Preparation and Analysis

10 µL of serum samples were diluted to a final volume of 1 mL in a methanol/water solution (1:1) (solution 1). After homogenization, the sample was further submitted to a second dilution of 10µL into a 0.1% solution of formic acid in methanol/water (1:1), to a final volume of 1 mL. All samples from each research participant were prepared in duplicates.

Samples submitted to HRMS were directly infused into an ESI-LTQ-XL Orbitrap Discovery instrument (Thermo Scientific, Bremen, Germany). Metabolic fingerprint data were acquired using a sample flow of 10µL/min, capillary temperature of 280°C, 5kV of source voltage and sheath gas at 10 arbitrary units. In addition to the biological duplicates, analytical triplicates were performed for each sample. The acquisition was performed in the mass-to-charge ratio (*m/z*) range of 700-1700, in the positive ion mode.

Machine Learning Method

The decision-making method we propose here for ZIKV detection has the following macro steps:

Data preparation: For our study herein, data samples of positive (with ZIKV) and negative's patients (without ZIKV condition) are normalized and randomly divided into main partitions (80% and 20% of the patients). The partition with 20% of the data (referred to as $\boldsymbol{P_{test}}$ is left untouched for the final blind test to evaluate

the designed diagnosis classifier. This is done to avoid any kind of overfitting to the available data. The remaining partition with 80% of the data (referred to as $\boldsymbol{P_{train}}$) is then used for training and validation tests in the process of determining most discriminant features for ZIKV detection. For reference, during training, a classifier is induced while during validation its performance on the validation set is checked. This process is iterative as we shall detail next. We further divide $\boldsymbol{P_{train}}$ into two subsets $\boldsymbol{P_{fit}}$, with 80% of the data in $\boldsymbol{P_{train}}$, and $\boldsymbol{P_{val}}$, with the remaining data in $\boldsymbol{P_{train}}$. $\boldsymbol{P_{fit}}$ is then used in the induction of the classifier (learning stage) and $\boldsymbol{P_{val}}$ in its evaluation. To account for possible variations in the splitting of fitting and validation sets, we repeat this process 10 times (here referred to as rounds) and report average performance numbers for the validation set with the corresponding standard deviation (stdv). A small stdv means there is no high variation across patients in the learning process of the algorithm.

Most discriminant features identification and ranking: Fitting and validation cycles of Random Forest classifier are iteratively executed, reducing the vector length representing each patient on each cycle by discarding the least significant ranked features. The feature importance measure is obtained in each cycle using the Out-of-Bag (OOB) calculation for the training samples over the trained trees. By sorting features in decreasing order of importance, we generate the feature ranking, which is updated on each step for the remaining ones after discarding part of the features located in ranking tail. The best performance achieved in this step determines the spectral signature features kept for further processing.

Generate the diagnosis classifier: Upon selecting the most discriminative features, we proceed to train the final classifier by using only such selected features. This allows us to now induce a simplified, yet powerful, classifier with only a subset of the original features (in our case a few dozen rather than thousands of initial features per patient). To train the final classifier, data from all patients in $\boldsymbol{P_{train}}$ is considered. Finally, the resulting classifier is tested with the blind-test data $\boldsymbol{P_{test}}$ and the final performance numbers are reported.

Values distribution analysis of the spectral signature features: Although the previous step resulted in a final classifier trained with the most important features to detect ZIKV, we take a step further to determine which of the selected best features have higher prevalence in the serum of positive patients. For that, we analyze the range of values of spectral signature features in positive and negative data samples. We refer to such features as *marker* (outstanding for the positive class) features. Probability distribution functions for the positive and negative values are compared using equality hypothesis test and higher-values cumulative probability comparison.

Marker features mapping into molecules: The *m/z* values for the marker features are then mapped onto physical molecules using the mass spectral techniques to corroborate evidences on the spectral mass signature used by the diagnosis classifier.

Data Preparation

In the data preparation step, we normalize the input *m/z* × intensity vectors of the samples using the relative intensity of each vector (we divided all vector elements by their maximum value), as defined in equation below. The normalization is needed to work with a more well-defined range of values for the features and is standard procedure in Machine Learning.

$$\boldsymbol{F} = [\boldsymbol{f}_{i,j}], \qquad \boldsymbol{f}_{i,j} = \frac{\boldsymbol{z}_{i,j}}{\mathbf{max}(\boldsymbol{z}_{i,j=1:k})}$$

$$\boldsymbol{L} = [\boldsymbol{l}_i], \quad \boldsymbol{l}_i = \{-\mathbf{1}, +\mathbf{1}\}, \qquad (\boldsymbol{vector\ label})$$

$$\boldsymbol{M} = [\boldsymbol{m}_j], \qquad \boldsymbol{m}_j = \boldsymbol{m/z\ value}\ (\boldsymbol{feature\ label})$$

where $\boldsymbol{F}$ comprises the measurements for all patients. Each row $\boldsymbol{f} \in \boldsymbol{F}$ represents data measurements from one patient. As each patient has five different sets of measurements (replicates) to account for possible variations $\boldsymbol{F}$ has 1,015 feature

vectors. Each feature vector of a patient, , comprises some 10,000 *m/z* values, many of which are missing upon different measurements.

As previously mentioned, *F* is divided into $\boldsymbol{P_{train}}$ and $\boldsymbol{P_{test}}$ and this latter set is left untouched for the final test of the developed classifier. It is important to mention that all splitting procedures are done so that all replicates of a patient are put in the same partition --- therefore the splitting is always performed per patient and not per feature vector.

Number of Trees Determination using Grid Search Approach

For experiments described in this article, we used the default of square root of number of total number of input features for the randomly selected features in each tree construction cycle, and the number of trees was defined by maximum between 40 and the square root of the total number of input variables. It is important to notice that during the reduction process, using this formula, the number of trees varies in each step according the vector length.

To select the number of trees used in the experiments, we performed a grid search varying the length of the ranked feature vectors, ranking them during the grid-search process, and the number of trees for each vector length from 1024 to 16. By dividing by two in each step, it generates a logarithmic grid, which could be plotted in the form of a contour surface, which colors regions delimited by isometric lines built from the grid z axis values (we use accuracy and also f1score), generating the chart shown in Figure 1. By analyzing the regions of best achieved accuracy for validation, we selected three functions to determine the number of trees. The first was to use the initially determined default described above nt = max(40, sqrt(len)), second a constant value crossing the regions of good accuracy nt = 230, and the third one as function that crosses the chart diagonally.

Comparing the validation results of the most discriminant features process using each of the options above, as Table 2 shows, we opted to use the number of trees as nt=max(40, sqrt(len)), because all three final results are statically comparable, and although the equation number 3 provides the smallest standard

deviation, the first choice runs much faster than the others, providing also the smallest number of signature features.

Ranking Most Discriminant Features

The objective of this step is to discover which features carry most information for the separation of positive and control (negative) patients. This is carried out through a ranking approach in which less relevant features are eliminated iteratively. By repeating the fitting and validation process of the random forest with fewer features in each step, the rank for the top features is refined, and the impact on the overall classification metrics is measured in the validation set.

In each iteration, the rank of remaining ranked features is updated using the descending order of the mean of the 10 feature importance vectors stored in each training round. Only the portion of the rank corresponding to the ranked length processed in the iteration is updated, the tail remains with the upper discarded rank. We evaluate the feature importance for each classifier through the out-of-bag calculation, which estimates the impact of a missing feature in the classification trees. To reduce the number of considered features in each step, we multiply the dimensionality (number of features) of feature vector $\boldsymbol{f}$ by a factor $0 < \gamma < 1$, retaining only the $\lfloor |\boldsymbol{f}| \times \boldsymbol{\gamma} \rfloor$ most important features to the next step, where $|\cdot|$ measures the number of features in vector $\boldsymbol{f}$. This process is repeated until convergence --- either by achieving a minimum set performance or when there is no feature to discard anymore. We determine the most discriminant features by the maximization of the classification performance metrics, e.g. using F1 score as the measure to maximize, and we call them spectral signature features. We shall define such measures later in this paper.

Generate Diagnosis Classifier

At this stage, we train the final diagnosis classifier using the most important features found in the previous step and all training data available in $\boldsymbol{P_{train}}$. Afterwards, we test the classifier using blind-test $\boldsymbol{P_{test}}$ and report final results for ZIKV detection.

Distribution Analysis to find Marker Features

In addition to generating a ZIKV classifier --- which can identify patients with the disease --- we set forth the objective of determining which metabolites appear with higher intensity on the positive patients than in the control group.

By relying on the ranges of values of each selected feature using our random forest classifier, we can identify dependencies between features which results in a good separation for the two classes of interest. As we are looking for features with the highest values, we are interested only in the ones which can be analyzed in isolation without further dependencies on other features. For that, values distribution analysis is performed comparing the features probability distribution functions, seeking the ones with higher values in the positive samples than in the set of negative ones. We refer to such features as *marker features* for the disease, or simply marker features. First, we apply an equality test to determine whether each feature has distinguishable distributions; if they are equal, we cannot test for the higher value condition. For this purpose, we use the Two-sample Kolmogorov-Smirnov (KS) test (Jr. 1951) (Miller 1956) over the two discrete probability functions $\boldsymbol{p}(\boldsymbol{y}), \boldsymbol{q}(\bar{\boldsymbol{y}})$ respectively, for *y* values of a feature in the spectral signature on positive patient's samples and $\bar{\boldsymbol{y}}$ values for same feature in the control group. After the equality hypothesis of KS test could not be confirmed, we apply the rule expressed in Equation $\boldsymbol{\Delta_j}$ to identify marker features. It means that for a marker feature, the probability to find a value over the median of that feature in the set of positive patients is $\boldsymbol{\beta}$ higher than finding the same order of values in the set of negative patients. For instance, by setting $\boldsymbol{\beta}$ to 40% means that over the median of positive samples, we will find only 10% of negative samples.

$$\boldsymbol{M_j \ni M \text{ is a positive feature to disease, } if}:$$

$$\boldsymbol{\Delta_j} = \int_{\boldsymbol{median}(\boldsymbol{y_j})}^{\max(\boldsymbol{F_j})} \boldsymbol{q}(\bar{\boldsymbol{y}}_{\boldsymbol{j}}) - \boldsymbol{p}(\boldsymbol{y_j}) > \beta$$

where

y_j is a F_j value for a positive patient;

$\bar{y_j}$ is a F_j value for a negative patient;

$p(y_j)$ is the probability distribution function of positive patients, and $q(\bar{y_j})$ the probability distribution function of negative patients;

$P(y_j)$ is the cumulative distribution function (CDF) of y values, and $Q(\bar{y_j})$ is the CDF of $\bar{y_j}$;

$0 < \beta < 0.5$ CDF difference over median of the feature j for the positive patients (e.g. $\beta = 40\%$).

Results and Discussion

The iteration of reducing feature vector length and ranking most discriminant features is summarized in Figure 2A, starting with 10,000 features and shrinking by a factor of 0.9, we finally identified 42 features, listed in Figure3A as the spectral features signature.

This is a remarkable result, as it allowed us not only to reduce the initial noisy 10,000 m/z measurements per patient to just 42 most discriminant for ZIKV virus, but also because it was the first time that the acute phase of ZIKV was accurately evaluated with patients 30 days after infection (i.e. non-acute phase). Thus, in order to visualize such features, we further projected them onto a 2D space through the t-distributed stochastic neighbor embedding (t-SNE) (Maaten and Hinton 2008) visualization technique for high dimension data resulting in the chart shown on **Figure 2B**. Although just using 2 dimensions out of the 42 selected as important for classification, we can see a very good separation between ZIKV and control group samples. We also split the positive group into the two categories of ZIKV infected patients, the acute phase samples and the 1 month after infection samples. As we can see, most of the acute phase are grouped into a consistent cluster on the left side of the chart while the 1-month infected cases are spread into 3 other consistent clusters. The relation between the positive and negative samples in each region can also be addressed by the reduced vector analysis pointing out which sample belongs to each group and which ions they have in common. Ultimately, we envision the TSNE chart analysis being useful to identify which ions are present in each cluster giving a physical clue about what those clusters have in

common further advancing the study toward more accountable models. This can be pursued in a future work.

Table 3 presents the average results for the validation set over the 10 rounds of training and validation along with the correspondent standard deviation, and the final numbers for the blind test. As expected, the blind test results are within the predicted range determined on the validation tests, and confirm the remarkable results achieved by the proposed technique.

The chart on **Figure 3A** shows the logarithmic standard deviation range for all 42 selected spectral signature features, identifying 12 markers for ZIKV, which are highlighted in green. The distribution analysis for the 42 spectral signature features was performed over all feature vectors as defined by Equation $\boldsymbol{\Delta_j}$, using $\boldsymbol{\beta = 40\%}$. For illustration, **Figure 3B** brings the distribution histogram of the first ranked feature (*m/z*=1295.6) and the rationale of Δ_j calculation.

This group of 12 markers can be grouped by their *m/z* proximity, composing four groups of correlated cations: (1295.6, 1296.6, 1297.6), (727.3, 728.3), (1307.9, 1308.9, 1309.9), (977.4, 977.9), and 2 other individual cations: 1544.2 and 717.2. This grouping occurs due to the chemical interpretation of the results; while these values are treated as independent variables among themselves, chemically, these features show an important correlation. For instance, in the group of values 1295.6, 1296.6, and 1297.6, the biomarker is actually only 1295.6, as the other two masses correspond to the natural isotopic distribution of carbon (i.e. ^{13}C and ^{14}C in the molecule). The same is true with all other groups, where the most relevant ion is that with the lowest nominal mass. It is noteworthy that this also occurs with divalent cations, as in the case of the group composed by 977.4 and 977.9, where the 1 Da difference is divided by 2 (*m/z*, where z = 2). This is an extremely important characteristic of mass spectra that provides even more reliability to the results, as this proves that the employed model effectively provided features/molecules that are discriminant of that particular group; since in the dataset these variables are completely independent, our results bring an outcome that is coherent chemically. Thus, the group of 12 marker features correspond to 6 actual molecules, i.e. biomarker candidates.

After metabolomics database search, all six features were elucidated and identified as a pentapeptide (717.2) and a tetrapeptide (727.3, 728.3), a divalent (977.4, 977.9) and a monovalent ganglioside (1295.6, 1296.6, 1297.6), a cardiolipin (1307.9, 1308.9, 1309.9), and a bisphosphoglycerol (1544.2500), which are the physical evidence of the positive ZIKV samples.

Computing Performance Metrics

All experiments were performed using a Samsung 500R5H-XD3BR, Intel Core i7-5500CPU @ 2.40GHz, 2 Cores, 4 Logical processors, 8 GB of physical memory, 1 TB HD 5400RPM SATA-III 6GB/s. Programs were written in MATLAB script language and ran on MATLAB R2017a 64-bit version 9.2.0.538062. All machine learning algorithms and analyses in the end-to-end process from data preparation to distribution analysis take about 15 seconds per patient in the training (considering the five different measurements per patient). The time to analyze a feature vector of a patient at testing time is less than a second.

Comparing Random Forest Classifier with Other Classifiers

Table 4 shows Random Forest compared with the well-known classification algorithm SVM using two different optimization algorithms: SMO (Sequential Minimal Optimization) and ISDA (Iterative Single Data Algorithm), and with a decision tree classifier, also with two different split criteria: GDI (Gini's diversity index) and DEVIANCE (maximum deviance reduction, also known as cross entropy). The 10-round training and validation tests were executed over the 1000 features full spectra vectors and also for the 42 signature features selected by the feature importance supervised reduction method. In short, RF performs best not only in the original complete feature space but also on the selected best features thus justifying its use.

Conclusion

The developed screening strategy using HRMS to assess ZIKV infection detects a set of 42 features, which are a spectral signature identified by a random forest classifier. 12 out of 42 features have high presence in the blood of patients due to ZIKV infection. This set of markers was validated using a powerful combination of statistical tools and are further supported by result comparison with those obtained with the current method for ZIKV diagnosis, RT-PCR. We hereby demonstrated that the combination between HRMS and the Random Forest algorithm is a robust platform that can be implemented in large-scale routine laboratories for rapid and straightforward detection of ZIKV, whether in patient screening or, as more recently recommended by the FDA, in donated blood and derivatives for transfusion. This approach is a work in progress, which will be the basis for the creation of a large database on molecules produced during ZIKV infection. This may lead to revealing new information on epidemiology, immunity, and pathogenesis of the ZIKV infection.

Due to the nature of the method and outstanding results achieved with ZIKV experiments, it is possible to envision that this method is a breakthrough technique in disease diagnosis tests.

Using our proposed platform, we envision that classifiers for many diseases can be developed. The only condition is that the serum of patients with the disease must contain information detected by the mass spectrometer; then, machine learning algorithms take care of extracting discriminative fingerprint for the condition of interest. Our aim is that, with one set of biofluids from any given patient with an unknown disease, we can submit such samples to multiple classifiers simultaneously, with a fast and reliable response to potential diagnostics.

References

Acharjee, Animesh, Zsuzsanna Ament, James A. West, Elizabeth Stanley, and Julian L. Griffin. 2016. "Integration of metabolomics, lipidomics and clinical data using a machine learning method." *BMC Bioinformatics* 17: 440. doi:10.1186/s12859-016-1292-2.

Altmann, André, Laura Tolosi, Oliver Sander, and Thomas Lengauer. 2010. "Permutation importance: a corrected feature importance measure." *Bioinformatics* 26: 1340-1347. doi:10.1093/bioinformatics/btq134.

Attar, Naomi. 2016. "ZIKA virus circulates in new regions." *Nature Reviews Microbiology* (Nature Publishing Group, a division of Macmillan Publishers Limited. All Rights Reserved. SN -) 14: 62. doi:10.1038/nrmicro.2015.28.

Breiman, Leo. 1996. "Out-of-bag estimation." Tech. rep., Statistics Department, University of California. https://www.stat.berkeley.edu/ breiman/OOBestimation.pdf.

Breiman, Leo. 2001. "Random Forests." *Machine Learning* 45: 5-32. doi:10.1023/A:1010933404324.

Cao-Lormeau, Van-Mai, Alexandre Blake, Sandrine Mons, Stéphane Lasère, Claudine Roche, Jessica Vanhomwegen, Timothée Dub, et al. 2016. "Guillain-Barré; Syndrome outbreak associated with Zika virus infection in French Polynesia: a case-control study." *The Lancet* (Elsevier) 387: 1531-1539. doi:10.1016/S0140-6736(16)00562-6.

Caruana, Rich, and Alexandru Niculescu-Mizil. 2006. "An Empirical Comparison of Supervised Learning Algorithms." *Proceedings of the 23rd International Conference on Machine Learning.* New York, NY, USA: ACM. 161-168. doi:10.1145/1143844.1143865.

Criminisi, Antonio, Jamie Shotton, and Ender Konukoglu. 2012. "Decision Forests: A Unified Framework for Classification, Regression, Density Estimation, Manifold Learning and Semi-Supervised Learning." *Foundations and Trends in Computer Graphics and Vision* 7: 81-227. doi:10.1561/0600000035.

Deng, Lu, David Chang, Rae R. Foshaug, Roman Eisner, Victor K. Tso, David S. Wishart, and Richard N. Fedorak. 2017. "Development and Validation of a High-Throughput Mass Spectrometry Based Urine Metabolomic Test for the Detection of Colonic Adenomatous Polyps." *Metabolites* 7. doi:10.3390/metabo7030032.

Diakopoulos, Nicholas, Sorelle Friedler, Marcelo Arenas, Solon Barocas, Michael Hay, Bill Howe, H. V. Jagadish, et al. 2017. "Principles for Accountable Algorithms and a Social Impact Statement for Algorithms." Tech. rep., FAT/ML Organization. http://www.fatml.org/resources/principles-for-accountable-algorithms.

Eiras, M. M., D. N. Oliveira, M. S. Ferreira, M. Benassi, S. O. S. Cazenavec, and R. R. Catharino. 2014. "Fast fingerprinting of cannabinoid markers by laser desorption ionization using silica plate extraction." *Analytical Methods* 6 (5): 1350-1352. doi:10.1039/C3AY41632A.

Eltzov, Evgeni, Danit Atias, Levy Gheber, and Robert S. Marks. 2010. "Dengue Virus Diagnostics." Chap. 12 in *Detection of Bacteria, Viruses, Parasites and Fungi*, 275-296. Springer. https://books.google.com.br/books?id=YqC5BQAAQBAJ.

Enfissi, Antoine, John Codrington, Jimmy Roosblad, Mirdad Kazanji, and Dominique Rousset. 2016. "Zika virus genome from the Americas." *The Lancet* (Elsevier) 387 (10015): 227-228. doi:10.1016/S0140-6736(16)00003-9.

Fauci, Anthony S., and David M. Morens. 2016. "Zika Virus in the Americas — Yet Another Arbovirus Threat." *New England Journal of Medicine* 374: 601-604. doi:10.1056/NEJMp1600297.

Fernández-Delgado, Manuel, Eva Cernadas, Senén Barro, and Dinani Amorim. 2014. "Do We Need Hundreds of Classifiers to Solve Real World Classification Problems?" *Journal of Machine Learning Research* 15: 3133-3181.

Gromski, Piotr S., Howbeer Muhamadali, David I. Ellis, Yun Xu, Elon Correa, Michael L. Turner, and Royston Goodacre. 2015. "A tutorial review: Metabolomics and partial least squares-discriminant analysis – a marriage of convenience or a shotgun wedding." *Analytica Chimica Acta* 879: 10-23. doi:10.1016/j.aca.2015.02.012.

Johnson, Caroline H., Julijana Ivanisevic, H. Paul Benton, and Gary Siuzdak. 2015. "Bioinformatics: The Next Frontier of Metabolomics." *Analytical Chemistry* (American Chemical Society) 87: 147-156. doi:10.1021/ac5040693.

Jr., Frank J. Massey. 1951. "The Kolmogorov-Smirnov Test for Goodness of Fit." *Journal of The American Statistical Association* 46 (253): 68-78. doi:10.1080/01621459.1951.10500769.

Kind, Tobias, Eunho Cho, Taeeun D. Park, Nan Deng, Zhenqiu Liu, Tack Lee, Oliver Fiehn, and Jayoung Kim. 2016. "Interstitial Cystitis-Associated Urinary Metabolites Identified by Mass-Spectrometry Based Metabolomics Analysis." *Scientific Reports* 6: 39227. doi:10.1038/srep39227.

Lanciotti, Robert S., Olga L. Kosoy, Janeen J. Laven, Jason O. Velez, Amy J. Lambert, Alison J. Johnson, Stephanie M. Stanfield, and Mark R. Duffy. 2008. "Genetic and Serologic Properties of Zika Virus Associated with an Epidemic, Yap State, Micronesia, 2007." *Emerging Infectious Diseases* 14: 1232. doi:10.3201/eid1408.080287.

Lima, Estela de Oliveira, Cristiana Santos Macedo, Cibele Zanardi Esteves, Diogo Noin Oliveira, Maria Cristina Vidal Pessolani, José Augusto da Costa Nery, Euzenir Nunes Sarno, and Rodrigo Ramos Catharino. 2015. "Skin Imprinting in Silica Plates: A Potential Diagnostic Methodology for Leprosy Using High-Resolution Mass Spectrometry." *Analytical Chemistry* 87: 3585-3592. doi:10.1021/acs.analchem.5b00097.

Louppe, Gilles, Louis Wehenkel, Antonio Sutera, and Pierre Geurts. 2013. "Understanding variable importances in forests of randomized trees." In *Advances in Neural Information Processing Systems 26*, edited by C. J. C. Burges, L. Bottou,

M. Welling, Z. Ghahramani and K. Q. Weinberger, 431-439. Curran Associates, Inc. https://tinyurl.com/ycrpfng9.

Maaten, Laurens, and Geoffrey Hinton. 2008. "Visualizing data using t-SNE." *Journal of Machine Learning Research* 9: 2579-2605. http://www.jmlr.org/papers/volume9/vandermaaten08a/vandermaaten08a.pdf.

Melo, Carlos Fernando O. R., Jeany Delafiori, Diogo N. Oliveira, Tatiane M. Guerreiro, Cibele Z. Esteves, Estela de O. Lima, Victoria Pando-Robles, et al. 2017. "Serum Metabolic Alterations upon Zika Infection." *Frontiers in Microbiology* 8: 1954. doi:10.3389/fmicb.2017.01954.

Miller, Leslie H. 1956. "Table of Percentage Points of Kolmogorov Statistics." *Journal of the American Statistical Association* 51: 111-121. doi:10.1080/01621459.1956.10501314.

Morizono, Kouki and Chen, Irvin S. Y. 2014. "Role of Phosphatidylserine Receptors in Enveloped Virus Infection." *Journal of Virology* 88 (8): 4275-4290. doi:10.1128/JVI.03287-13.

Motta, Iara J. F., Bryan R. Spencer, Suely G. Cordeiro da Silva, Monica B. Arruda, Jane A. Dobbin, Yung B. M. Gonzaga, Ingrid P. Arcuri, et al. 2016. "Evidence for Transmission of Zika Virus by Platelet Transfusion." *New England Journal of Medicine* 375: 1101-1103. doi:10.1056/NEJMc1607262.

Murphy, Kevin P. 2012. "Adaptive basis function models." Chap. 16 in *Machine Learning: A Probabilistic Perspective*, 543-587. The MIT Press. https://books.google.com.br/books?id=NZP6AQAAQBAJ.

Musso, D., T. Nhan, E. Robin, C. Roche, D. Bierlaire, K. Zisou, A. Shan Yan, M. Cao-Lormeau V, and J. Broult. 2014. "Potential for Zika virus transmission through blood transfusion demonstrated during an outbreak in French Polynesia, November 2013 to February 2014." *Eurosurveillance* 19 (14). doi:10.2807/1560-7917.ES2014.19.14.20761.

Narayanan, A., E. Shi, and B. I. P. Rubinstein. 2011. "Link prediction by de-anonymization: How We Won the Kaggle Social Network Challenge." *The 2011 International Joint Conference on Neural Networks.* 1825-1834. doi:10.1109/IJCNN.2011.6033446.

Pardee, Keith, Alexander A. Green, Melissa K. Takahashi, Dana Braff, Guillaume Lambert, Jeong Wook Lee, Tom Ferrante, et al. 2016. "Rapid, Low-Cost Detection of Zika Virus Using Programmable Biomolecular Components." *Cell* (Elsevier) 165: 1255-1266. doi:10.1016/j.cell.2016.04.059.

Rouet, Francois, Didier K. Ekouevi, Marie-Laure Chaix, Marianne Burgard, Andre Inwoley, Thomas D'Aquin Tony, Christine Danel, et al. 2005. "Transfer and Evaluation of an Automated, Low-Cost Real-Time Reverse Transcription-PCR Test

for Diagnosis and Monitoring of Human Immunodeficiency Virus Type 1 Infection in a West African Resource-Limited Setting." *Journal of Clinical Microbiology* 43: 2709-2717. doi:10.1128/JCM.43.6.2709-2717.2005.

Schuler-Faccini, Lavinia, Erlane M. Ribeiro, Ian M. L. Feitosa, Dafne D. G. Horovitz, Denise P. Cavalcanti, André Pessoa, Maria Juliana R. Doriqui, et al. 2016. "Possible Association Between Zika Virus Infection and Microcephaly — Brazil, 2015." *MMWR Morbidity and Mortality Weekly Report* 65(3): 59–62. doi:10.15585/mmwr.mm6503e2.

Shotton, Jamie, Toby Sharp, Alex Kipman, Andrew Fitzgibbon, Mark Finocchio, Andrew Blake, Mat Cook, and Richard Moore. 2013. "Real-time Human Pose Recognition in Parts from Single Depth Images." *Commun. ACM* (ACM) 56: 116-124. doi:10.1145/2398356.2398381.

Smith, Rob, Andrew D. Mathis, Dan Ventura, and John T. Prince. 2014. "Proteomics, lipidomics, metabolomics: a mass spectrometry tutorial from a computer scientist's point of view." *BMC Bioinformatics* 15: S9. doi:10.1186/1471-2105-15-S7-S9.

Steinhagen, Katja, Christian Probst, Jonas Radzimski, Petra Emmerich, Marjan Esbroeck, Janke Schinkel, Martin P. Grobusch, et al. 2016. "Serodiagnosis of Zika virus (ZIKV) infections by a novel NS1-based ELISA devoid of cross-reactivity with dengue virus antibodies: a multicohort study of assay performance, 2015 to 2016." *Eurosurveillance* 21. doi:https://doi.org/10.2807/1560-7917.ES.2016.21.50.30426.

Suna, Guanglu, Shaobo Lia, Yanzhen Caoa, and Fei Lang. 2017. "Cervical Cancer Diagnosis based on Random Forest." *International Journal of Performability Engineering* (Totem Publisher, Inc) 13: 446-457. doi:10.23940/ijpe.17.04.p12.446457.

Sylvester, Emma V. A., Paul Bentzen, Ian R. Bradbury, Marie Clément, Jon Pearce, John Horne, and Robert G. Beiko. 2017. "Applications of random forest feature selection for fine-scale genetic population assignment." *Evolutionary Applications* In press. doi:10.1111/eva.12524.

Takayama, Takahiro, Haruhito Tsutsui, Ippei Shimizu, Tatsuya Toyama, Nobuyasu Yoshimoto, Yumi Endo, Koichi Inoue, et al. 2016. "Diagnostic approach to breast cancer patients based on target metabolomics in saliva by liquid chromatography with tandem mass spectrometry." *Clinica Chimica Acta* 452: 18-26. doi:10.1016/j.cca.2015.10.032.

To, Kelvin K. W., Kim-Chung Lee, Samson S. Y. Wong, Ka-Ching Lo, Yin-Ming Lui, Akhee S. Jahan, Andrea L. Wu, et al. 2015. "Lipid mediators of inflammation as novel plasma biomarkers to identify patients with bacteremia." *Journal of Infection* (Elsevier) 70: 433-444. doi:10.1016/j.jinf.2015.02.011.

Vinaixa, Maria, Emma L. Schymanski, Steffen Neumann, Miriam Navarro, Reza M. Salek, and Oscar Yanes. 2016. "Mass spectral databases for LC/MS- and GC/MS-based metabolomics: State of the field and future prospects." *TrAC Trends in Analytical Chemistry* 78: 23-35. doi:10.1016/j.trac.2015.09.005.

Xia, Jianguo, Igor V. Sinelnikov, Beomsoo Han, and David S. Wishart. 2015. "MetaboAnalyst 3.0—making metabolomics more meaningful." *Nucleic Acids Research* 43: W251-W257. doi:10.1093/nar/gkv380.

Zheng, Bichen, Sang Won Yoon, and Sarah S. Lam. 2014. "Breast cancer diagnosis based on feature extraction using a hybrid of K-means and support vector machine algorithms." *Expert Systems with Applications* 41: 1476-1482. doi:10.1016/j.eswa.2013.08.044.

Conflict of Interest

The authors declare that the research was conducted in the absence of any commercial or financial relationships that could be construed as a potential conflict of interest.

Authors and contributions

CFORM, MZD, JD, ALLA and CTA performed mass spectrometry experiments. CFORM, LCN, SEFA and ARR conceived and executed the machine learning method. CFORM and LCN wrote the manuscript. DNO, TMG, CZE, EOL, MM, MR, RGMR and KNM performed data analysis. PLP, GPM, GMN, FTMC, CWA and JLPM processed serum samples and performed all molecular biology experiments. ARRF, RA, MRR. EA, RPJ, CCRV, HM and MLM performed patient recruitment, biofluids management, and clinical support. CFORM, LCN, DNO, SEFA, ARR and RRC performed manuscript proofreading and prepared tables and figures. RRC idealized all experiments and managed the research group. The Zika Unicamp Network is mentioned as an initiative from the University of Campinas of mutual collaboration in the Brazilian Plan for Fighting Zika Virus.

Funding

The authors would like to thank the São Paulo Research Foundation (FAPESP) for the fellowships of CFORM (16/17066-2) and CZE (14/00302-0), and the grants for

RRC (11/50400-0, 15/06809-1 and 17/20614-4). We also acknowledge CAPES for the scholarships for EOL (PNPD 1578388) and TMG (PROEX 1489740). DNO acknowledges the *Plano Nacional de Enfrentamento ao* Aedes aegypti *e Microcefalia* from the Brazilian Ministry of Health for the fellowship (88887.137889/2017-00). ARR thanks CNPq for his grant No. 304472/2015-8.

Acknowledgements

The authors acknowledge the Zika Unicamp Network for the support during the conceptual development of the initiative.

Figure captions

Figure 1. Number of trees given by grid search as function of vector length. Cross marks inside the chart denotes values evaluated during the grid search. Lines 1, 2 and 3 correspond to functions as expressed in Table 2 used to compute the number of trees on the evaluation of discriminant features reduction.

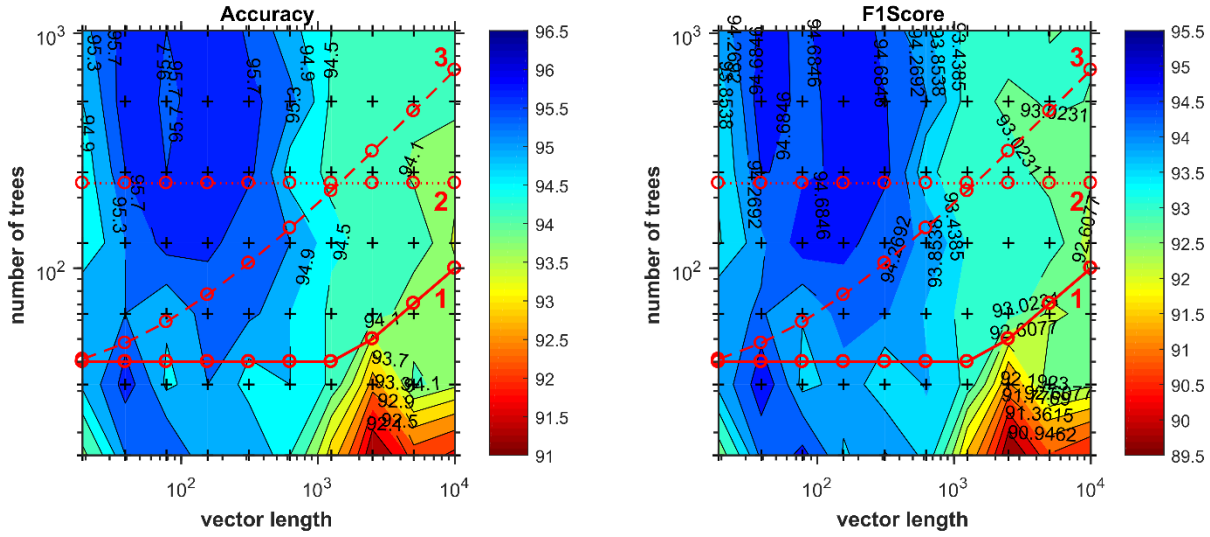

Figure 2. (A) Iterative process to determine the most discriminant ranked features. (B) Visualization of vectors with spectral signature features (length 42) using t-SNE technique. Vectors corresponding to positive ZIKV infected patients are separated into two categories: acute phase and 1 month after infection.

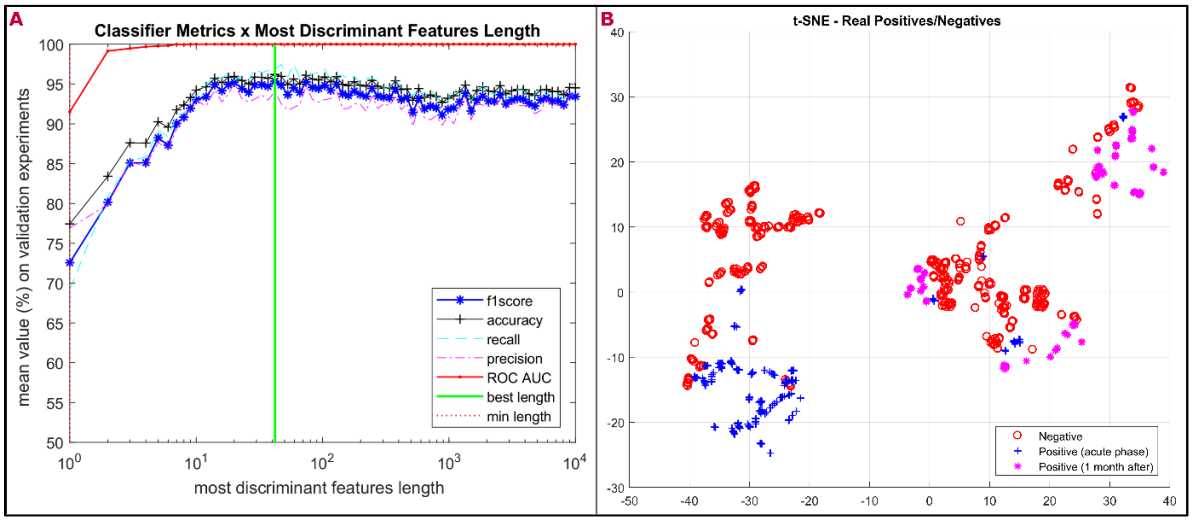

Figure 3. (A) Ranked features standard deviation range in log scale for ZIKV positive and control group (negative) vectors. The green highlight identifies the marker features for ZIKV, selected using the rationale of $\Delta_j > 40\%$. (B) Example of probability distribution and cumulative distribution charts for the main ranked feature for ZIKV, ion *m/z* 1295.6 (Ganglioside); the rationale for Δ_j calculation is given on the right chart.

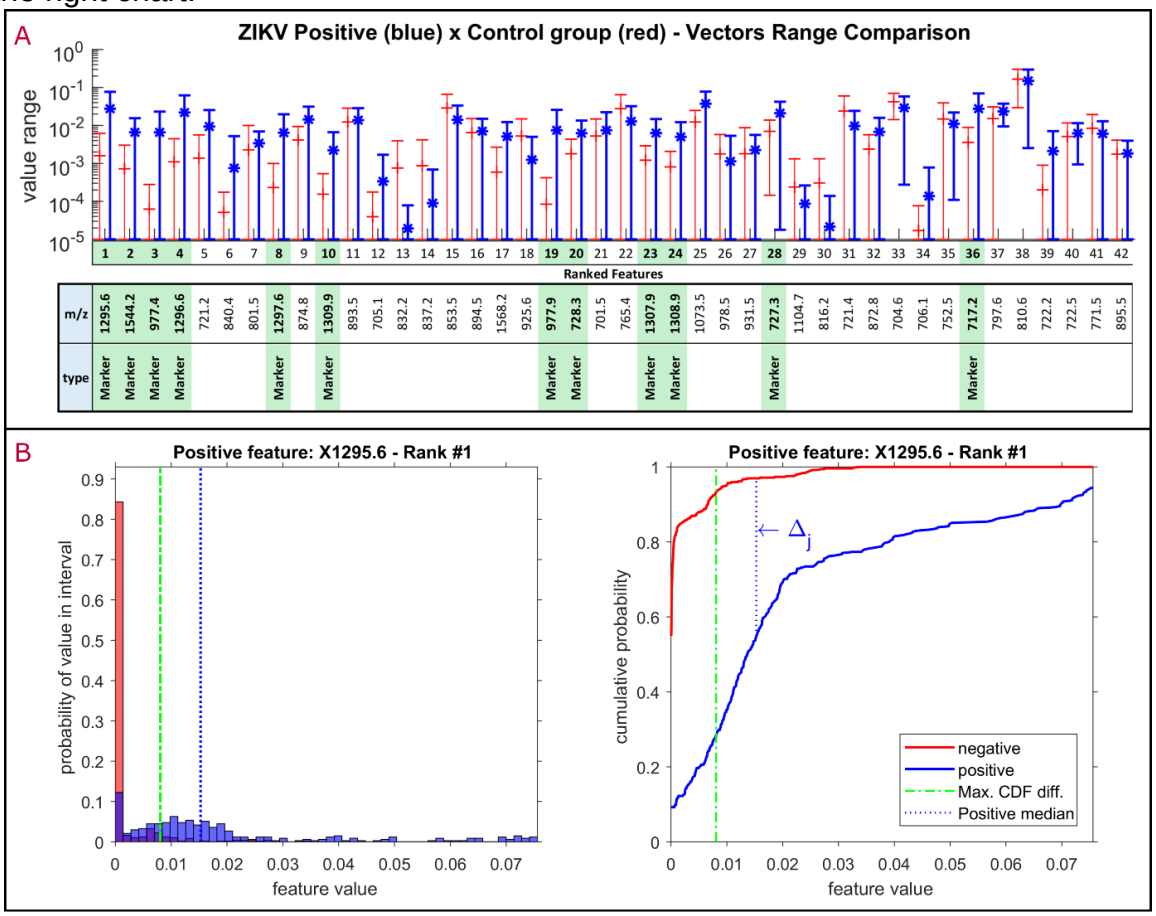

Tables

Table 1. Summary of the specimens included in the study regarding demographic information, clinical conditions and results from RT-PCR performed during the high viremia period.

	ZIKV symptomatic and current infected	ZIKV 1 month after infection	Symptomatic, but not ZIKV	Symptomatic Dengue RT-PCR+	Healthy, asymptomatic more than 30 days
RT-PCR	+	+	-	-	-
Pos./Neg.	Positive	Positive	Negative	Negative	Negative
DEMOGRAPHICS					
Male	27	23	48	25	6
Female	16	16	16	21	5
Total of specimens	43	39	64	46	11
Mean age (median)	33.23 (33)	32.85 (32.2)	32.53 (31)	33.21 (33)	32.76 (30)

Table 2. Comparison of the most discriminant 10-round training and validation results using the 3 selected equations for the number of trees in each iteration as function of the ranked vector length.

Num. of Trees Equation (v = vector length)	*max(40,sqrt(v))*		*230*		*32+(log2(v)/2.sqrt(v))*	
	Grid chart line 1		*Grid chart line 2*		*Grid chart line 3*	
	μ	σ	μ	σ	μ	σ
Best Vector Length	42		59		93	
Accuracy	96.54%	3.58%	96.03%	2.61%	96.12%	2.00%
Sensitivity	97.74%	3.66%	97.74%	3.66%	96.99%	3.71%
Specificity	95.34%	5.23%	94.31%	5.81%	95.26%	3.79%
Precision	93.99%	6.29%	92.82%	6.46%	93.66%	4.61%
NPV	98.46%	2.50%	98.55%	2.34%	98.02%	2.31%
F1Score	95.74%	4.23%	95.03%	3.17%	95.18%	2.42%
F1Neg	96.82%	3.38%	96.26%	2.78%	96.55%	1.78%
green	metric's best value					
rose	metric's worst value					

Table 3. ZIKV Diagnosis Classifier's tests results.

Metric	Formula	10 rounds Validation Tests		Blind Final Test
		Mean	σ	
Feature Vector Length		42		42
Real Positives	$P = TP + FN$			15
Real Negatives	$N = TN + FP$			24
Predicted Positives	$TP + FP$			15
Predicted Negatives	$TN + FN$			24
True Negatives	TN			23
False Positives	FP			1
False Negatives	FN			1
True Positives	TP			14
Accuracy	$ACC = \frac{(SEN + SPC)}{2}$	96.54%	3.58%	94.49%
Sensitivity	$SEN = \frac{TP}{TP + FN}$	97.74%	3.66%	93.33%
Specificity	$SPC = \frac{TN}{TN + FP}$	95.34%	5.23%	95.65%
Precision	$PRC = \frac{TP}{TP + FP}$	93.99%	6.29%	93.33%
Neg. Pred. Value	$NPV = \frac{TN}{TN + FN}$	98.46%	2.50%	95.65%
F1Score	$F1S = 2 \cdot \frac{SEN.PRC}{SEN + PRC}$	95.74%	4.23%	93.33%

Table 4. Comparison of 10-round training and validation results between classifiers using same datasets for the full-length input vectors and for the signature features selected by the reduction method proposed in the article.

	SVM				Random Forest		Tree			
	SMO		ISDA				GDI		Deviance	
	μ	σ	μ	σ	μ	σ	μ	σ	μ	σ
Vector Length 10000 (full spectra)										
Accuracy	90.16%	5.96%	90.84%	6.28%	94.19%	3.59%	89.62%	5.60%	90.07%	5.91%
Sensitivity	87.88%	11.58%	89.25%	9.62%	94.06%	4.81%	87.41%	9.37%	88.83%	8.10%
Specificity	92.44%	7.58%	92.44%	7.58%	94.31%	5.25%	91.83%	5.47%	91.31%	4.23%
Precision	89.74%	10.05%	89.58%	10.34%	92.45%	6.29%	88.32%	7.41%	87.42%	6.22%
NPV	92.54%	6.78%	93.24%	6.05%	95.93%	3.13%	91.59%	5.89%	92.31%	5.42%
F1Score	88.08%	7.50%	89.00%	7.73%	93.11%	4.21%	87.54%	6.49%	88.08%	6.91%
F1Neg	92.17%	4.59%	92.63%	5.14%	95.03%	3.27%	91.59%	4.41%	91.79%	4.63%
Vector Length 42 (signature features)										
Accuracy	93.13%	2.80%	93.42%	4.05%	96.54%	3.58%	91.22%	3.54%	91.24%	4.60%
Sensitivity	93.93%	5.10%	92.45%	5.20%	97.74%	3.66%	89.60%	3.62%	89.60%	6.28%
Specificity	92.34%	5.02%	94.39%	5.66%	95.34%	5.23%	92.84%	5.01%	92.89%	4.86%
Precision	89.91%	6.34%	92.39%	7.47%	93.99%	6.29%	89.87%	6.56%	89.81%	7.14%
NPV	95.89%	3.07%	94.93%	3.40%	98.46%	2.50%	92.83%	2.68%	92.92%	4.25%
F1Score	91.65%	3.26%	92.24%	4.84%	95.74%	4.23%	89.64%	4.31%	89.57%	5.60%
F1Neg	93.98%	2.62%	94.58%	3.66%	96.82%	3.38%	92.78%	3.32%	92.84%	3.74%
green	metric's best value									
rose	metric's worst value									

4.1.4. Artigo IV

The role of lipids in the inception, maintenance and complications of dengue virus infection[119]

Carlos Fernando Odir Rodrigues Melo[1], Jeany Delafiori[1], Mohamad Ziad Dabaja[1], Diogo Noin de Oliveira[1], Tatiane Melina Guerreiro[1], Tatiana Elias Colombo[2], Maurício Lacerda Nogueira[2], Jose Luiz Proenca-Modena[3], Rodrigo Ramos Catharino[1]*,

[1]INNOVARE Biomarkers Laboratory, School of Pharmaceutical Sciences, University of Campinas, Brazil.

[2]School of Medicine from São José do Rio Preto (FAMERP), Brazil.

[3]Laboratory of Study of Emerging Viruses (LEVE), Department of Genetic, Evolution and Bioagents, Institute of Biology, University of Campinas, Brazil.

* Corresponding author: Rodrigo Ramos Catharino [e-mail: rrc@g.unicamp.br]

DOI:10.1038/s41598-018-30385-x

Abstract

Dengue fever is a viral condition that has become a recurrent issue for public health in tropical countries, common endemic areas. Although viral structure and composition have been widely studied, the infection phenotype in terms of small molecules remains poorly established. This contribution providing a comprehensive overview of the metabolic implications of the virus-host interaction using a lipidomic-based approach through direct-infusion high-resolution mass spectrometry. Our results provide further evidence that lipids are part of both the immune response upon Dengue virus infection and viral infection maintenance mechanism in the organism. Furthermore, the species described herein provide evidence that such lipids may be part of the mechanism that leads to blood-related complications such as hemorrhagic fever, the severe form of the disease.

Keywords: Dengue virus; mass spectrometry; metabolomics; viromics; physiopathology.

Introduction

Dengue virus (DENV) is an arbovirus transmitted by mosquitoes of the genus *Aedes*, such as *Aedes aegypti* and *Aedes albopictus*. DENV is associated

with outbursts of febrile diseases in the tropics since the 80's[1]. The large number of DENV-infected patients every year, estimated by the World Health Organization in 390 million, makes DENV the most hazardous arbovirus in the world.

DENV is a series of enveloped viruses belonging to the family *Flaviviridae*, genus *Flavivirus*, which are classified in four closely related and antigenically distinct serotypes (DENV-1, DENV-2, DENV-3 and DENV-4). Similary to other flavivirus, the DENV genome consist of a single-stranded positive sense RNA (ssRNA) of almost 11 kb, which encodes a polyprotein that is cleaved into three structural proteins (the capsid (C), the pre-membrane (prM) and the envelope (E) and seven nonstructural proteins, named NS1, NS2A, NS2B, NS3, NS4A, NS4B, and NS5[2].

Although the spectrum of clinical outcomes of patients' responses to DENV varies from a subclinical infection to death, the majority of symptomatic patients develop an acute, self- limiting febrile manifestation. Lasting approximately [4–7] days, it is characterized by fever, chills, retro-orbital headache, myalgia, malaise, leukopenia, thrombocytopenia (sometimes severe) and elevated levels of hepatic transaminases[3]. In contrast, a small percentage of infected patients, usually children or adults during a second infection with a different DENV serotype, may develop severe dengue, characterized by spontaneous bleeding, plasma leakage, shock, and organ failure[3].

The available knowledge indicates that the outcome of DENV infection depends on several factors produced during the beginning of the viral infection such as viral load, presence of non-neutralizing antibodies, immune cells recruitment and production of immune mediators[2]. These factors determine whether the environment is favorable or unfavorable for disease progression by either controlling the viral infection or impairing inflammatory reaction, associated with vascular permeability. Nevertheless, the lack of reliable immunological and other metabolic markers for either protective or pathological responses still an

important gap that hinders the development of new diagnostic or prognostic tests or vaccine candidates[4,5].

Within this context[4,5], this work aimed to verify the changes in serum lipidome of patients infected with DENV-4, since lipids have been shown to be of great importance in the viral infection process[6–8]. Although the lipid profile of patients infected with DENV has already been established in other studies, most of them performed using liquid chromatography coupled to mass spectrometry (LC-MS) techniques [9–11], whereas the present study used no chromatographic approach. We intended to analyze samples with the least possible preparation and manipulation, attempting to minimize as much as possible changes in the biological matrix used. Additionally, direct infusion high-resolution mass spectrometry allows us to analyze a wide range of lipids, a characteristic that is impaired when using LC-MS, since the column separates lipids by their respective physicochemical characteristics such as polarity, isomerism and others[12,13].

Metabolomic approach of serum of patients infected with DENV-4

PCA clearly shows the separation between Control and DENV-infected patients, as shown in Fig. 1. This multivariate data analysis method was chosen because it is an unsupervised approach, capable of reducing the number of variables (reduction of dimensions) in the original dataset (raw data) based on the similar features between the samples, helping to find the most representative variables (features) responsible for each of the two clusters formed[14], according to Fig. 1. This enabled the election of a feature set that is characteristic for each analyzed group, namely DENV-infected patients and healthy individuals. The bidimensional score plot in Fig. 1 is derived from the analysis performed with the data collected by mass spectrometry in the positive mode; from this clustering, we selected and characterized the features (potential metabolomic markers) that presented the greatest relevance in discriminating both groups. To illustrate the characteristic markers chosen by PCA, a heatmap of all features selected by this model was built using Pearson’s distance measurement and Ward’s clustering

algorithm (Fig. 2).The Fig. 2 clearly illustrates the differences in the pool of metabolites between both analyzed groups. Following structure elucidations by mass accuracy and MS/MS reactions[15] (*Supplementary Information 1*), three precursors of Platelet Activation Factor (PAF) [*m/z* 768.5917, *m/z* 770.6043 and *m/z* 792.5917], three Phosphatidylcholine derivatives (PC) [*m/z* 762.6022, *m/z* 838.6336 and *m/z* 796.6231] and four triglycerides [*m/z* 743.6169, *m/z* 769.6327, *m/z* 795.6412 and *m/z* 859.7765] were identified as characteristic for the DENV group; a list of characterized molecules is available in Table 1. Moreover, by elucidating relevant species such as the above mentioned, this work has confirmed that it is possible to identify *in vivo* which are the lipids associated with the phenotype of viral infection process by directly infusing the serum of infected patients in an HRMS instrument, regardless of any previous chromatographic approach.

Compounds involved in the pathophysiological mechanism of DENV-4 infection

Our findings corroborate previous reports by other groups, in studies that identified the production of a series of polypeptides that act as inflammatory mediators during the immune response of the host[3], participating in the autophagy process by signaling between virus and host cell[2] and in their replication process[16]. These studies have also reported the synthesis of lipid mediators during viral infection, which are related to the signaling, control, and maintenance of both the immune response and DENV pathogenesis. [6,17–19]

Phosphatidylcholines (PC) and Triglycerides (TG)

The importance of lipid changes during DENV cell infection is evident when the virus assumes control of the cellular metabolism by controlling and regulating autophagy mechanisms to meet the needs of the viral replication[20].

Autophagy is a general term used to refer to pathways by which cytoplasmic material (soluble macromolecules and organelles) are delivered to

the lysosomes for degradation[21]. There are three different processes characterized by autophagy: macroautophagy, autophagy mediated by chaperones, and microautophagy[21]. By these processes, an eukaryotic cell is able to promote essential lysosomal degradation for survival, differentiation, development and homeostasis, presenting an important adaptive role in the protection of organisms against several pathologies[22]. Eliminating defective proteins and organelles with the potential to trigger pathogenic processes prevents the abnormal accumulation of protein aggregates and the removal of obligate intracellular parasites (OIPs); additionally, the autophagic process also plays an important role in the innate and adaptive immunity: it is responsible for the formation of epitopes presented by MHC complexes[23]. Autophagy is rapidly and positively regulated by cells that need to obtain intracellular nutrients, either during a period of nutrient deprivation or absence of growth factors, as well when there is high energy demand[22]. In this way, DENV, like any other virus, controls the cellular mechanisms in its favor[20]. By taking control of the autophagy processes, the virus is able to control cellular lipid metabolism[24], providing the demands required in the viral infection process[20].

Viral growth occurs through the formation of viral replication complexes (VRCs)[25], consisting of lipid vesicles constructed by all positive-strand RNA viruses from the reorganization of the host intracellular membranes; within this vesicle, viral assembly occurs[26].

Zhang, Jiantao, *et al*. (2016) demonstrated that a significant increase in PC is associated with viral replication, and occurs mainly in the perinuclear membrane of the endoplasmic reticulum (ER), where viral replication occurs; additionally, their data showed that PC accumulation is due to the formation of this lipid class at the region where the VRC will remain, and not due to the transport of preexisting PC in the cellular interior [25]. Thus, the 3 PCs identified herein as characteristic molecules for the group of infected patients (Table 1) are putatively related to the pool of PCs synthesized by the infected cells for viral

replication. These data are not only in agreement with the role of PCs during viral infection by positive-chain RNA viruses[6 11,25], but also demonstrate that the results obtained by direct *in vitro* analysis are corroborated *in vivo*.

Since DENV controls the lipid metabolism of the host cell[20,24], and there is a urge for an additional bioenergetic demand in the viral replication process, the virus promotes the mobilization and recruitment of lipid droplets responsible for the cellular stock of TGs and cholesteryl esters[7]. Recruited TGs undergo the action of lipases in order to provide the necessary fatty acids (FA) for the additional energy supply, since these TGs are used for the production of ATP through the β-oxidation pathway[28]. Cholesterol, also released during this process, will be used to form VRC for viral replication, as well as PCs [9–31]. Thus, TGs identified in this study (Table 1) were indicated as markers present in serum of patients infected with DENV, since the increased bioenergetic demand for viral replication leads to a higher recruitment of TGs as an energy source[24].

The role of platelet activation factor in DENV infection

Platelet activation factor (PAF) is the trivial name of a phospholipid that has the chemical structure of 1-O-alkyl-2-acetyl-sn-glycero-3-phosphocholine, characterized by an alkyl ether bond at the sn-1 position in the glycerol chain (Fig. 3)[32]. The hexadecyl (16:0) moiety as the linker at the sn-1 position provides greater biological activity to the PAF; however, chain length specificity is low, and this leads to the natural formation of a significant amount of 1-O-octadecyl species, i.e. with an octadecyl (18:0) moiety as the linker at the sn-1 position[33]. Given the variation in the length of the side chain of O-alkyl bound at the sn-1 position, as well as the variation of the 2-acetyl chain attached at the sn-2 position, a series of different PAFs may be formed at the same time[34,35]. The formation of PAFs occurs either by *de novo* synthesis, or by the lipid remodeling pathway[36]. The formation of PAFs by *de novo* synthesis is related to the maintenance of the physiological concentrations of this mediator when the organism is in

homeostasis, i.e. constitutive PAF concentrations[37]. The synthesis of PAFs from the remodeling pathway, on the other hand, is regulated by extracellular stimuli, i.e. under inflammation or infection, and is responsible for the PAF pool that occurs under these conditions[38,39]. The synthesis of a pool of PAFs occurring under infection/inflammation is mediated by the activation of cytosolic PLA2 (cPLA2), which recruits and hydrolyzes phosphatidylcholines for the formation of lysoPAF[38,39]. cPLA2 is a member of a superfamily of phospholipases responsible for the recruitment of a series of lipids involved in inflammatory and immune response processes[10]. Therefore, with the activation of cPLA2 due to extracellular stimuli (phosphorylation and Ca^{2+}), PAFs synthesis is initiated by the remodeling pathway, with the formation of 1-O-alkyl-sn-glycer-3-phosphocholine (lyso-PAF) from the hydrolysis of 2-Acyl-1-alkyl-sn-glycero-3-phosphocholine by cPLA2, which has the characteristic of hydrolyzing fatty acids linked to the sn-2 position of the glycerol chain[37]. Thus, the action of the platelet-activating factor acetylhydrolase, activated by Ca^{2+}, and phosphorylation of lyso-PAF[40], leads to PAF formation (Fig. 3).

PAFs exhibit biological activity in various cells and tissues[41] and the interaction of PAF agonists occur through the PAF receptor (PAFR). PAFR is comprised of seven transmembrane helixes coupled to the G protein, and is present in both plasma membrane and nuclear membrane. Activation of this receptor leads to the influx of Ca^{2+} into the cell, promoting a series of simultaneous signaling of kinases and phospholipases, such as MAPK, PKC, phosphatidylinositol-3-kinase (PI3K), protein tyrosine kinase (PTK), phospholipase Cβ (PLC β), and PLA[42]. Thus, cPLA2 itself is activated by increasing Ca^{2+} concentrations and phosphorylations promoted by the interaction of PAF with its receptor, generating a positive feedback for the production of a PAF pool[40,43].

The simultaneous activation cascade resulting from PAF promotes a multitude of effects involved in the immune and inflammatory responses, such as

the production of superoxide, thromboxane B2 and leukotriene C4[44], increased endothelial permeability[45], increased production of proinflammatory interleukins[46], eosinophils recruitment[47], among other effects involved in the immune response against viral infection. PAFR is present in the membranes of various cell types such as eosinophils, leukocytes, macrophages, neutrophils and platelets[43].

The correlation between PAF and platelet activation is important in the viral infection process, especially for DENV; the endogenous release of PAF is related to a number of acute inflammation effects in DENV infection, such as increased vascular permeability, altered leukocyte numbers, thrombocytopenia, and degrees of bleeding[48]. Thus, the identification of 4 PAF precursors as biomarkers becomes a strong indication for representing this process.

It has recently been shown that platelets are also involved in the detection of pathogen- associated molecular patterns (PAMPs)[49] by standard-recognition receptors (PRRs) on the surface, such as Toll-like receptors (TLRs), and associated with other members of the interleukin-1 (IL-1)-TLR superfamily. Moreover, it has been reported that the number of constitutive PRR on the surface of the platelet undergoes specific upregulation when the platelet is active by a given microorganism[50], which would increase the sensitivity to the immune response to the pathogen, assisting in the fight against infection. This mechanism indicates that platelets are part of the first-line recognition process for both microbial pathogens and immune response. Given the fact that platelets have direct antimicrobial functions mediated by the secretion of antimicrobial molecules, including platelet microbicidal proteins (PMPs) and kinocidins[49]; Tsegaye *et al.* 2013 demonstrated that the release of CXCL4 by platelets inhibited *in vitro* HIV-1 infection in T cells. Thus, it is feasible to infer that platelet activation may play an important role during the viral immune response process[51].

The identification of precursor species involved in the synthesis of PAFs in this study is in line with the findings proposed by Berthet *et al*. 2012, where peripheral blood platelets exposed to *S. minnesota* led to increased

concentrations of IL-6, IL-8 and TNFα, whereas platelets exposed to *E. coli* did not[52]. This behavior evidences that the secretion of platelet cytokines is distinct due to the activation pattern, and suggests a specific response where lipids are responsible for such specificity[53,54].

In contrast to helping fight viral infections, one of the major complications manifested as a result of the interaction between viral infection and platelets, and which is directly related to the activation of PAF, is thrombocytopenia[55,56]. This characteristic manifestation of DENV infection is even used as one of the criteria for the diagnosis of this infection[56].

Thrombocytopenia has been used as a parameter for the identification of patients with a more severe clinical picture, which also encompass other symptoms such as increased vascular permeability and hematocrit, alterations in the number of leukocytes and hemorrhage (varying degrees)[48]. A study by Yang *et al*. demonstrated greater release of PAF by macrophages in patients with DENV-1 virus than control subjects[57]. In addition, in studies with mice deficient in PAFR, primary infection by DENV was less severe. This occurs because inhibition of the PAF-PAFR interaction decreases the production of proinflammatory cytokines and TNF-α, in addition to decreasing vascular permeability[57,58]. The increase in intracellular Ca^{2+}, which may be promoted by the PAF-PAFR interaction, is a crucial factor in the activation of platelet response, including the translocation of P-selectin to the membrane[59].

Thrombocytopenia in DENV infection occurs due to the immunological destruction of virus- platelet complexes; viral activation of platelets induces overexpression of P-selectin, functioning as a receptor for macrophages[60]. In cases of recurrent DENV infections, antibodies against the prM structural viral protein facilitate efficient binding of their immature particles to cells expressing the Fc receptor, such as platelets (FccRIIa), which bind to these anti-prM- DENV complexes susceptible to destruction by the immune system[61]. In addition, the DENV- platelet complex also binds to complement C3 molecules and to platelet-

associated IgM or IgG antibodies, resulting in their clearance by immune system cells[62], which would result in thrombocytopenia. Additionally to the mechanisms of destruction of the platelet-DENV complex mentioned above, anti-DENV antibodies react against platelet glycoproteins mediating their destruction by the complement or monocyte-macrophage system[63].

Therefore, all PAF precursors identified and elucidated in this study highlight the importance of increasing the synthesis of PAF performed by the remodeling pathway in the inflammatory process, confirming its activation by external factors[36]. In addition, the synthesis of PAF pools represents the extensive activation of PAFR, a factor related to the severity of dengue cases, which leads to increased cytokines, increased vascular permeability and, consequently, severe hemorrhage and shock[48]. Moreover, platelet activation correlates with the initiation and maintenance of the immune response, as platelets participate in the front line detection and initiation of the immune response[49]. Platelets still play an ambiguous role in the literature, in which they collaborate in the fight against the infection in the organism[49], while at the same time are involved in the degree of severity of the disease, being responsible for provoking hemorrhagic fever due to thrombocytopenia[56].

A previous contribution by our research group has confirmed that it is possible to carry out a study on viral infection mechanism through the direct analysis of the serum of infected patients[7], assertively providing the metabolomics profile of the pathophysiology of the viral infection process, without further degrees of sample preparation and (pre-)processing.

Remarkably, this is possible thanks to the integration between mass spectrometry and bioinformatics to analyze the large amount of data generated. All biomarkers were chosen and validated by statistical analysis and are in line with previous studies on the changes arising from DENV infection both *in vivo* and *in vitro*[19,20,25,64]. Thus, the use of these biomarkers opened the possibility to systemically assess the alterations on the lipid pool due to DENV infection, which

occurred through the increase of PC synthesis and the recruitment of TGs to supply the bioenergetic needs due to the infection. This study also clarifies the possible mediators of the most severe form of the disease, the hemorrhagic form, since the direct analysis of serum allowed to identify a series of precursors of PAFs. According to data in the literature, the increase in PAFs is closely related to two of the main characteristics of this infection: hemorrhagic fever[16] and thrombocytopenia[59]. These symptoms, nonetheless, are not exclusively a result of DENV infection: they occur in other infectious diseases as well[55,56,61]. Hence, future efforts in identifying metabolites directly related to several infection processes, as performed herein, will allow us to verify whether the mechanism involved in these diseases is common or specific for each pathogen. Also, our results may enables and encourages the medical community to screen patients with conditions that have potential for hemorrhagic aggravations with a higher degree of confidence for clinical prognosis.

Methods

Patients

In this study, serum samples stored in the Research Laboratory of Virology from the Faculty of Medicine of São José do Rio Preto (SJRP), a city located in the northwestern region of São Paulo State, Brazil, were analyzed. All 20 sera samples infected with DENV were obtained from febrile patients serviced in healthcare centers in SJRP during the year of 2014, when Zika virus and Chikungunya virus were not detected in São Paulo State. The control group was composed of 10 healthy adults, i.e. asymptomatic individuals who did not present any signs of infection within 30 days prior to sample collection and presented a negative result in RT-PCR for DENV. All sera were transported in dry ice to the INNOVARE Biomarkers Laboratory in Campinas, SP. This study was conducted according to the Declaration of Helsinki and was approved by the Ethics Committee from the Faculty of Medicine of SJRP (FAMERP), São José do Rio Preto, São Paulo, Brazil (Process Number n° 02078812.8.0000.5415). The

collected specimens from all participants consisted of blood samples. Table 2 organizes the structure of sample collection and provides a view of the total number of analyzed specimens. A written informed consent was obtained from all patients prior to enrollment. All samples were obtained from the Base Hospital of SJRP. All experiments were performed in accordance with relevant guidelines and regulations regarding samples from human origin.

DENV detection

All clinical samples used in this study were positive for DENV-NS1 antigen using the NS1 Ag rapid assay kit according to the manufacturer's instructions. In addition, all samples were positive for DENV by a specific RT Multiplex-Nested-PCR performed after RNA extraction from 140 uL of serum with the QIAamp Viral RNA mini kit (QIAGEN), according to the manufacturer's protocol. The Multiplex-Nested-PCR to DENV 1-4 were performed according Colombo and collaborators, 2016[65].

Sample preparation

Serum preparation was performed as described by Melo *et al*. 2017[7]. In summary, 20 µL of each biological sample (blood serum) were diluted in 200 µL of tetrahydrofuran and homogenized and then the volume was completed to 1 mL with methanol, with further homogenization. The obtained solution was centrifuged and 20 µL of the supernatant was collected and diluted in 980 µL of methanol and 0.1% of formic acid was added to the final solution.

High Resolution Mass Spectrometry Analysis

All samples were directly injected for survey scan analysis in an ESI-LTQ-XL Orbitrap Discovery instrument (Thermo Scientific, San Jose, California) with nominal resolution of 30,000 (FWHM), under the following parameters: flow rate of 10 $\mu L.min^{-1}$, capillary temperature of 280 °C, 5 kV as spray voltage and sheath gas at 10 arbitrary units. HRMS analyses were performed in technical

quintuplicates for each sample using the mass range of 500–2000 *m/z* in the positive ion mode. Spectra were analyzed using XCalibur software (v. 2.4, Thermo Scientific, San Jose, CA)

Statistical analysis

Statistical analysis to choose chemical markers for each group was performed using Principal Component Analysis (PCA). PCA is a multivariate model of covariance structure modeling; it is used with the specific purpose of analyzing correlation structures, and it is characterized as a statistical analysis technique for potential biomarkers screening by a given "omic" platform[14].

To perform PCA analyses, raw data were used as a pool of all samples within the same data matrix, i.e. all mass spectrometric data from all replicates of both Control and DENV group were organized in a single database, which was inputted in the online platform environment.

Prior to PCA analyses, interquartile range was used as data filtering method, with quantile normalization and auto scaling. A heatmap of the all features selected by PCA analyses was built using the Pearson's distance measurement and Ward's clustering algorithm. Fold Change analysis was performed for all features selected by PCA and elucidated by HRMS and MS/MS analysis. All statistical analyses were performed using the online platform MetaboAnalyst 3.0[66,67].

Identification of markers

METLIN (Scripps Center for Metabolomics, La Jolla, CA) was consulted to elect the most suitable markers based on the exact mass of each species, adopting a maximum error of 2 ppm for mass accuracy from the experimental exact mass obtained in the study and adducts of $[M+H^+]$ and $[M+Na^+]$ available on the platform[15]. The markers selected on METLIN were confirmed across MS/MS data acquired in the same instrument used for the HRMS analyses and with the same setup. MS/MS reactions were carried out

using Helium as the collision gas, with energies for collision-induced dissociation (CID) ranging from 16 to 31 (arbitrary units). The fragmentation analysis profile spectra of MS/MS were analyzed using XCalibur software (v.2.4, Thermo Scientific, San Jose, CA) and structures were confirmed using theoretical calculations modeling for molecular fragmentation using Mass Frontier software (v. 6.0, Thermo Scientific, San Jose, CA) (Table 1 and *Supplementary Information 1*).

Acknowledgements

CFORM would like to thank the São Paulo Research Foundation by the grant (16/17066-2). We also thank the Coordination for the Improvement of Higher Level Personnel (CAPES) for the fellowships from TMG (PROEX: 1489740) and MZD. DNO would like to thank the Brazilian Ministry of Health (Plano Nacional de Enfrentamento ao Aedes aegypti e à Microcefalia [Brazilian Plan for Fighting Aedes aegypti and Microcephaly]) for the fellowship under process No. 88887.137889/2017-00. JLPM and RRC thank MCTIC-CNPq/MEC-CAPES/MS-Decit/FNDCT No. 14/2016 for the grant. MLN would like to thank the São Paulo Research Foundation for the grant (FAPESP, Process No. 13/21719-3). Finally, RRC would like to thank the São Paulo Research Foundation for the grant (FAPESP, Process Nos. 11/50400-0 and 15/06809-1).

Author contributions

CFORM performed experiments, data collection, analyzed data and wrote the manuscript. MZD performed experiments and data collection. JD, DNO and TMG analyzed data and revised the manuscript. TEC, MLN and JLPM performed patient selection, diagnosis, sample collection and preparation and revised the manuscript. MLN, JLPM and RRC coordinated the team, revised the manuscript and idealized all experiments.

Competing interests

The authors declare no competing interests of any nature.

References

1. Simmons, C. P. *et al.* Dengue. *N. Engl. J. Med.* **366,** 1423–32 (2012).

2. Diamond, M. S. & Pierson, T. C. Molecular Insight into Dengue Virus Pathogenesis and Its Implications for Disease Control. *Cell* **162,** 488–492 (2015).

3. Rothman, A. L. Immunity to dengue virus: A tale of original antigenic sin and tropical cytokine storms. *Nature Reviews Immunology* **11,** 532–543 (2011).

4. Guzman, M. G. *et al.* Dengue: A continuing global threat. *Nat. Rev. Microbiol.* **8,** S7– S16 (2010).

5. Amâncio, F. F. *et al.* FATAL OUTCOME OF INFECTION BY DENGUE 4 IN A PATIENT WITH THROMBOCYTOPENIC PURPURA AS A COMORBID CONDITION IN BRAZIL. *Rev. Inst. Med. Trop. Sao Paulo* **56,** 267–270 (2014).

6. Melo, C. F. O. R. *et al.* A lipidomics approach in the characterization of zika-infected mosquito cells: Potential targets for breaking the transmission cycle. *PLoS One* **11,** (2016).

7. Melo, C. F. O. R. Serum Metabolic Alterations upon Zika Infection. *Front. Microbiol.* **8,** (2017).

8. Nolte-'t Hoen, E., Cremer, T., Gallo, R. C. & Margolis, L. B. Extracellular vesicles and viruses: Are they close relatives? *Proc. Natl. Acad. Sci.* **113,** 9155–9161 (2016).

9. Soto-Acosta, R. *et al.* The increase in cholesterol levels at early stages after dengue virus infection correlates with an augment in LDL particle uptake and HMG-CoA reductase activity. *Virology* **442,** 132–147 (2013).

10. Chandrasekharan, J. A., Marginean, A. & Sharma-Walia, N. An insight into the role of arachidonic acid derived lipid mediators in virus associated pathogenesis and malignancies. *Prostaglandins and Other Lipid Mediators* **126,** 46–54 (2016).

11. Perera, R. *et al.* Dengue virus infection perturbs lipid homeostasis in infected mosquito cells. *PLoS Pathog.* **8,** (2012).

12. Ortmayr, K., Hann, S. & Koellensperger, G. Complementing reversed-phase selectivity with porous graphitized carbon to increase the metabolome coverage in an on-line two- dimensional LC-MS setup for metabolomics. *Analyst* **140,** 3465–3473 (2015).

13. Matuszewski, B. K., Constanzer, M. L. & Chavez-Eng, C. M. Strategies for the assessment of matrix effect in quantitative bioanalytical methods based on HPLC- MS/MS. *Anal. Chem.* **75,** 3019–3030 (2003).

14. Blekherman, G. *et al.* Bioinformatics tools for cancer metabolomics. *Metabolomics* **7,**
329–343 (2011).
15. Guijas, C. *et al.* METLIN: A Technology Platform for Identifying Knowns and Unknowns. *Anal. Chem.* acs.analchem.7b04424 (2018). doi:10.1021/acs.analchem.7b04424
16. Martina, B. E. E., Koraka, P. & Osterhaus, A. D. M. E. Dengue virus pathogenesis: An
integrated view. *Clinical Microbiology Reviews* **22,** 564–581 (2009).
17. Gong, W. *et al.* Serum metabolomic profiling of piglets infected with virulent classical swine fever virus. *Front. Microbiol.* **8,** (2017).
18. Murakami, M. *Bioactive lipid mediators: Current reviews and protocols*. *Bioactive Lipid*
Mediators: Current Reviews and Protocols (2015). doi:10.1007/978-4-431-55669-5
19. Cui, L. *et al.* Serum Metabolome and Lipidome Changes in Adult Patients with Primary Dengue Infection. *PLoS Negl. Trop. Dis.* **7,** (2013).
20. Heaton, N. S. & Randall, G. Dengue virus-induced autophagy regulates lipid metabolism. *Cell Host Microbe* **8,** 422–432 (2010).
21. Mizushima, N., Yoshimori, T. & Levine, B. Methods in Mammalian Autophagy
Research. *Cell* **140,** 313–326 (2010).
22. Levine, B. & Kroemer, G. Autophagy in the Pathogenesis of Disease. *Cell* **132,** 27–42 (2008).
23. Qian, M., Fang, X. & Wang, X. Autophagy and inflammation. *Clin. Transl. Med.* **6,** 24 (2017).
24. Singh, R. *et al.* Autophagy regulates lipid metabolism. *Nature* **458,** 1131–1135 (2009).
25. Zhang, J. *et al.* Positive-strand RNA viruses stimulate host phosphatidylcholine synthesis at viral replication sites. *Proc. Natl. Acad. Sci.* **113,** E1064–E1073 (2016).
26. Lee, W.-M. & Ahlquist, P. Membrane synthesis, specific lipid requirements, and
localized lipid composition changes associated with a positive-strand RNA virus RNA
replication protein. *J. Virol.* **77,** 12819–12828 (2003).
27. Martin, S. & Parton, R. G. Lipid droplets: A unified view of a dynamic organelle. *Nature*
Reviews Molecular Cell Biology **7,** 373–378 (2006).
28. Carneiro, L. A. M. & Travassos, L. H. Autophagy and viral diseases transmitted by
Aedes aegypti and Aedes albopictus. *Microbes Infect.* **18,** 169–171 (2016).

29. Sagan, S. M. *et al.* The influence of cholesterol and lipid metabolism on host cell structure and hepatitis C virus replication. *Biochem Cell Biol* **84,** 67–79 (2006).

30. Stoeck, I. K. *et al.* Hepatitis C virus replication depends on endosomal cholesterol homeostasis. *J. Virol.* JVI.01196-17 (2017). doi:10.1128/JVI.01196-17

31. Albulescu, L., Wubbolts, R., van Kuppeveld, F. J. M. & Strating, J. R. P. M. Cholesterol shuttling is important for RNA replication of coxsackievirus B3 and encephalomyocarditis virus. *Cell. Microbiol.* **17,** 1144–1156 (2015).

32. Benveniste, J. *et al.* Semi-synthesis and proposed structure of platelet-activating factor (PAF): PAF-acether an alkyl ether analog of lysophosphatidylcholine. *C. R. Seances Acad. Sci. D.* **289,** 1037–1040 (1979).

33. Hanahan, D. J. Platelet activating factor: a biologically active phosphoglyceride. *Annu. Rev. Biochem.* **55,** 483–509 (1986).

34. Gale, T. V., Horton, T. M., Grant, D. S. & Garry, R. F. Metabolomics analyses identify platelet activating factors and heme breakdown products as Lassa fever biomarkers. *PLoS Negl. Trop. Dis.* **11,** (2017).

35. Itabe, H. Oxidized phospholipids as a new landmark in atherosclerosis. *Prog. Lipid Res.* **37,** 181–207 (1998).

36. Snyder, F. Platelet-activating factor: the biosynthetic and catabolic enzymes. *Biochem. J.* **305,** 689 (1995).

37. Blank, M. L., Lee, Y. J., Cress, E. A. & Snyder, F. Stimulation of the de novo pathway for the biosynthesis of platelet-activating factor (PAF) via cytidylyltransferase activation in cells with minimal endogenous PAF production. *J. Biol. Chem.* **263,** 5656–5661 (1988).

38. Uozumi, N. *et al.* Role of cytosolic phospholipase A2 in allergic response and parturition. *Nature* **390,** 618–622 (1997).

39. Shindou, H., Ishii, S., Uozumi, N. & Shimizu, T. Roles of cytosolic phospholipase A(2) and platelet-activating factor receptor in the Ca-induced biosynthesis of PAF. *Biochem. Biophys. Res. Commun.* **271,** 812–7 (2000).

40. Prescott, S. M., Zimmerman, G. A., Stafforini, D. M. & McIntyre, T. M. Platelet- activating factor and related lipid mediators. *Annu. Rev. Biochem.* **69,** 419–445 (2000).

41. Ishii, S. & Shimizu, T. Platelet-activating factor (PAF) receptor and genetically engineered PAF receptor mutant mice. *Prog Lipid Res* **39,** 41–82 (2000).

42. Liscovitch, M. & Cantley, L. C. Lipid second messengers. *Cell* **77,** 329–334 (1994).

43. Liu, Y. *et al.* Current Understanding of Platelet-Activating Factor Signaling in Central

Nervous System Diseases. *Molecular Neurobiology* **54,** 5563–5572 (2017).

44. Dent, G. *et al.* Protein kinase C inhibition enhances platelet-activating factor-induced eicosanoid production in human eosinophils. *Am. J. Respir. Cell Mol. Biol.* **18,** (1998).

45. Liu, L. *et al.* Triple role of platelet-activating factor in eosinophil migration across monolayers of lung epithelial cells: eosinophil chemoattractant and priming agent and epithelial cell activator. *J. Immunol.* **161,** 3064–70 (1998).

46. Roth, M. *et al.* Platelet-activating factor exerts mitogenic activity and stimulates expression of interleukin 6 and interleukin 8 in human lung fibroblasts via binding to its functional receptor. *J Exp Med* **184,** 191–201 (1996).

47. Lou, Y. P. *et al.* Platelet-activating factor induces goblet cell hyperplasia and mucin gene expression in airways. *Am. J. Respir. Crit. Care Med.* **157,** 1927–1934 (1998).

48. Souza, D. G. *et al.* Essential role of platelet-activating factor receptor in the pathogenesis of Dengue virus infection. *Proc. Natl. Acad. Sci. U. S. A.* **106,** 14138–43 (2009).

49. Yeaman, M. R. Platelets: At the nexus of antimicrobial defence. *Nature Reviews*

Microbiology **12,** 426–437 (2014).

50. Shiraki, R. *et al.* Expression of Toll-like receptors on human platelets. *Thromb. Res.* **113,**

379–385 (2004).

51. Solomon Tsegaye, T. *et al.* Platelet activation suppresses HIV-1 infection of T cells.

Retrovirology **10,** (2013).

52. Berthet, J. *et al.* Human platelets can discriminate between various bacterial LPS

isoforms via TLR4 signaling and differential cytokine secretion. *Clin. Immunol.* **145,**

189–200 (2012).

53. Anderson, H. A. & Roche, P. A. MHC class II association with lipid rafts on the antigen presenting cell surface. *Biochim. Biophys. Acta - Mol. Cell Res.* **1853,** 775–780 (2015).

54. Kallikourdis, M. *et al.* Phosphatidylinositol 4-Phosphate 5-Kinase β Controls

Recruitment of Lipid Rafts into the Immunological Synapse. *J. Immunol.* **196,** 1955–

1963 (2016).

55. Assinger, A. Platelets and infection - An emerging role of platelets in viral infection.

Frontiers in Immunology **5,** (2014).

56. Zapata, J. C., Cox, D. & Salvato, M. S. The Role of Platelets in the Pathogenesis of Viral

Hemorrhagic Fevers. *PLoS Negl. Trop. Dis.* **8,** (2014).

57. Yang, K. D., Wang, C. L. & Shaio, M. F. Production of cytokines and platelet activating factor in secondary dengue virus infections. *J. Infect. Dis.* **172,** 604–605 (1995).

58. Costa, V. V., Fagundes, C. T., Souza, D. G. & Teixeira, M. M. Inflammatory and innate immune responses in dengue infection: Protection versus disease induction. *American Journal of Pathology* **182,** 1950–1961 (2013).

59. De Azeredo, E. L., Monteiro, R. Q. & De-Oliveira Pinto, L. M. Thrombocytopenia in dengue: Interrelationship between virus and the imbalance between coagulation and fibrinolysis and inflammatory mediators. *Mediators of Inflammation* **2015,** (2015).

60. Von Hundelshausen, P. *et al.* RANTES deposition by platelets triggers monocyte arrest on inflamed and atherosclerotic endothelium. *Circulation* **103,** 1772–1777 (2001).

61. Rodenhuis-Zybert, I. A. *et al.* Immature dengue virus: A veiled pathogen? *PLoS Pathog.* **6,** (2010).

62. Noisakran, S. *et al.* Role of CD61+ cells in thrombocytopenia of dengue patients. *Int. J. Hematol.* **96,** 600–610 (2012).

63. Lin, C. F. *et al.* Generation of IgM anti-platelet autoantibody in dengue patients. *J. Med. Virol.* **63,** 143–149 (2001).

64. Geoghegan, V. *et al.* Perturbed cholesterol and vesicular trafficking associated with dengue blocking in Wolbachia-infected Aedes aegypti cells. *Nat. Commun.* **8,** (2017).

65. Colombo, T. E. *et al.* Dengue virus surveillance: Detection of DENV-4 in the city of São José do Rio Preto, SP, Brazil. *Acta Trop.* **164,** 84–89 (2016).

66. Xia, J. & Wishart, D. S. Using metaboanalyst 3.0 for comprehensive metabolomics data analysis. *Curr. Protoc. Bioinforma.* **2016,** 14.10.1-14.10.91 (2016).

67. Xia, J., Sinelnikov, I. V., Han, B. & Wishart, D. S. MetaboAnalyst 3.0-making metabolomics more meaningful. *Nucleic Acids Res.* **43,** W251–W257 (2015).

Figure Legends

Figure 1. Scores plot between the first two principal components (PCs) selected from the Principal Component Analysis.

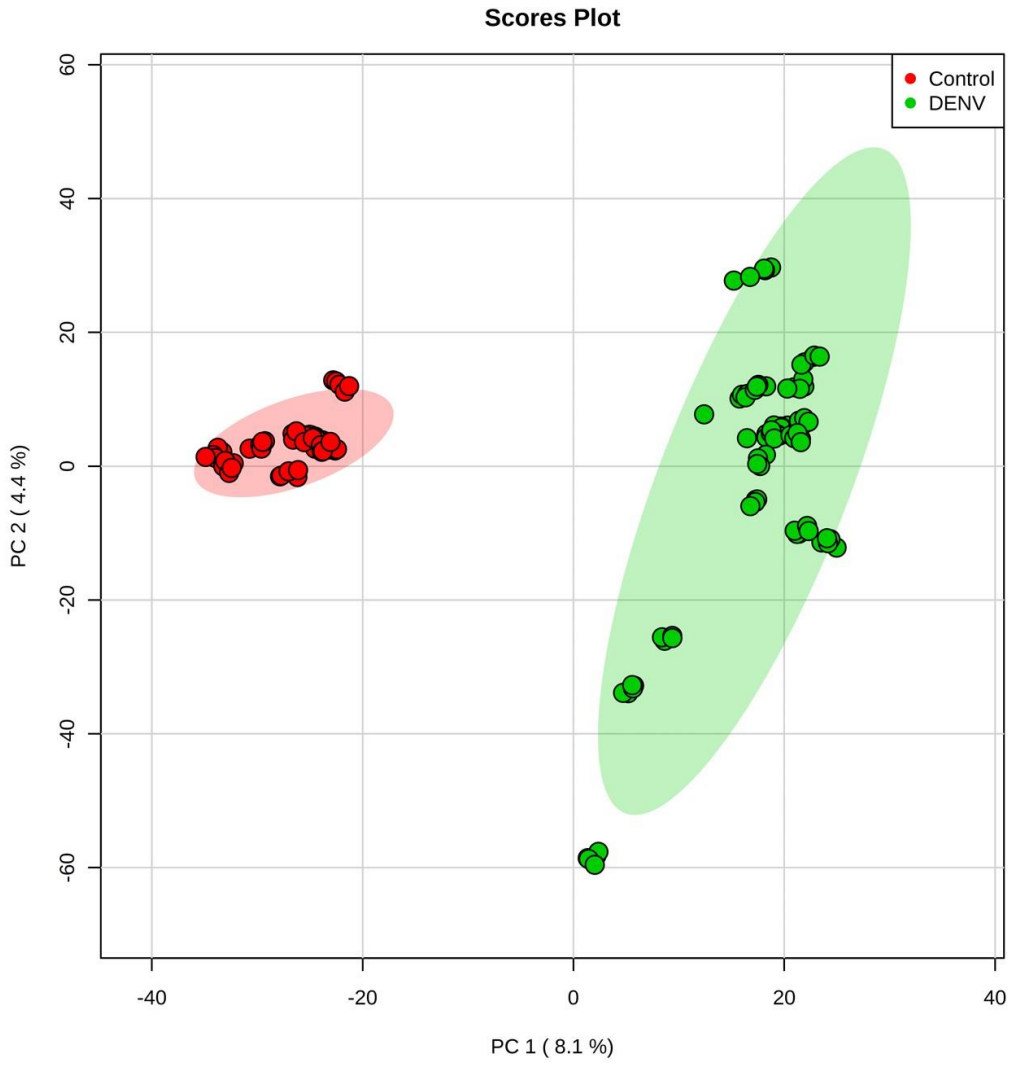

Figure 2: Clustering result for the 27 top features selected by Principal Component Analysis shown as a heatmap (distance measured by Pearson's distance measurement and Ward's clustering algorithm). The color-coded thermometer (bottom) indicates the relative presence of metabolites among the groups.

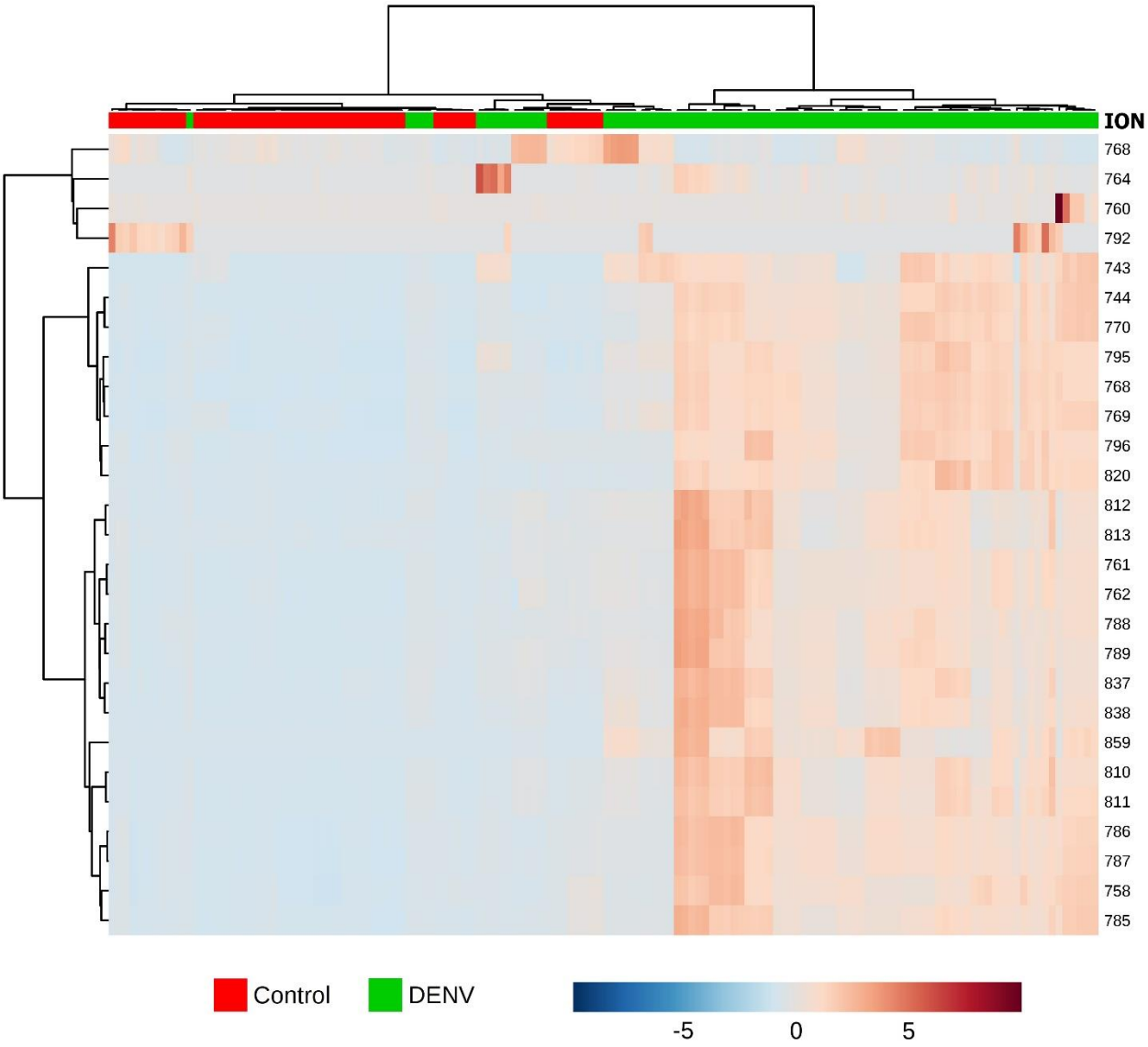

Figure 3: The pool in the synthesis of PAFs that occurs under infection it is mediated by the activation of cPLA2, which recruits and hydrolyzes phosphatidylcholines for the formation of lysoPAF. The activation of cPLA2 due to extracellular stimuli (intracellular phosphorylation and Ca^{2+} influx) upon PAFs synthesis is initiated by the formation of lyso-PAF. Also, the action of the PAF acetylhydrolase, activated by Ca^{2+}, and phosphorylation of lyso-PAF leads to PAF formation. PAF, Platelet activation factor; PAFR, Platelet activation factor receptor; PLC, Phospholipase; DAG, Diacylglycerol; IP3, Inositol trisphosphate; Ca^{2+}, Calcium ions; cPLA2, Cytosolic phospholipase A2; PC, Phosphatidylcholine; AA, Arachidonic acid; Lysp-PAF, 1-O-alkyl-sn-glycer-3-phosphocholine; LPCAT, Lysophosphatidylcholine acyltransferase; Acetyl- CoA, Acetyl coenzyme A.

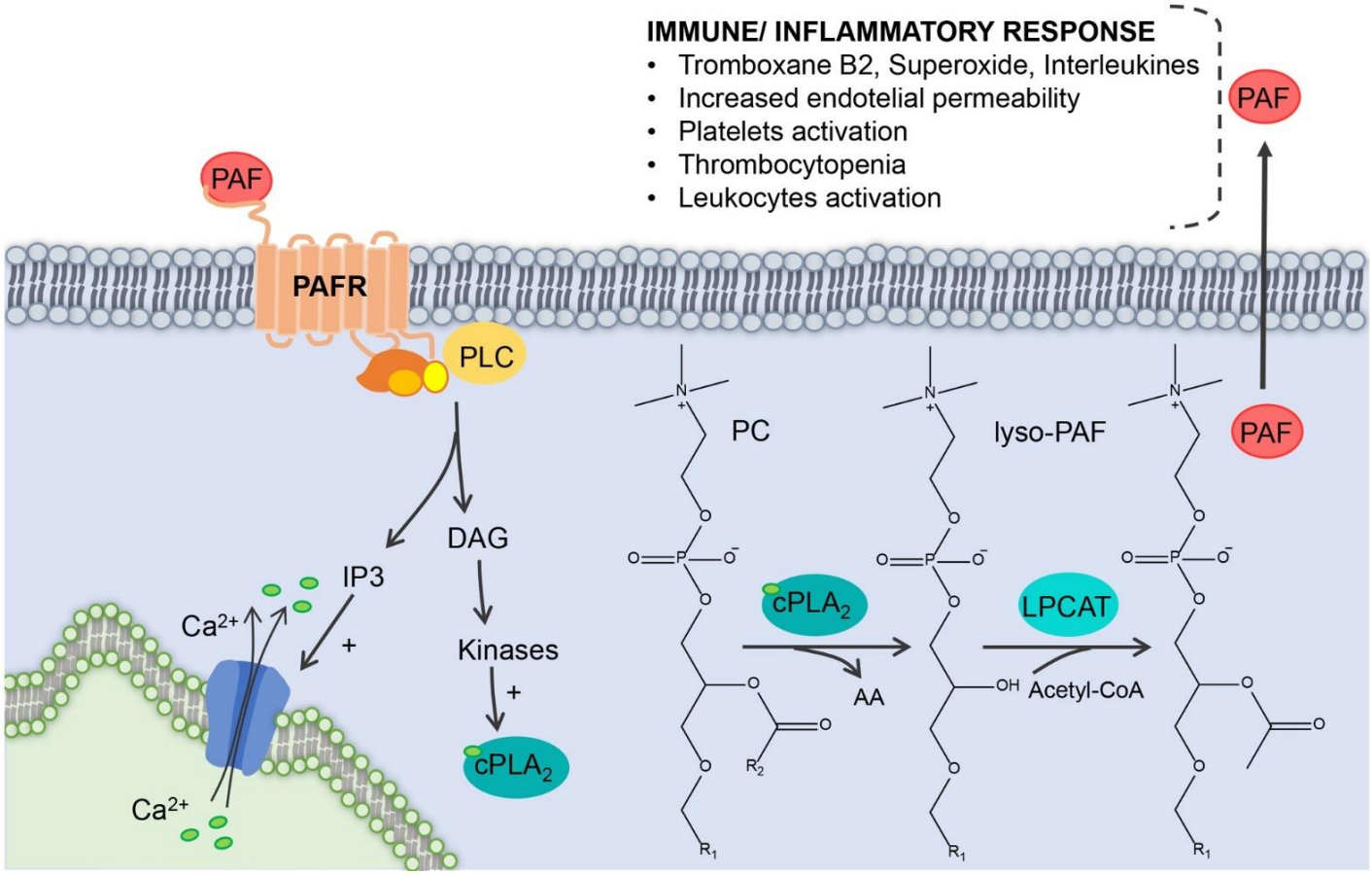

Tables

Table 1. Lipid markers elected by Principal Component Analysis from the serum of patients infected with DENV (DENV group). Characterization was performed with the assistance of METLIN database[15].

Exact mass	Theoretical Mass	Error (ppm)[1]	MS/MS fragmentation	Adducts	Platform [2]	Molecule	Log 2 (FC) [3]
743.6169	743.6184	2.0172	684,619,555,487	[M+H]+	MID 98508 MID 99076	TG(44:4)	4.245
769.6327	769.6341	-1.8190	709,645,581,587	[M+H]+	MID 99084 MID 98516	TG(46:5)	2.9707
795.6412	795.6424	-1.5082	736,612,607,590	[M+H]+	MID 99092 MID 98531	TG(48:6)	3.7961
859.7765	859.7749	1.8610	799,676,842,671	[M+H]+	MID 4798	TG(52:2)	7.4812
762.6022	762.6007	1.9670	575,704,621,719	[M+H]+	MID 59328 MID 39142 MID 59482 MID 59708 MID 39823	PC(34:0)	2.6625
784.5836	784.5851	-1.9118	579,595,725,601	[M+H]+	MID 59843 MID 59614	PC(36:0)	8.9199
838.6336	838.6320	1.9079	779,649,655,721	[M+H]+	MID 59917 MID 59982 MID 39855	PC(40:0)	4.8301
768.5917	768.5902	1.9516	709,581,585, 563	[M+H]+	MID 43414 MID 40083 MID 76437	PC(O-36:4)	3.2534
770.6043	770.6058	-1.9465	711,583,726, 567	[M+H]+	MID 76435 MID 40080 MID 43415	PC(O-36:3)	3.6014
792.5917	792.5902	1.8925	733,416,609, 605	[M+H]+	MID 62936 MID 40092	PC(O-38:6)	2.7396
796.6231	796.6215	2.0085	737,613,778, 752	[M+H]+	MID 76462 MID 76423 MID 40129	PC(O-38:4)	2.9874

1- Error = ((Exact Mass-Theoretical Mass)/Exact mass)*10^6

2- METLIN: A Technology Platform for Identifying Knowns and Unknowns – the provided IDs refer to the possible isomers that can be found within that mass range

3 - Log_2 (FC) where *FC* = Fold Change (DENV/Control) prior normalization

SupplementaryMaterial #1

MS/MS Reactionsofthe Species Elected by PCA

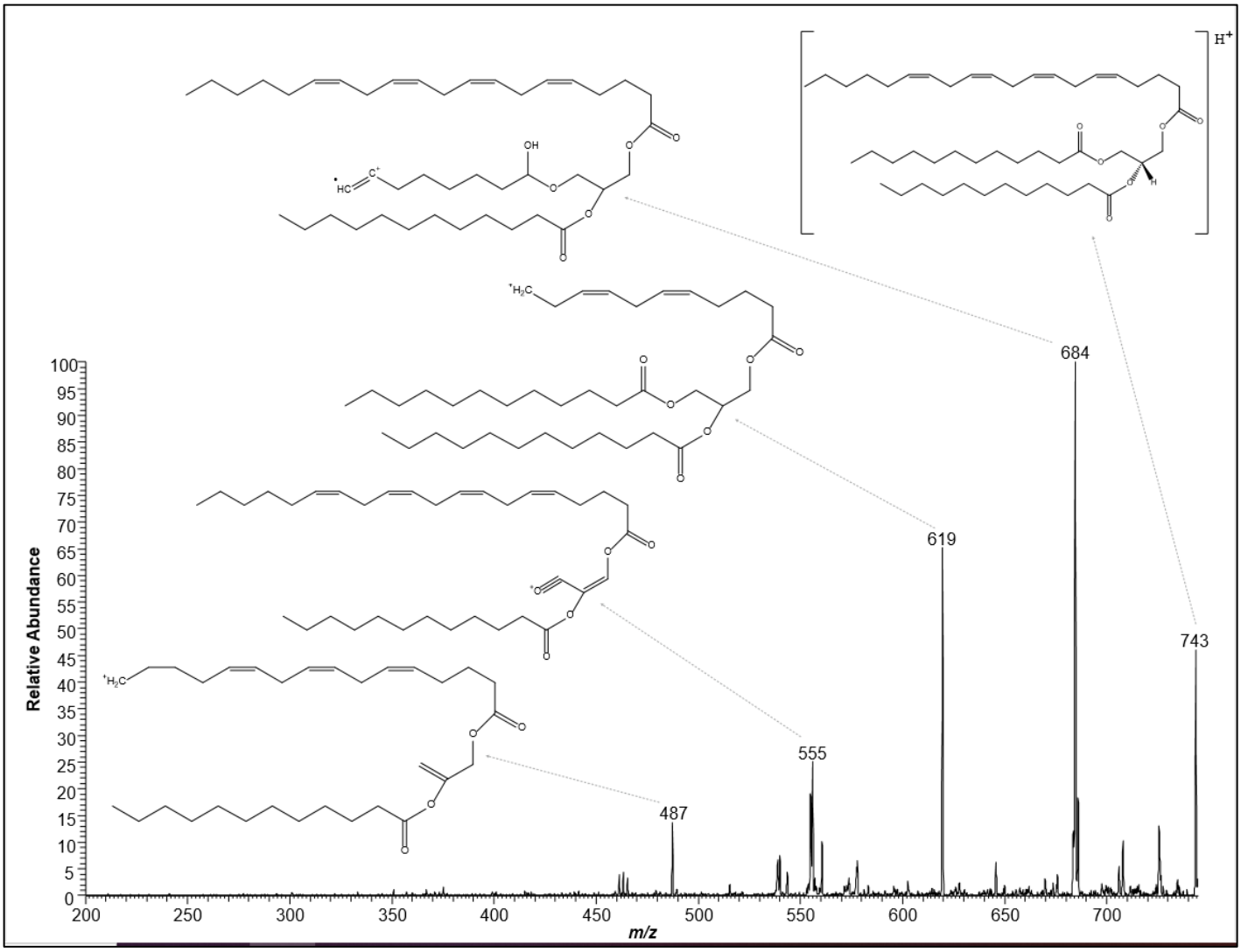

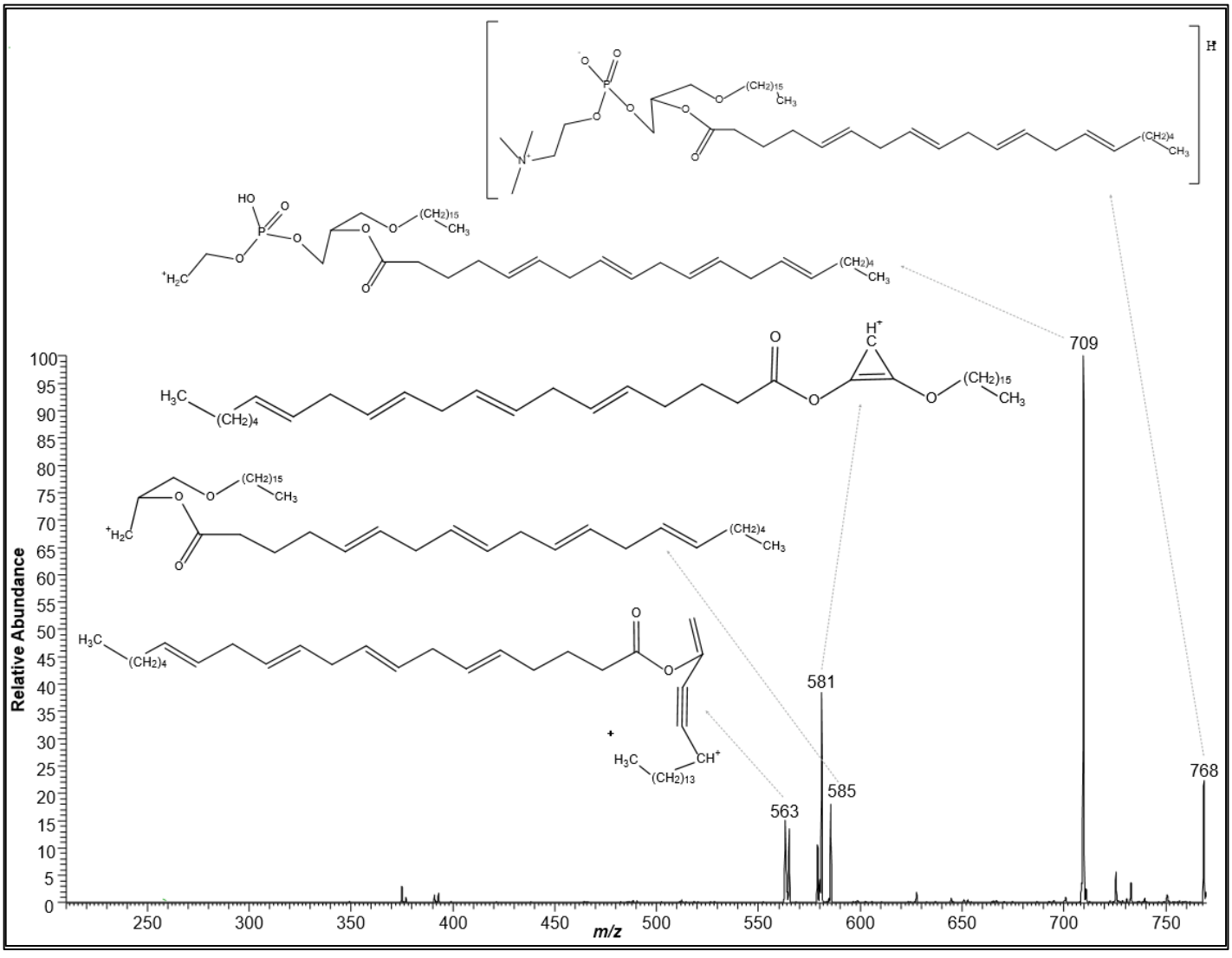
Relative Abundance
m/z
709
581
585
563
768

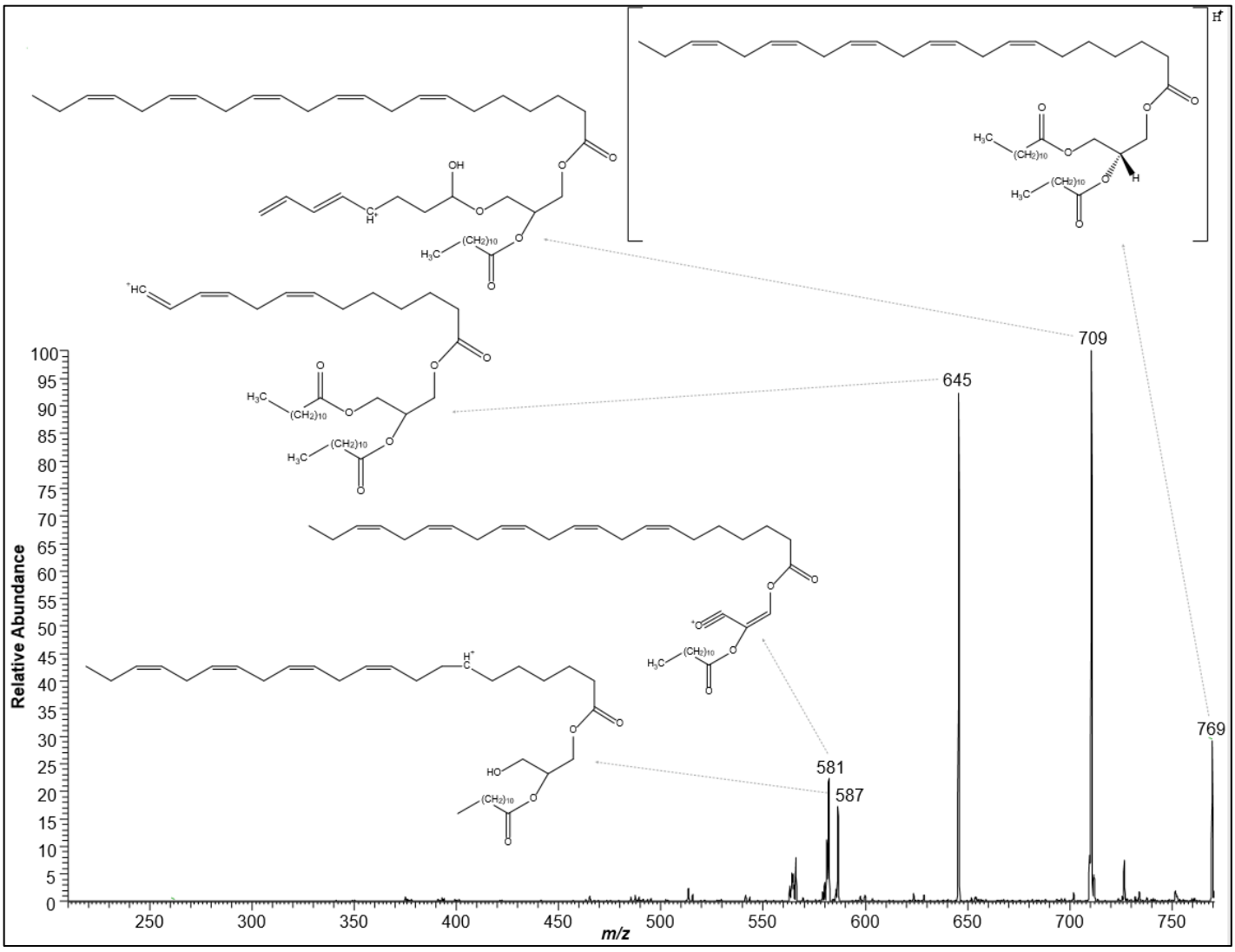
Relative Abundance
m/z
709
645
769
581
587
OH
HO
H
100
95
90
85
80
75
70
65
60
55
50
45
40
35
30
25
20
15
10
5
0
250
300
350
400
450
500
550
600
650
700
750

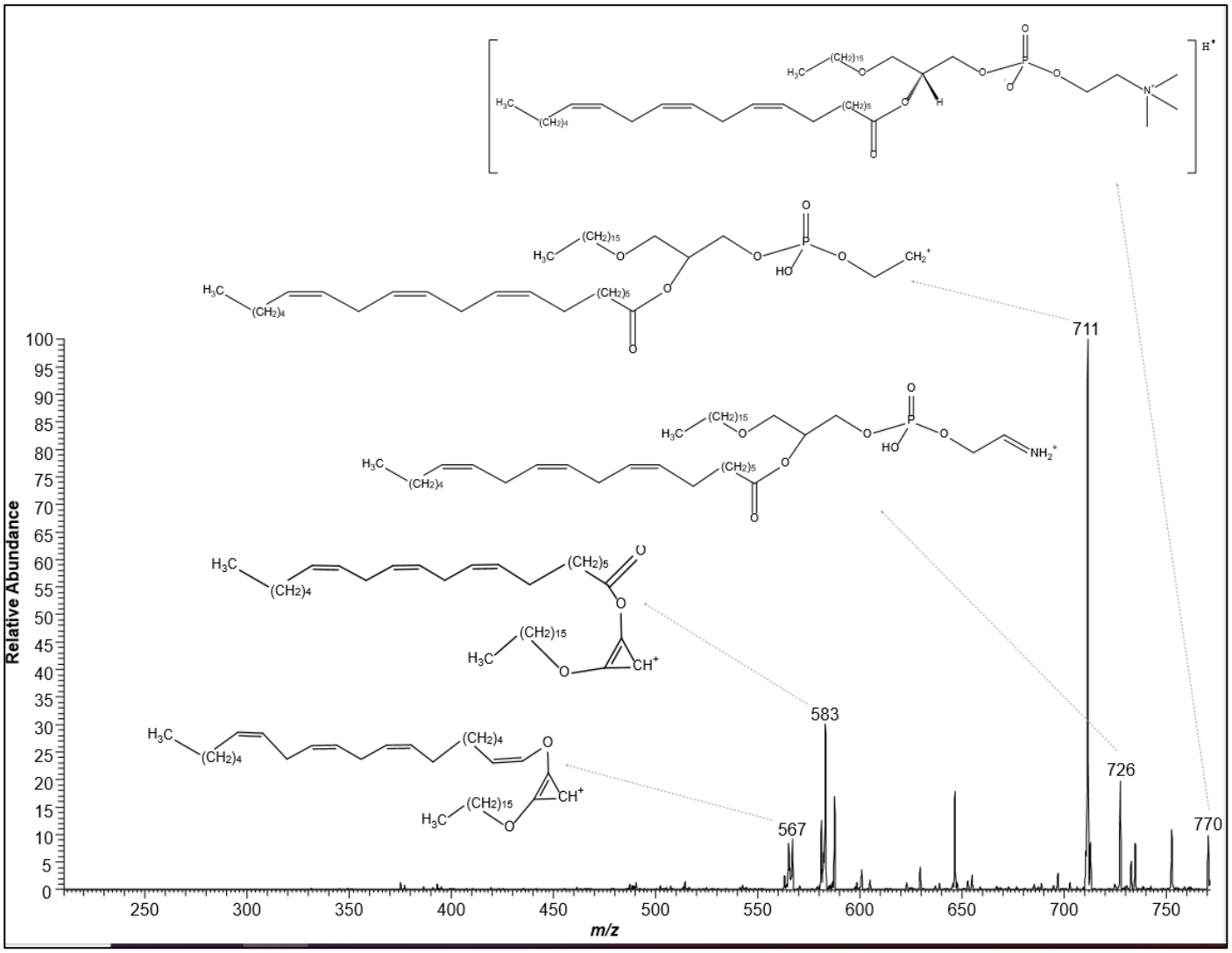
Relative Abundance
m/z
711
583
726
770
567
100
95
90
85
80
75
70
65
60
55
50
45
40
35
30
25
20
15
10
5
0
250
300
350
400
450
500
550
600
650
700
750


Relative Abundance
m/z
733
792
609
605
416
OH
CH3
(CH2)15
CH2+
H+

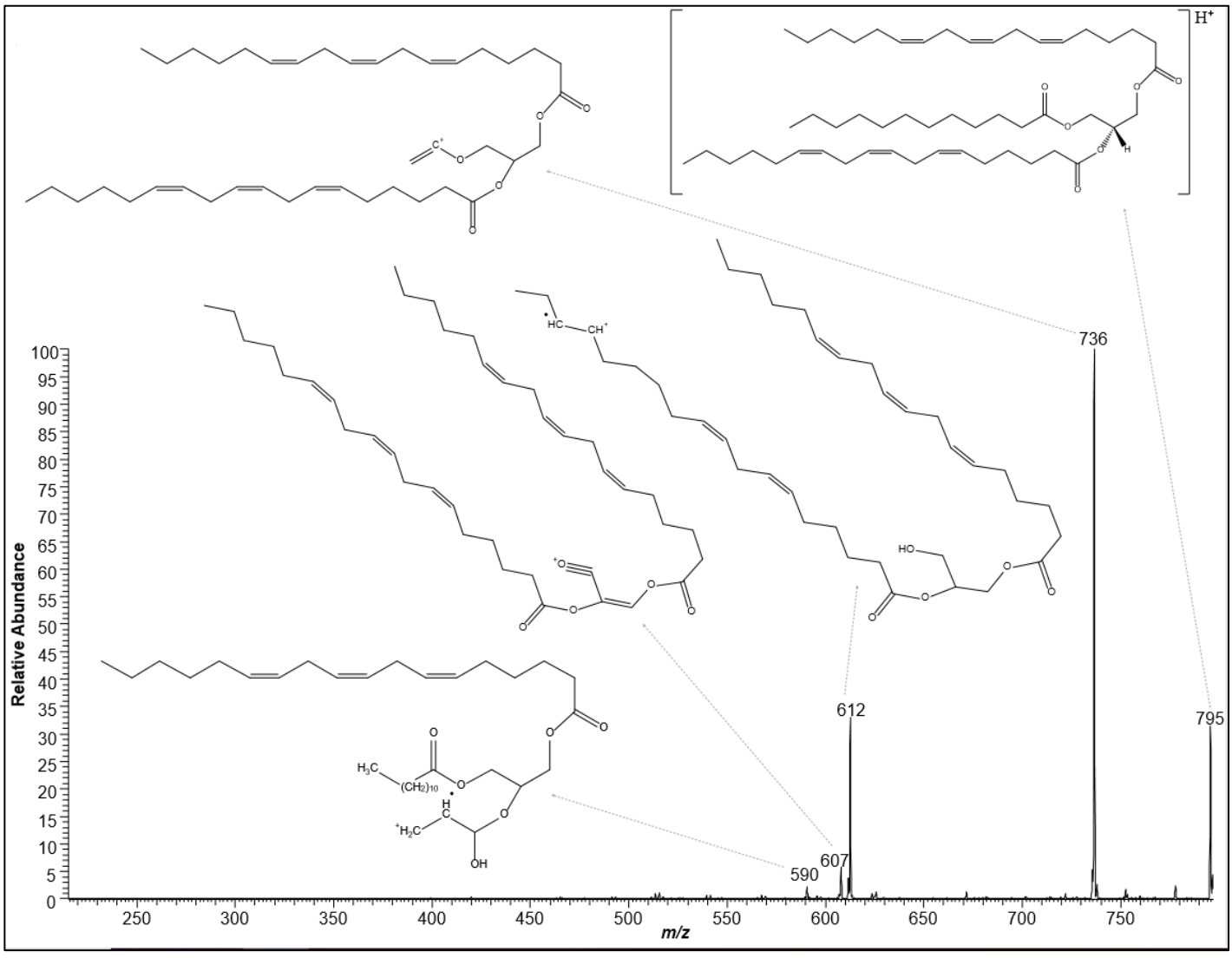
H+
736
795
612
607
590
Relative Abundance
m/z
100
95
90
85
80
75
70
65
60
55
50
45
40
35
30
25
20
15
10
5
0
250
300
350
400
450
500
550
600
650
700
750


Relative Abundance
m/z
737
796
778
752
613

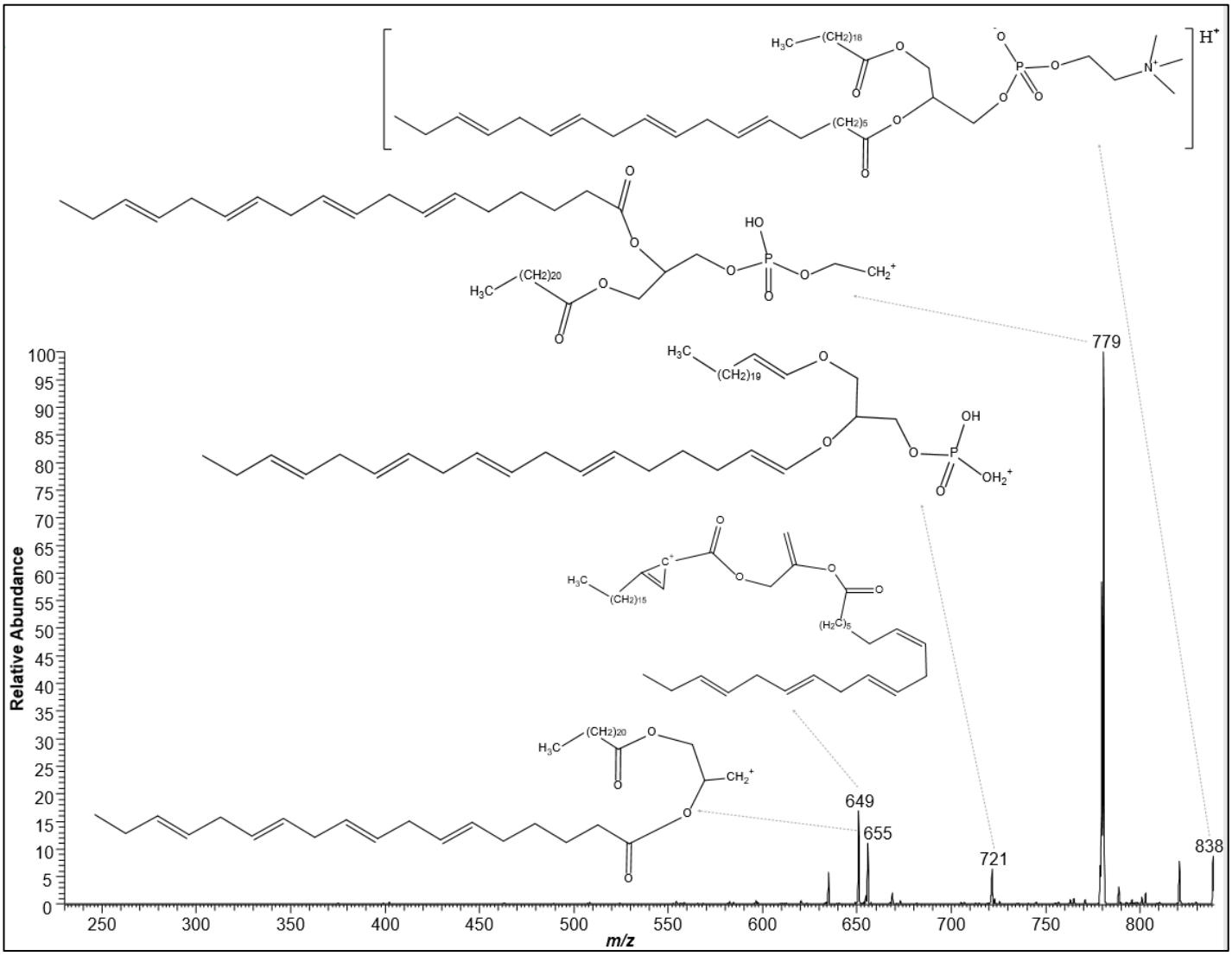
Relative Abundance
m/z
779
649
655
721
838


Relative Abundance
m/z
799
676
671
842
859

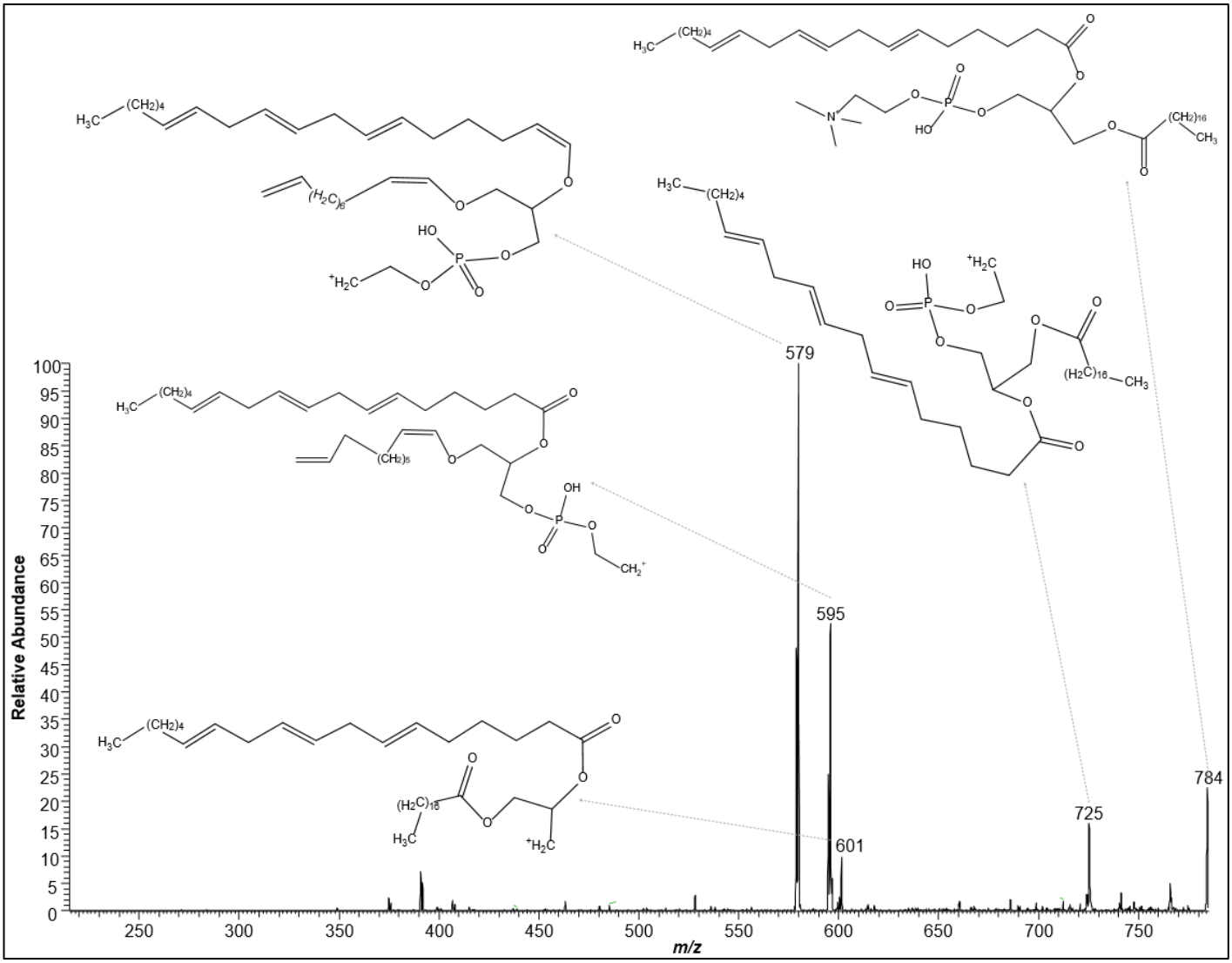
Relative Abundance
m/z
579
595
601
725
784

5. DISCUSSAO GERAL

Os resultados alcançados neste projeto fornecem informações de extrema importância tanto para o processo de infecção viral do ZIKA em mosquitos e em humanos como o mecanismo de infecção da DENV que leva à forma grave da doença.

Na abordagem da infecção viral em mosquitos (Anexo 6) foi possível verificar quais são os lipídios envolvidos nas primeiras 12 horas da infecção viral e conseguintemente os lipídios responsáveis pelo processo de instalação da maquinaria de replicação viral logo que o agente patogênico entra em contado com o hospedeiro. Os lipídios encontrados foram 3 triglicerídeos (TG), 1 esfingolípido (ESF), 3 colesteróis (Col), 2 diacilgliceróis (Diac) e 1 gangliosídeo (Gang); todos envolvidos nas primeiras fazes da formação do complexo de replicação viral, bem como na liberação, pelas células infectadas, de estruturas virais responssáveis pela evazão do sistema imune, como hexamero de NS1 e não permitindo que as células infectadas sejam reconhecidas e a replicação interrompida (mais detalhes estam apresentados no anexo 6).

No trabalho que foram analisadas as alterações metabólicas em humanos após a infecção por Zika (Anexo 3) foi possível verificar a presença de Angiotensina I, Angiotensina (1-7), PIP e PIP2 nos pacientes infectados por ZIKV. Os primeiros dois marcadores fazem parte do Sistema Renina-Angiotensina (SRA) que está envolvido na captação e excreção de sódio e potássio no rins, promovendo a vasoconstrição e regulação da pressão arterial, respectivamente [67,68]. O SRA sempre foi estudado com foco em seu papel na síndrome metabólica [69–71], entretanto mais recentemente tem-se verificado sua importância no processo de infecção viral conforme demonstrado em experimentos realizados com ratos knockout para a Enzima Conversora de Angiotensina II (ECA2) ou com medicamentos inibidores da ECA [72], esses estudos foram realizados com diversos vírus como H5N1 [73], H7N9 e DENV [74]; e mostram que a Ang(1-7) diminui a gravidade da infecção por patógenos em razão de alterar a maquinaria celular necessária para a replicação do patógeno, quebrando seu ciclo de vida [75,76]. Os resultados obtidos neste trabalho apontaram os peptídeos Ang I e Ang(1-7) como marcadores para os paciente infectados, sugerindo que o SRA é parte do processo da resposta imunológica com o ZIKV em seres humanos e também são os responsáveis pela ativação da via PI3K-Akt [77,78], desencadeando uma série de

fosforilações em lipídios pela atuação do receptor MAS que modula a ativação da PI3K e a ativação da Phosphatidylinositol Signaling System, sistema de sinalização celular que modula a autofagia e também a neurogênese.

Uma vez que no processo de infecção viral por ZIKV existem duas proteínas não estruturais, a NS4A e NS4B que inibem a via de sinalização Akt/mTOR [79], e essa inibição leva ao acúmulo dos metabólitos intermediários e precursores envolvidos na sinalização da via PI3K-Akt , sendo neste trabalho a primeira vez que são identificados lipídios específicos envolvidos no processo fisiopatológico da infecção por ZIKV e que podem estar relacionados diretamente com a resposta imune do organismos frente à infecção e, ao mesmo tempo, ,relacionados com a microcefalia em filhos de mães infectadas com ZIKV [1], podendo os marcadores apresentados neste trabalho (Anexo 3), serem de grande valia no entendimento da fisiopatologia da infecção viral e da microcefalia.

No terceiro trabalho desenvolvido neste projeto, que objetivava o diagnóstico da infecção de ZIKA utilizando espectrometria de massas (Anexo 4) foi apresentado uma abordagem por aprendizado de máquina utilizando Random Forest como ferramenta de análise, e onde foi possível criar uma plataforma *online* para o diagnóstico *in sílico* e identificar 42 marcadores com os quais é possível fazer este diagnóstico *in sílico* com base na assinatura espectral obtida por espectrometria de massas de alta resolução a partir das amostras biológicas dos pacientes utilizados no estudo. Alguns dos valores de resultados obtidos pela plataforma criada nesta abordagem foram 94,49% de acurácia, 93,33% de sensibilidade, 95,65 % de especificidade e 93,33% de precisão; que permitem pensar nesta técnica como perfeitamente viável para estudos epidemiológicos e como técnica de *screening* em casos de surtos. Isto se faz possível uma vez que a ferramenta diagnóstica é facilmente automatizável e pode ser operada por qualquer pessoa com um rápido curso em como operar o equipamento tendo em vista que o equipamento pode ser configurado para seu uso na rotina diagnóstica, sendo a assinatura espectral podendo ser analisada em outro lugar que não o do exame, ou seja, a técnica permite sua aplicação com dispositivos de telemedicina, que torna o exame rápido, prático e com baixo custo quando comparados as técincas convencionais de biologia molecular.

No trabalho com pacientes infectados com DENV os achados identificaram mediadores lipídicos que durante a infecção viral estão relacionados à sinalização, controle e manutenção da resposta imune e da patogênese do DENV. Estes lipídios foram fosfatidilcolinas (PC), triglicerídeos (TG) e precursores de fatores de ativação plaquetária (PAF). As PCs e TGs são alterações lipídicas encontradas quando o vírus assume o controle do metabolismo celular, controlando e regulando os mecanismos de autofagia para atender às necessidades da replicação viral [80]. Já as PAFs apontadas como marcadores tem sua formação por síntese de novo ou pela via de remodelação lipídica36. A formação de PAFs por síntese de novo está relacionada à manutenção das concentrações fisiológicas desse mediador quando o organismo está em homeostase, ou seja, concentrações constitutivas de PAF [81]. Os PAFs exibem atividade biológica em várias células e tecidos [82] e a interação dos agonistas do PAF ocorre através do receptor do PAF (PAFR) que e está presente na membrana plasmática e na membrana nuclear e sua ativação gera um feedback positivo para a produção de um pool de PAF [83,84].

A cascata de ativação da PAF promove uma infinidade de efeitos envolvidos nas respostas imunes e inflamatórias, como a produção de superóxido, tromboxano B2 e leucotrieno C4 [85], aumento da permeabilidade endotelial [86], aumento da produção de interleucinas pró-inflamatórias [87], recrutamento de eosinófilos [88], entre outros efeitos envolvidos na resposta imune contra a infecção viral; sendo a correlação entre o PAF e a ativação plaquetária importante no processo de infecção viral, especialmente para o DENV; a liberação endógena do PAF está relacionada a vários efeitos da inflamação aguda na infecção por DENV, como aumento da permeabilidade vascular, número de leucócitos alterados, trombocitopenia e graus de sangramento [89]. Assim, a identificação dos precursores do PAF como biomarcadores pode indicar alvos susceptiveis de intervenção com a finalidade de impedir uma possível resposta imune acentuada e que provoque efeitos deletórios ao hospeideiro como no casa da DENV em sua forma hemorrágica, como mostrado em detalhes no ANEXO 5.

6. CONCLUSÃO

Os resultados mostram que é perfeitamente possível realizar estudos abordando o mecanismo de infecção viral através da análise direta de amostras

biológicas oriundas de individuoas intectados, sendo estes individuoas pacientes infectados ou mosquitos infectados

Na abordagem da infecção viral em mosquitos, devido a presença de lipídios que compõem a lipoproteína solúvel formada por um hexâmero de NS1 mais éster de colesterol, esfingolípido, di e triacilglicerol como biomarcadores da infecção, é possível verificar se o pool lipídico encontrado nas primeiras horas de infecção corrobora com os novos estudos. que apontam para as células de mosquitos infectadas por flavivírus como capazes de secretar sNS1 [90–92]. Verificou-se também que essas três classes de lipídios são responsáveis pela formação da subunidade lipídica onde está instalado o mecanismo de replicação viral do ZIKV: a balsa lipídica [93], que também participa da via pela qual o sNS1 é secretado pela célula [92]; processos que correm já nas primeiras horas de infecção viral.

No trabalho que foram analisadas as alterações metabólicas em humanos após a infecção por Zika, todos os biomarcadores são substratos/produtos da ECA e quinases envolvidas na via PI3K-AKT-mTOR [40], resultado que amplia o conhecimento dos aspectos fisiopatológicos da doença, elucidando alvos moleculares da resposta imune celular no enfrentamento de infecçoes virais; fornecendo bases para novos desenvolvimentos no campo da farmacologia para terapias diferenciadas, intervenções e insights no gerenciamento de infecções por ZIKV.

No terceiro trabalho desenvolvido neste projeto, que objetivava o diagnóstico da infecção de ZIKA utilizando espectrometria de massas e a criação de uma plataforma *online* para o diagnostico *in sílico;* devido à natureza do método e aos excelentes resultados alcançados com o ZIKV, é possível afirmar que esse método consiste em uma técnica inovadora nos testes de diagnóstico de doenças. Usando a plataforma criada neste trabalho, imaginamos que classificadores para muitas doenças possam ser desenvolvidos e tendo como condição única que o soro dos pacientes com a doença a ser investigada conteha informações detectadas pelo espectrômetro de massa (ionizáveis); então, os algoritmos de aprendizado de máquina, Random Forest no caso específico, cuidam da extração de assitaturas discriminativas para a condição de interesse.

No trabalho com pacientes infectados com DENV o uso dos biomarcadores apresentados esclarece os possíveis mediadores da forma mais grave da doença, a

forma hemorrágica, uma vez que foram identificados uma série de precursores dos PAFs. Segundo dados da literatura, o aumento dos PAFs está intimamente relacionado a duas das principais características dessa infecção: febre hemorrágica16 e trombocitopenia [94]. Esses sintomas, no entanto, não resultam exclusivamente da infecção por DENV: eles também ocorrem em outras doenças infecciosas [95,96]. Portanto, futuros esforços na identificação de metabólitos diretamente relacionados a vários processos de infecção, conforme aqui realizado, permitirão verificar se o mecanismo envolvido nessas doenças é comum ou específico para cada patógeno. Além disso, nossos resultados podem possibilitar e incentivar a comunidade médica a rastrear pacientes com condições com potencial de agravamentos hemorrágicos com maior grau de confiança para prognóstico clínico.

7. REFERÊNCIAS

1. Dick, G. W. A. Zika Virus (I). Isolations and serological specificity. *Trans. R. Soc. Trop. Med. Hyg.* (1952). doi:10.1016/0035-9203(52)90042-4
2. Dick, G. W. A. Zika virus (II). Pathogenicity and physical properties. *Trans. R. Soc. Trop. Med. Hyg.* (1952). doi:10.1016/0035-9203(52)90043-6
3. Hennessey, M., Fischer, M. & Staples, J. E. Zika Virus Spreads to New Areas - Region of the Americas, May 2015-January 2016. *Am. J. Transplant.* (2016). doi:10.1111/ajt.13743
4. MacNamara, F. N. Zika virus: A report on three cases of human infection during an epidemic of jaundice in Nigeria. *Trans. R. Soc. Trop. Med. Hyg.* (1954). doi:10.1016/0035-9203(54)90006-1
5. Olson, J. G., Ksiazek, T. G., Suhandiman, G. & Triwibowo, V. Zika virus, a cause of fever in central java, indonesia. *Trans. R. Soc. Trop. Med. Hyg.* (1981). doi:10.1016/0035-9203(81)90100-0
6. Petersen, L. R., Jamieson, D. J., Powers, A. M. & Honein, M. A. Zika Virus. *New Engl J Med* (2016). doi:10.1056/NEJMra1602113
7. Grard, G. *et al.* Zika Virus in Gabon (Central Africa) - 2007: A New Threat from Aedes albopictus? *PLoS Negl. Trop. Dis.* (2014). doi:10.1371/journal.pntd.0002681

8. Brasil, P. *et al.* Zika Virus Infection in Pregnant Women in Rio de Janeiro — Preliminary Report. *N. Engl. J. Med.* NEJMoa1602412 (2016). doi:10.1056/NEJMoa1602412
9. Roehrig, J. T., Hombach, J. & Barrett, A. D. T. Guidelines for plaque-reduction neutralization testing of human antibodies to dengue viruses. in *Viral Immunology* (2008). doi:10.1089/vim.2008.0007
10. Bearcroft, W. G. C. Zika virus infection experimentally induced in a human volunteer. *Trans. R. Soc. Trop. Med. Hyg.* (1956). doi:10.1016/0035-9203(56)90091-8
11. ECDC. Rapid risk assessment - Zika virus infection outbreak, French Polynesia. 14 february 2014. *ECDC. Eur. Cent. Dis. Prev. Control* (2014).
12. Salge, A. K. M. *et al.* Infecção pelo vírus Zika na gestação e microcefalia em recém-nascidos: revisão integrativa de literatura. *Rev. Eletrônica Enferm.* (2016). doi:10.5216/ree.v18.39888
13. Cameron P. Simmons, Ph.D., Jeremy J. Farrar, M.D., Ph.D., Nguyen van Vinh Chau, M.D., Ph.D., and Bridget Wills, M.D., D. M. Dengue — NEJM. *The New England journal of medicine* (2012).
14. Diamond, M. S. & Pierson, T. C. Molecular Insight into Dengue Virus Pathogenesis and Its Implications for Disease Control. *Cell* **162**, 488–492 (2015).
15. Rothman, A. L. Immunity to dengue virus: A tale of original antigenic sin and tropical cytokine storms. *Nature Reviews Immunology* **11**, 532–543 (2011).
16. Guzman, M. G. *et al.* Dengue: A continuing global threat. *Nat. Rev. Microbiol.* (2010). doi:10.1038/nrmicro2460
17. Yacoub, S. & Wills, B. Predicting outcome from dengue. *BMC Medicine* (2014). doi:10.1186/s12916-014-0147-9
18. Tabachnick, W. J. Nature, nurture and evolution of intra-species variation in mosquito arbovirus transmission competence. *International Journal of Environmental Research and Public Health* (2013). doi:10.3390/ijerph10010249
19. Kröpelin, S. *et al.* Climate-driven ecosystem succession in the Sahara: The past 6000 years. *Science (80-.).* (2008). doi:10.1126/science.1154913

20. King, L. S. Plagues and Peoples. *JAMA* **236**, 2800 (1976).
21. Cloudsley-Thompson, J. L. Insects and history. *Br. Med. J.* **1**, 1220 (1977).
22. Vega-Rua, A., Zouache, K., Girod, R., Failloux, A.-B. & Lourenco-de-Oliveira, R. High Level of Vector Competence of Aedes aegypti and Aedes albopictus from Ten American Countries as a Crucial Factor in the Spread of Chikungunya Virus. *J. Virol.* (2014). doi:10.1128/jvi.00370-14
23. McFarlane, M. *et al.* Characterization of Aedes aegypti Innate-Immune Pathways that Limit Chikungunya Virus Replication. *PLoS Negl. Trop. Dis.* (2014). doi:10.1371/journal.pntd.0002994
24. Blair, C. D. & Olson, K. E. Mosquito immune responses to arbovirus infections. *Current Opinion in Insect Science* (2014). doi:10.1016/j.cois.2014.07.005
25. Rainey, S. M., Shah, P., Kohl, A. & Dietrich, I. Understanding the wolbachia-mediated inhibition of arboviruses in mosquitoes: Progress and challenges. *Journal of General Virology* (2014). doi:10.1099/vir.0.057422-0
26. Machain-Williams, C. *et al.* Association of human immune response to Aedes aegypti salivary proteins with dengue disease severity. *Parasite Immunol.* (2012). doi:10.1111/j.1365-3024.2011.01339.x
27. Ocampo, C. B. *et al.* Differential Expression of Apoptosis Related Genes in Selected Strains of Aedes aegypti with Different Susceptibilities to Dengue Virus. *PLoS One* (2013). doi:10.1371/journal.pone.0061187
28. Tanabe, M. & Kanehisa, M. Using the KEGG database resource. *Curr. Protoc. Bioinforma.* (2012). doi:10.1002/0471250953.bi0112s38
29. Harkewicz, R. & Dennis, E. A. Applications of Mass Spectrometry to Lipids and Membranes. *Annu. Rev. Biochem.* (2011). doi:10.1146/annurev-biochem-060409-092612
30. Carrasco-Pancorbo, A., Navas-Iglesias, N. & Cuadros-Rodríguez, L. From lipid analysis towards lipidomics, a new challenge for the analytical chemistry of the 21st century. Part I: Modern lipid analysis. *TrAC - Trends Anal. Chem.* **28**, 263–278 (2009).
31. Dabaja, M. Z. *et al.* Metabolic alterations induced by attenuated Zika virus in glioblastoma cells. *Cell Biosci.* **8**, (2018).
32. Melo, C. F. O. R. *et al.* A lipidomics approach in the characterization of zika-

infected mosquito cells: Potential targets for breaking the transmission cycle. *PLoS One* **11**, (2016).

33. Koriem, K. M. M. A lipidomic concept in infectious diseases. *Asian Pacific Journal of Tropical Biomedicine* **7**, 265–274 (2017).
34. Melo, C. F. O. R. *et al.* The role of lipids in the inception, maintenance and complications of dengue virus infection. *Sci. Rep.* (2018). doi:10.1038/s41598-018-30385-x
35. Amâncio, F. F. *et al.* Fatal Outcome of Infection By Dengue 4 in a Patient With Thrombocytopenic Purpura As a Comorbid Condition in Brazil. *Rev. Inst. Med. Trop. Sao Paulo* **56**, 267–270 (2014).
36. Melo, C. F. O. R. *et al.* A machine learning application based in random forest for integrating mass spectrometry-based metabolomic data: A simple screening method for patients with Zika virus. *Front. Bioeng. Biotechnol.* **6**, (2018).
37. Lam, S. M. & Shui, G. Lipidomics as a Principal Tool for Advancing Biomedical Research. *Journal of Genetics and Genomics* (2013). doi:10.1016/j.jgg.2013.06.007
38. Loizides-Mangold, U. On the future of mass-spectrometry-based lipidomics. *FEBS Journal* (2013). doi:10.1111/febs.12202
39. van der Meer-Janssen, Y. P. M., van Galen, J., Batenburg, J. J. & Helms, J. B. Lipids in host-pathogen interactions: Pathogens exploit the complexity of the host cell lipidome. *Progress in Lipid Research* (2010). doi:10.1016/j.plipres.2009.07.003
40. Melo, C. F. O. R. *et al.* Serum Metabolic Alterations upon Zika Infection. *Front. Microbiol.* **8**, (2017).
41. Sandra, K. & Sandra, P. Lipidomics from an analytical perspective. *Current Opinion in Chemical Biology* (2013). doi:10.1016/j.cbpa.2013.06.010
42. Navas-Iglesias, N., Carrasco-Pancorbo, A. & Cuadros-Rodríguez, L. From lipids analysis towards lipidomics, a new challenge for the analytical chemistry of the 21st century. Part II: Analytical lipidomics. *TrAC - Trends Anal. Chem.* (2009). doi:10.1016/j.trac.2008.12.004
43. Thi, E. P. *et al.* Lipid nanoparticle siRNA treatment of Ebola-virus-Makona-infected nonhuman primates. *Nature* (2015). doi:10.1038/nature14442

44. Schaefer, E. A. K. & Chung, R. T. HCV and host lipids: An intimate connection. *Semin. Liver Dis.* (2013). doi:10.1055/s-0033-1358524
45. Griffiths, W. J., Ogundare, M., Williams, C. M. & Wang, Y. On the future of 'omics': Lipidomics. in *Journal of Inherited Metabolic Disease* (2011). doi:10.1007/s10545-010-9274-4
46. Carrasco-Pancorbo, A., Navas-Iglesias, N. & Cuadros-Rodríguez, L. From lipid analysis towards lipidomics, a new challenge for the analytical chemistry of the 21st century. Part I: Modern lipid analysis. *TrAC - Trends Anal. Chem.* (2009). doi:10.1016/j.trac.2008.12.005
47. Hu, C. *et al.* Analytical strategies in lipidomics and applications in disease biomarker discovery. *Journal of Chromatography B: Analytical Technologies in the Biomedical and Life Sciences* (2009). doi:10.1016/j.jchromb.2009.01.038
48. BLIGH, E. G. & DYER, W. J. A rapid method of total lipid extraction and purification. *Can. J. Biochem. Physiol.* (1959). doi:10.1139/o59-099
49. FOLCH, J., LEES, M. & SLOANE STANLEY, G. H. A simple method for the isolation and purification of total lipides from animal tissues. *J. Biol. Chem.* (1957).
50. Fahy, E., Sud, M., Cotter, D. & Subramaniam, S. LIPID MAPS online tools for lipid research. *Nucleic Acids Res.* (2007). doi:10.1093/nar/gkm324
51. O'Donnell, V. B., Dennis, E. A., Wakelam, M. J. O. & Subramaniam, S. LIPID MAPS: Serving the next generation of lipid researchers with tools, resources, data, and training. *Sci. Signal.* (2019). doi:10.1126/scisignal.aaw2964
52. Chong, J. *et al.* MetaboAnalyst 4.0 : towards more transparent and integrative metabolomics analysis. *Nucleic Acids Res.* 1–9 (2018). doi:10.1093/nar/gky310
53. Guijas, C. *et al.* METLIN: A Technology Platform for Identifying Knowns and Unknowns. *Anal. Chem.* acs.analchem.7b04424 (2018). doi:10.1021/acs.analchem.7b04424
54. Molloy, J. C., Sommer, U., Viant, M. R. & Sinkins, S. P. Wolbachia modulates lipid metabolism in Aedes albopictus mosquito cells. *Appl. Environ. Microbiol.* (2016). doi:10.1128/AEM.00275-16
55. Chukkapalli, V., Heaton, N. S. & Randall, G. Lipids at the interface of virus-host interactions. *Current Opinion in Microbiology* (2012).

doi:10.1016/j.mib.2012.05.013

56. Alvisi, G., Madan, V. & Bartenschlager, R. Hepatitis C virus and host cell lipids: An intimate connection. *RNA Biology* (2011). doi:10.4161/rna.8.2.15011
57. Sheridan, D. A., Neely, R. D. G. & Bassendine, M. F. Hepatitis C virus and lipids in the era of direct acting antivirals (DAAs). *Clinics and Research in Hepatology and Gastroenterology* (2013). doi:10.1016/j.clinre.2012.07.002
58. Clark, A. E., Kaleta, E. J., Arora, A. & Wolk, D. M. Matrix-Assisted laser desorption ionization-time of flight mass spectrometry: A fundamental shift in the routine practice of clinical microbiology. *Clin. Microbiol. Rev.* **26**, 547–603 (2013).
59. Simmons, C. P. *et al.* Dengue. *N. Engl. J. Med.* **366**, 1423–32 (2012).
60. Petricoin, E. F. & Liotta, L. A. Mass spectrometry-based diagnostics: The upcoming revolution in disease detection. *Clinical Chemistry* (2003). doi:10.1373/49.4.533
61. Callesen, A. K. *et al.* Serum protein profiling by solid phase extraction and mass spectrometry: A future diagnostics tool? *Proteomics* (2009). doi:10.1002/pmic.200800382
62. Liang, Q., Liu, H., Xie, L. xiang, Li, X. & Zhang, A. H. High-throughput metabolomics enables biomarker discovery in prostate cancer. *RSC Adv.* (2017). doi:10.1039/C6RA25007F
63. Colombo, T. E. *et al.* Dengue virus surveillance: Detection of DENV-4 in the city of São José do Rio Preto, SP, Brazil. *Acta Trop.* **164**, 84–89 (2016).
64. Wishart, D. S. *et al.* HMDB 4.0: The human metabolome database for 2018. *Nucleic Acids Res.* (2018). doi:10.1093/nar/gkx1089
65. Guijas, C. *et al.* METLIN: A Technology Platform for Identifying Knowns and Unknowns. *Anal. Chem.* (2018). doi:10.1021/acs.analchem.7b04424
66. Kanehisa, M. *et al.* Data, information, knowledge and principle: Back to metabolism in KEGG. *Nucleic Acids Res.* (2014). doi:10.1093/nar/gkt1076
67. Tikellis, C. & Thomas, M. C. Angiotensin-converting enzyme 2 (ACE2) is a key modulator of the renin angiotensin system in health and disease. *International Journal of Peptides* (2012). doi:10.1155/2012/256294
68. Passos-Silva, D. G., Verano-Braga, T. & Santos, R. A. S. Angiotensin-(1--7):

beyond the cardio-renal actions. *Clin. Sci.* **124**, 443–456 (2012).

69. Van Vark, L. C. *et al.* Angiotensin-converting enzyme inhibitors reduce mortality in hypertension: A meta-analysis of randomized clinical trials of renin-angiotensin-aldosterone system inhibitors involving 158 998 patients. *Eur. Heart J.* (2012). doi:10.1093/eurheartj/ehs075
70. Santos, R. A. S., Ferreira, A. J., Verano-Braga, T. & Bader, M. Angiotensin-converting enzyme 2, angiotensin-(1-7) and Mas: New players of the renin-angiotensin system. *J. Endocrinol.* (2013). doi:10.1530/JOE-12-0341
71. Cabandugama, P. K., Gardner, M. J. & Sowers, J. R. The Renin Angiotensin Aldosterone System in Obesity and Hypertension: Roles in the Cardiorenal Metabolic Syndrome. *Medical Clinics of North America* (2017). doi:10.1016/j.mcna.2016.08.009
72. Hernández-Fonseca, J. P., Durán, A., Valero, N. & Mosquera, J. Losartan and enalapril decrease viral absorption and interleukin 1 beta production by macrophages in an experimental dengue virus infection. *Arch. Virol.* (2015). doi:10.1007/s00705-015-2581-1
73. Zou, Z. *et al.* Angiotensin-converting enzyme 2 protects from lethal avian influenza A H5N1 infections. *Nat. Commun.* (2014). doi:10.1038/ncomms4594
74. Lumbers, E. R. & Pringle, K. G. Roles of the circulating renin-angiotensin-aldosterone system in human pregnancy. *American Journal of Physiology - Regulatory Integrative and Comparative Physiology* (2014). doi:10.1152/ajpregu.00034.2013
75. Fedson, D. S. Treating the host response to emerging virus diseases: lessons learned from sepsis, pneumonia, influenza and Ebola. *Ann. Transl. Med.* (2016). doi:10.21037/atm.2016.11.03
76. Saraiva, V. B. *et al.* Impairment of the Plasmodium falciparum erythrocytic cycle induced by angiotensin peptides. *PLoS One* (2011). doi:10.1371/journal.pone.0017174
77. Giani, J. F. *et al.* Angiotensin-(1-7) stimulates the phosphorylation of JAK2, IRS-1 and Akt in rat heart in vivo: Role of the AT1 and Mas receptors. *Am. J. Physiol. - Hear. Circ. Physiol.* (2007). doi:10.1152/ajpheart.01395.2006
78. Sampaio, W. O. *et al.* Angiotensin-(1-7) through receptor Mas mediates

endothelial nitric oxide synthase activation via Akt-dependent pathways. *Hypertension* (2007). doi:10.1161/01.HYP.0000251865.35728.2f

79. Liang, Q. *et al.* Zika Virus NS4A and NS4B Proteins Deregulate Akt-mTOR Signaling in Human Fetal Neural Stem Cells to Inhibit Neurogenesis and Induce Autophagy. *Cell Stem Cell* (2016). doi:10.1016/j.stem.2016.07.019
80. Heaton, N. S. & Randall, G. Dengue virus-induced autophagy regulates lipid metabolism. *Cell Host Microbe* **8**, 422–432 (2010).
81. Blank, M. L., Lee, Y. J., Cress, E. A. & Snyder, F. Stimulation of the de novo pathway for the biosynthesis of platelet-activating factor (PAF) via cytidylyltransferase activation in cells with minimal endogenous PAF production. *J. Biol. Chem.* **263**, 5656–5661 (1988).
82. Ishii, S. & Shimizu, T. Platelet-activating factor (PAF) receptor and genetically engineered PAF receptor mutant mice. *Prog Lipid Res* **39**, 41–82 (2000).
83. Prescott, S. M., Zimmerman, G. A., Stafforini, D. M. & McIntyre, T. M. Platelet-activating factor and related lipid mediators. *Annu. Rev. Biochem.* **69**, 419–445 (2000).
84. Liu, Y. *et al.* Current Understanding of Platelet-Activating Factor Signaling in Central Nervous System Diseases. *Molecular Neurobiology* **54**, 5563–5572 (2017).
85. Dent, G. *et al.* Protein kinase C inhibition enhances platelet-activating factor-induced eicosanoid production in human eosinophils. *Am. J. Respir. Cell Mol. Biol.* **18**, (1998).
86. Liu, L. *et al.* Triple role of platelet-activating factor in eosinophil migration across monolayers of lung epithelial cells: eosinophil chemoattractant and priming agent and epithelial cell activator. *J. Immunol.* **161**, 3064–70 (1998).
87. Roth, M. *et al.* Platelet-activating factor exerts mitogenic activity and stimulates expression of interleukin 6 and interleukin 8 in human lung fibroblasts via binding to its functional receptor. *J Exp Med* **184**, 191–201 (1996).
88. Lou, Y. P. *et al.* Platelet-activating factor induces goblet cell hyperplasia and mucin gene expression in airways. *Am. J. Respir. Crit. Care Med.* **157**, 1927–1934 (1998).
89. Souza, D. G. *et al.* Essential role of platelet-activating factor receptor in the

pathogenesis of Dengue virus infection. *Proc. Natl. Acad. Sci. U. S. A.* **106**, 14138–43 (2009).

90. Accepted, J. V. I., Posted, M., Society, A. & Reserved, A. R. Secretion of the non-structural protein 1 of dengue virus from infected mosquito cells: facts and speculations. *J. Virol.* 1–18 (2018). doi:10.1128/JVI.00275-18
91. Thiemmeca, S. *et al.* Secreted NS1 Protects Dengue Virus from Mannose-Binding Lectin–Mediated Neutralization. *J. Immunol.* **197**, 4053–4065 (2016).
92. Alcalá, A. C. *et al.* The dengue virus non-structural protein 1 (NS1) is secreted from infected mosquito cells via a non-classical caveolin-1- dependent pathway. *J. Gen. Virol.* **98**, 2088–2099 (2017).
93. Martï¿½n-Acebes, M. A., Vï¿½zquez-Calvo, ï¿½ngela & Saiz, J. C. Lipids and flaviviruses, present and future perspectives for the control of dengue, Zika, and West Nile viruses. *Progress in Lipid Research* **64**, 123–137 (2016).
94. De Azeredo, E. L., Monteiro, R. Q. & De-Oliveira Pinto, L. M. Thrombocytopenia in dengue: Interrelationship between virus and the imbalance between coagulation and fibrinolysis and inflammatory mediators. *Mediators of Inflammation* **2015**, (2015).
95. Assinger, A. Platelets and infection - An emerging role of platelets in viral infection. *Frontiers in Immunology* **5**, (2014).
96. Zapata, J. C., Cox, D. & Salvato, M. S. The Role of Platelets in the Pathogenesis of Viral Hemorrhagic Fevers. *PLoS Negl. Trop. Dis.* **8**, (2014).
97. Chang, C., Ortiz, K., Ansari, A. & Gershwin, M. E. The Zika outbreak of the 21st century. *J. Autoimmun.* **68**, 1–13 (2016).
98. Faria, N. R. *et al.* Zika virus in the Americas: Early epidemiological and genetic findings. *Science (80-.).* **352**, 345–349 (2016).
99. Cao-Lormeau, V.-M. *et al.* Guillain-Barre; Syndrome outbreak associated with Zika virus infection in French Polynesia: a case-control study. *Lancet* **387**, 1531–1539 (2016).
100. Lindenbach, B. D. & Rice, C. M. Molecular Biology of Flavivirus. *Adv. Virus Res.* **59**, 23–62 (2003).
101. Moradpour, D. & Penin, F. *Hepatitis C Virus: From Structure to Function*. *Current topics in microbiology and immunology* **369**, (2013).

102. Bollati, M. *et al.* Structure and functionality in flavivirus NS-proteins: Perspectives for drug design. *Antiviral Research* **87**, 125–148 (2010).
103. Rastogi, M., Sharma, N. & Singh, S. K. Flavivirus NS1: A multifaceted enigmatic viral protein. *Virology Journal* **13**, (2016).
104. Noisakran, S. *et al.* Association of dengue virus NS1 protein with lipid rafts. *J. Gen. Virol.* **89**, 2492–2500 (2008).
105. Asif, A. *et al.* Zika Virus: Immune Evasion Mechanisms, Currently Available Therapeutic Regimens, and Vaccines. *Viral Immunol.* vim.2017.0046 (2017). doi:10.1089/vim.2017.0046
106. Conde, J. N., Silva, E. M., Barbosa, A. S. & Mohana-Borges, R. The complement system in flavivirus infections. *Frontiers in Microbiology* **8**, (2017).
107. Beatty, P. R. *et al.* Dengue virus NS1 triggers endothelial permeability and vascular leak that is prevented by NS1 vaccination. *Sci. Transl. Med.* **7**, (2015).
108. Mackenzie, J. M., Jones, M. K. & Young, P. R. Immunolocalization of the Dengue virus nonstructural glycoprotein NS1 suggests a role in viral RNA replication. *Virology* (1996). doi:10.1006/viro.1996.0307
109. Young, P. R., Hilditch, P. A., Bletchly, C. & Halloran, W. An antigen capture enzyme-linked immunosorbent assay reveals high levels of the dengue virus protein NS1 in the sera of infected patients. *J. Clin. Microbiol.* (2000). doi:10.1002/anie.201411533
110. Muller, D. A., Corrie, S. R., Coffey, J., Young, P. R. & Kendall, M. A. Surface modified microprojection arrays for the selective extraction of the dengue virus NS1 protein as a marker for disease. *Anal. Chem.* (2012). doi:10.1021/ac2034387
111. Ricciardi-Jorge, T. *et al.* Development of a quantitative NS1-capture enzyme-linked immunosorbent assay for early detection of yellow fever virus infection. *Sci. Rep.* **7**, (2017).
112. Lim, J. M. *et al.* An electrochemical peptide sensor for detection of dengue fever biomarker NS1. *Anal. Chim. Acta* **1026**, 109–116 (2018).
113. Wasik, D., Mulchandani, A. & Yates, M. V. Point-of-Use Nanobiosensor for Detection of Dengue Virus NS1 Antigen in Adult Aedes aegypti: A Potential Tool for Improved Dengue Surveillance. *Anal. Chem.* **90**, 679–684 (2018).

114. Xie, Q. *et al.* Structure and Function of the Non-Structural Protein of Dengue Virus and its Applications in Antiviral Therapy. *Curr. Top. Med. Chem.* **17**, 371–380 (2017).
115. Alcalá, A. C. *et al.* The dengue virus non-structural protein 1 (NS1) is secreted efficiently from infected mosquito cells. *Virology* **488**, 278–287 (2016).
116. Brown, W. C. *et al.* Extended surface for membrane association in Zika virus NS1 structure. *Nat. Struct. Mol. Biol.* **23**, 865–867 (2016).
117. Mason, P. W. Maturation of Japanese encephalitis virus glycoproteins produced by infected mammalian and mosquito cells. *Virology* **169**, 354–364 (1989).
118. Muller, D. A. & Young, P. R. The flavivirus NS1 protein: Molecular and structural biology, immunology, role inpathogenesis and application asadiagnostic biomarker. *Antiviral Research* **98**, 192–208 (2013).
119. Melo, C. F. O. R. *et al.* The role of lipids in the inception, maintenance and complications of dengue virus infection. *Sci. Rep.* **8**, (2018).
120. Niu, Z., Zhang, W., Yu, C., Zhang, J. & Wen, Y. Recent advances in biological sample preparation methods coupled with chromatography, spectrometry and electrochemistry analysis techniques. *TrAC - Trends in Analytical Chemistry* **102**, 123–146 (2018).
121. Nagana Gowda, G. A. & Djukovic, D. Overview of mass spectrometry-based metabolomics: Opportunities and challenges. *Methods Mol. Biol.* **1198**, 3–12 (2014).
122. Tisoncik-Go, J. *et al.* Integrated Omics Analysis of Pathogenic Host Responses during Pandemic H1N1 Influenza Virus Infection: The Crucial Role of Lipid Metabolism. *Cell Host Microbe* **19**, 254–266 (2016).
123. Hofmann, S. *et al.* Complex lipid metabolic remodeling is required for efficient hepatitis C virus replication. *Biochim. Biophys. Acta (BBA)-Molecular Cell Biol. Lipids* (2018).
124. Madigan, C. A. *et al.* Lipidomic Analysis Links Mycobactin Synthase K to Iron Uptake and Virulence in M. tuberculosis. *PLoS Pathog.* **11**, 1–21 (2015).
125. Gao, Q. *et al.* Phospholipid homeostasis maintains cell polarity, development and virulence in Metarhizium robertsii. *Environ. Microbiol.* **18**, 3976–3990

(2016).

126. Lima, E. O. *et al.* MALDI imaging detects endogenous digoxin in glioblastoma cells infected by Zika virus—Would it be the oncolytic key? *J. Mass Spectrom.* **53**, (2018).
127. Gutsche, I. *et al.* Secreted dengue virus nonstructural protein NS1 is an atypical barrel-shaped high-density lipoprotein. *Proc. Natl. Acad. Sci.* **108**, 8003–8008 (2011).
128. Pike, L. J. Lipid rafts: bringing order to chaos. *J. Lipid Res.* **44**, 655–67 (2003).
129. Takahashi, T., Suzuki, T., Takahashi, T. & Suzuki, T. Function of Membrane Rafts in Viral Lifecycles and Host Cellular Response, Function of Membrane Rafts in Viral Lifecycles and Host Cellular Response. *Biochem. Res. Int. Biochem. Res. Int.* **2011**, **2011**, e245090 (2011).
130. Edeling, M. A., Diamond, M. S. & Fremont, D. H. Structural basis of Flavivirus NS1 assembly and antibody recognition. *Proc. Natl. Acad. Sci.* **111**, 4285–4290 (2014).
131. Akey, D. L. *et al.* Flavivirus NS1 structures reveal surfaces for associations with membranes and the immune system. *Science (80-.).* **343**, 881–885 (2014).
132. Xu, X. *et al.* Contribution of intertwined loop to membrane association revealed by Zika virus full-length NS1 structure. *EMBO J.* **35**, 2170–2178 (2016).
133. Avirutnan, P. *et al.* Binding of Flavivirus Nonstructural Protein NS1 to C4b Binding Protein Modulates Complement Activation. *J. Immunol.* **187**, 424–433 (2011).
134. Watterson, D., Modhiran, N. & Young, P. R. The many faces of the flavivirus NS1 protein offer a multitude of options for inhibitor design. *Antiviral Research* **130**, 7–18 (2016).
135. Akey, D. L., Brown, W. C., Jose, J., Kuhn, R. J. & Smith, J. L. Structure-guided insights on the role of NS1 in flavivirus infection. *BioEssays* **37**, 489–494 (2015).
136. Falconar, A. K. I. & Young, P. R. Immunoaffinity purification of native dimer forms of the flavivirus non-structural glycoprotein, NS1. *J. Virol. Methods* **30**, 323–332 (1990).
137. Gibson, C. A., Schlesinger, J. J. & Barrett, A. D. Prospects for a virus non-

structural protein as a subunit vaccine. *Vaccine* **6**, 7–9 (1988).

138. Shi, P. Y. Unraveling a flavivirus enigma. *Science* **343**, 849–850 (2014).
139. Xia, H. *et al.* An evolutionary NS1 mutation enhances Zika virus evasion of host interferon induction. *Nat. Commun.* **9**, (2018).
140. Chung, K. M. *et al.* West Nile virus nonstructural protein NS1 inhibits complement activation by binding the regulatory protein factor H. *Proc. Natl. Acad. Sci. U. S. A.* **103**, 19111–6 (2006).
141. Avirutnan, P. *et al.* Antagonism of the complement component C4 by flavivirus nonstructural protein NS1. *J. Exp. Med.* **207**, 793–806 (2010).
142. Levashina, E. A. *et al.* Conserved role of a complement-like protein in phagocytosis revealed by dsRNA knockout in cultured cells of the mosquito, Anopheles gambiae. *Cell* **104**, 709–718 (2001).
143. Juárez-Martínez, A. B. *et al.* Detection and sequencing of defective viral genomes in C6/36 cells persistently infected with dengue virus 2. *Arch. Virol.* **158**, 583–599 (2013).
144. Youn, S., Cho, H., Fremont, D. H. & Diamond, M. S. A Short N-Terminal Peptide Motif on Flavivirus Nonstructural Protein NS1 Modulates Cellular Targeting and Immune Recognition. *J. Virol.* **84**, 9516–9532 (2010).
145. Lee, J. M., Crooks, A. J. & Stephenson, J. R. The synthesis and maturation of a non-structural extracellular antigen from Tick-borne encephalitis virus and its relationship to the intracellular NS1 protein. *J. Gen. Virol.* **70**, 335–343 (1989).
146. Pietiäinen, V. M., Marjomäki, V., Heino, J. & Hyypiä, T. Viral entry, lipid rafts and caveosomes. *Annals of Medicine* **37**, 394–403 (2005).
147. Obayashi, T. K., Akahashi, M. T., Agatsuka, Y. N. & Irabayashi, Y. H. Lipid Dynamics and Pathobiology in Membrane Lipid Rafts Lipid Rafts. *Biol Pharm Bill* **29**, 1526–1531 (2006).
148. Huang, J. H. *et al.* Identification of the HIV-1 gp41 core-binding motif in the scaffolding domain of caveolin-1. *J. Biol. Chem.* **282**, 6143–6152 (2007).
149. Diwaker, D., Mishra, K. P., Ganju, L. & Singh, S. B. Protein Disulfide Isomerase Mediates Dengue Virus Entry in Association with Lipid Rafts. *Viral Immunol.* **28**, 153–160 (2015).
150. Simons, K. & Toomre, D. Lipid rafts and signal transduction. *Nat. Rev. Mol. Cell*

Biol. **1**, 31–39 (2000).

151. Vazeille, M., Gaborit, P., Mousson, L., Girod, R. & Failloux, A. B. Competitive advantage of a dengue 4 virus when co-infecting the mosquito Aedes aegypti with a dengue 1 virus. *BMC Infect. Dis.* (2016). doi:10.1186/s12879-016-1666-0
152. Worley, B., Halouska, S. & Powers, R. Utilities for quantifying separation in PCA/PLS-DA scores plots. *Anal. Biochem.* **433**, 102–104 (2013).
153. Kalivodová, A. *et al.* PLS-DA for compositional data with application to metabolomics. *J. Chemom.* **29**, 21–28 (2015).

8. APENDICE

8.1. Autorização da revista para uso dos artigos publicados no periódico Frontiers:

Sob os Termos e Condições do Periodico Frontiers, os autores mantêm os direitos autorais de seus trabalhos. Além disso, todos os artigos da Frontiers são de acesso aberto e distribuídos sob os termos da Licença de atribuição Creative Commons (CC-BY 3,0), que permite o uso, distribuição e reprodução de material de artigos publicados, desde que os autores e a fonte originais sejam creditados, e sujeito a quaisquer avisos de direitos autorais sobre qualquer conteúdo de terceiros.
Mais informações sobre o CC-BY podem ser encontradas em:

https://www.frontiersin.org/about/author-guidelines#GuidelinesLicence
(acessado em 25/10/2019)

https://creativecommons.org/licenses/by/4.0/ (acessado em 25/10/2019)

8.2. Autorização da revista para uso dos artigos publicados no periódico Scientific Reports:

O periodico Scientific Reports não exige que os autores atribuam direitos autorais de seus trabalhos de pesquisa originais publicados na revista. Os artigos são

ANEXOS

ANEXO 1: CEP - Projeto de Pesquisa: Síndrome congênita do Zika: investigação da susceptibilidade à infecção congênita a partir de uma coorte oriunda de várias regiões do Brasil

MINISTÉRIO DA SAÚDE - Conselho Nacional de Saúde - Comissão Nacional de Ética em Pesquisa – CONEP
PROJETO DE PESQUISA ENVOLVENDO SERES HUMANOS

Projeto de Pesquisa:
Síndrome congênita do Zika: investigação da susceptibilidade à infecção congênita a partir de uma coorte oriunda de várias regiões do Brasil

Informações Preliminares

Responsável Principal

CPF/Documento: 323.464.414-49	Nome: Denise Pontes Cavalcanti
Telefone: 1935210385	E-mail: denisepcavalcanti@gmail.com

Instituição Proponente

CNPJ:	Nome da Instituição: Faculdade de Ciências Medicas - UNICAMP

Essa submissão de emenda é exclusiva do seu Centro Coordenador?
A emenda é exclusiva de seu Centro Coordenador, então as alterações realizadas em seu projeto, em virtude da emenda, NÃO serão replicadas nos Centros Participantes vinculados e nos Comitês de Ética das Instituições Coparticipantes, quando da sua aprovação.

É um estudo Internacional? Sim

Assistentes

CPF/Documento	Nome
368.452.888-95	CYNTHIA SILVEIRA
094.355.286-94	KARINA DA COSTA SILVEIRA

Equipe de Pesquisa

CPF/Documento	Nome
216.012.148-71	Jose Luiz Proenca Modena
309.706.013-87	erlane marques ribeiro
326.422.468-25	DANILO CICCONE MIGUEL
214.063.228-14	Rodrigo Ramos Catharino
390.953.980-72	LAVINIA SCHULER FACCINI
004.672.507-58	Dafne Dain Gandelman Horovitz
613.728.113-20	Ian Mikardo Lima Feitosa
271.855.160-72	Clarice Weis Arns
004.112.558-43	Saulo Duarte Passos
000.484.038-06	Paolo Marinho de Andrade Zanotto
698.671.271-53	BENILTON DE SA CARVALHO

Área de Estudo

Área Temática Especial
Genética Humana:
(Haverá envio para o exterior de material genético ou qualquer material biológico humano para obtenção de material genético, salvo nos casos em que houver cooperação com o Governo Brasileiro;)

Grandes Áreas do Conhecimento (CNPq)
- Grande Área 4. Ciências da Saúde

Propósito Principal do Estudo (OMS)
- Outros

Título Público da Pesquisa: Síndrome congênita do Zika: investigação da susceptibilidade à infecção congênita a partir de uma coorte oriunda de várias regiões do Brasil

Contato Científico: Denise Pontes Cavalcanti

Desenho de Estudo / Apoio Financeiro

Desenho:

Estudo de coorte retrospectivo de uma série de crianças acometidas pela síndrome congênita do Zika e suas mães, oriundas de várias regiões do Brasil, sobretudo do nordeste brasileiro.A coleta dos materiais biológicos será realizada durante os mutirões nos respectivos locais onde contamos com médicos colaboradores do presente projeto, a saber Fortaleza e São Luís. Normalmente esses mutirões têm por finalidade a avaliação clínica e orientação das famílias. Para fins desse projeto incluiremos a informação sobre o TCLE e a coleta de exames.

Apoio Financeiro

CNPJ	Nome	E-mail	Telefone	Tipo
01.263.896/0004-07	MINISTERIO DA CIENCIA, TECNOLOGIA E INOVACAO		2121232703	Institucional Principal

Palavra Chave

Palavra-chave
zika vírus
microbioma
microcefalia
susceptibilidade genética
viroma
lipidoma

Detalhamento do Estudo

Resumo:

O vírus Zika (ZIKV) é um vírus emergente no Brasil que pode levar ao desenvolvimento de uma doença exantemática, muitas vezes associada à febre baixa, fadiga, mialgia e conjuntivite. O ZIKV também está relacionado a quadros graves de complicações neurológicas, como a Síndrome de Guillain-Barré, e anomalias fetais, como a microcefalia. Entretanto, os fatores de risco determinantes para o desenvolvimento dessas manifestações graves ainda não são conhecidos. Desse modo, o objetivo principal desse estudo é buscar fatores que possam explicar essas diferenças de susceptibilidade materno-fetal e que possam estar envolvidos com o papel teratogênico desse vírus. Com esse propósito é preciso investigar uma série de mães e crianças expostas ao ZIKV durante o pré-natal, incluindo aquelas afetadas pelo que se convencionou chamar de síndrome congênita do Zika, e crianças sem sequelas. De um lado a investigação dar-se-á por meio da investigação do exoma expandido com o objetivo de avaliar incialmente genes relacionados à microcefalia e, em seguida buscar variações genéticas preferencialmente associadas às crianças afetadas que possam ser caracterizadas como polimorfismos que conferem maior ou menor susceptibilidade à ação teratogênica do ZIKV. De outra parte, sabendo que o microbioma intestinal humano é essencial, entre outros, pelo desenvolvimento do tecido linfóide secundário e na promoção de uma imunidade heteróloga, interferindo na permeabilidade da barreira hematoencefálica e hematoplacentária e modulando a resposta contra infecções virais, pretendemos também investigar o microbioma em mulheres que foram expostas ao ZIKV e que tiveram ou não filhos afetados pela síndrome congênita do Zika.

Introdução:

O Zika vírus (ZIKV) - as consequências da infecção, o diagnóstico e a prevenção O Zika vírus (ZIKV) é um arbovírus, transmitido por mosquitos do gênero Aedes, pertencente ao gênero Flavivirus da família Flaviviridae (ICTV, 2016). Ele é um vírus pequeno, com 50nm de diâmetro e genoma composto por RNA fita simples de polaridade positiva de aproximadamente 10.800 nucleotídeos. O ZIKV expressa três proteínas estruturais (capsídeo, pré-membrana/membrana e envelope) e sete proteínas não estruturais: NS1, NS2a, NS2b, NS3, NS4a, NS4b e NS5 (Pierson e Diamond, 2013). Embora o ZIKV tenha sido isolado pela primeira vez em 1947 em macacos Rhesus na floresta de Zika, Uganda, até 2007 apenas um pequeno número de casos esporádicos de infecção por ZIKV foi documentado em humanos. Esse cenário foi alterado com a introdução da cepa asiática desse vírus e sua circulação em ilhas do pacífico (Duffy et al., 2009). Entre janeiro de 2007 e março de 2016 foram relatados casos de ZIKV em aproximadamente 52 países, principalmente nas Américas e no Pacífico Ocidental (Broutet et al., 2016). No início de 2015 foram confirmados no nordeste brasileiro os primeiros casos de infecção pelo ZIKV, e em fevereiro de 2016 vinte e dois estados brasileiros confirmaram transmissão autóctone do ZIKV (Zanluca e Santos, 2016). De um modo geral, o ZIKV causa uma doença que se apresenta com febre baixa ou ausente, prurido, artralgia, edema de membros inferiores, conjuntivite e sobretudo exantema maculopapular que pode se estender por 4 a 7 dias. Geralmente, essa doença tem evolução benigna e a infecção pode ser assintomática em aproximadamente 80% dos infectados, sugerindo que uma resposta imunológica eficiente durante o início do ciclo infeccioso pode eliminar o vírus (European Centre For Disease Prevention And Control, 2015). Além disso, há relatos de manifestações graves associadas ao ZIKV, como Guillain-Barré, meningoencefalite (Marrs et al, 2016; Carteaux et al, 2016) e o desenvolvimento de anomalias fetais, sobretudo a microcefalia, a partir da transmissão vertical. No Brasil, dois óbitos em adultos em decorrência de infecção por ZIKV foram confirmados (Brasil, 2016). Essa possível associação do ZIKV com anomalias do sistema nervoso central (SNC) em fetos a partir da infecção congênita, inicialmente suspeitada por clínicos nos estados de Pernambuco e da Paraíba, foi, de fato, levantada pelo Ministério da Saúde do Brasil em meados de 2015, devido ao aumento do número de crianças com microcefalia ao nascimento em áreas acometidas pelo ZIKV. As informações sobre a evolução da infecção por ZIKV na gravidez ainda são limitadas. Aparentemente, a infecção por ZIKV pode ocorrer em qualquer trimestre da gestação e não há evidência de que a doença seja mais grave em gestantes (Besnard et al, 2014). Entretanto, há fortes e contundentes evidências de transmissão vertical do ZIKV, mostrando que o conjunto de efeitos da infecção congênita por esse vírus pode ser devastador para a feto (Oliveira Melo et al, 2016, Mlakar et al, 2016; Driggers et al, 2016; Brasil et al, 2016). A despeito da ausência de estudos epidemiológicos de ambos os desenhos, caso-controle e coorte, uma revisão da literatura recente avaliando ambos os critérios – critérios para provar a teratogenicidade de um agente e os critérios de Bradford Hill para evidenciar causalidade de uma doença, conclui que existe uma relação causal entre a infecção pré-natal pelo ZIKV e as graves anomalias cerebrais induzindo clinicamente à microcefalia (Rasmussen et al., 2016). Estudos em modelos animais também corroboram com essa associação, uma vez que foi demonstrado em modelo murino a habilidade do ZIKV em cruzar a barreira placentária e induzir dano neurológico e no desenvolvimento do feto (Cugola et al, 2016, Miner et al, 2016). Uma vez estabelecida a relação causal entre a infecção pré-natal

pelo ZIKV e os efeitos deletérios no SNC fetal, os principais esforços da comunidade científica deveriam ser intensificados sobretudo em medidas preventivas. No entanto, pelo menos três questões são críticas para as tais medidas preventivas: 1 – o entendimento sobre o espectro de anomalias fetais causadas pelo ZIKV, 2 – os reais riscos, relativo e absoluto, dos efeitos adversos nos fetos, cujas mães se infectarem durante a gestação e 3 – os fatores que poderiam influenciar o risco fetal de uma mulher que tem a infecção durante a gestação (Rasmussen et al, 2016). Sobre o entendimento do espectro fenotípico das crianças expostas ao ZIKV, além de relatos isolados de crianças com microcefalia associada sobretudo a lesões cerebrais como atrofia cerebral e calcificações cerebrais (Vasco Aragão et al., 2016; Hazin et al., 2016), hidropisia (Sarno et al, 2016) e letalidade (Brasil et al, 2016), a avaliação preliminar de 35 bebês expostos à infecção pelo ZIKV mostrou também outras anomalias (excesso de pele em couro cabeludo e dorso, contraturas articulares e alterações neurológicas características), possivelmente associadas à teratogenicidade do ZIKV (Schuler-Faccini et al, 2016). Mais recentemente, seguindo o trabalho da força-tarefa que avaliou esses primeiros 35 bebês mostrando um possível espectro fenotípico (Schuler-Faccini et al, 2016), concluímos um estudo detalhando o espectro fenotípico da infecção congênita pelo ZIKV. Este quadro se estende desde crianças com microcefalia de leve/moderada a quadros fenotipicamente típicos e, portanto, reconhecíveis, de microcefalias muito graves acompanhadas de importante quadro neurológico e dismórfico e, por vezes associado a um quadro mais complexo e generalizado e que inclui contraturas de membros (artrogripose) (manuscrito submetido à publicação). Os demais itens, 2 e 3, mencionados acima e que são críticos para as medidas preventivas vão depender dos estudos epidemiológicos para entendimento dos riscos fetais quando uma mulher se infecta durante a gestação e dos estudos que visam entender quais fatores, genéticos ou não, podem produzir diferentes susceptibilidades contribuindo ou não para o risco fetal à exposição pré-natal ao ZIV. Especificamente sobre a investigação de fatores que poderiam influenciar o risco fetal de uma mulher que tem a infecção durante a gestação, ou seja fatores relacionados à susceptibilidade, ocupar-se-á o presente projeto. A esse respeito vale ressaltar recente estudo de análise de bioinformática mostrando que a infecção pelo ZIKV induz alterações na expressão gênica da resposta imune de células neurais progenitoras, indicando que essas células são capazes de ativar vias do sistema imune pró-inflamação a partir da infecção viral (Rolfe et al, 2016).Ainda levando em conta o fenótipo ou o espectro fenotípico da exposição pré-natal ao ZIKV que se está delineando, alguns pontos relacionados ao diagnóstico diferencial devem ser levados em conta. Hoje são conhecidos mais de 16 diferentes tipos de microcefalia primária e mais de 25 genes relacionados à microcefalia (OMIM; Mahmood et al., 2011; Morris-Rosendhal et al., 2015; Rump et al., 2016; Passemard et al., 2016). Portanto, uma vez estabelecido o fenótipo, ou espectro fenotípico relacionado à infecção congênita pelo ZIKV, as próximas investigações devem, para aprimorar a delineação desse fenótipo, investigar os genes relacionados a microcefalias primárias, maioria delas com padrão de herança AR, sobretudo aqueles quadros cuja neuroimagem é muito similar com os achados associados às infecções congênitas, tipo a síndrome Pseudo- TORCH ou Band-like intracranial calcification with simplified gyration and polymicrogyria (Abdel-Salam et al, 208; Briggs et al., 2008). Microcefalia com padrão de herança autossômico dominante com lesões em fundo olho semelhante às que tem sido observadas nas crianças com a síndrome congênita do Zika, também foram recentemente identificadas (Mears et al., 2015). Por último, se considerarmos os casos mais graves de infecção congênita pelo Zika e que incluem as artrogriposes, um número de quadros sindrômicos de origem genética, que vão desde síndromes decorrentes de microrrearranjos cromossômicos a quadros sindrômicos monogênicos, também deve ser considerado no processo de diagnóstico diferencial (OMIM; Vogt et al., 2009; Ravenscroft et al., 2013; Hall et al., 2014). Desse modo, à tentativa de se investigar fatores genéticos relacionados à susceptibilidade da ação teratogênica do ZIKV, deve-se ter em conta a tarefa de bem realizar o(s) diagnóstico(s) diferencial(is), antes de pesquisar fatores genéticos associados à susceptibilidade à infecção pelo ZIKV. Em outras palavras, uma vez clinicamente bem definido o espectro fenotípico associado à infecção congênita pelo ZIKV, este deve ser então investigado do ponto de vista molecular para afastar os possíveis diagnósticos diferenciais. Portanto, a investigação do material genético de crianças afetadas pela síndrome congênita do Zika se faz necessária nesse momento, seja aprimorar o fenótipo afastando possíveis diagnósticos diferenciais que mimetizariam essa síndrome, seja para procurar fatores genéticos que podem estar preferencialmente associados a esses quadros, determinando uma susceptibilidade genética à infecção congênita pelo ZIKV. Quanto a questão da confirmação da infecção pelo ZIKV, o diagnóstico laboratorial específico baseia-se, principalmente, na detecção de RNA viral a partir de espécimes clínicos nos primeiros dias dos sintomas. O período virêmico é de curta duração e por isso recomenda-se que o diagnóstico seja realizado até o 5º dia a partir do aparecimento dos sintomas. No Brasil, até o momento, o método padrão ouro para o diagnóstico é a reação em cadeia da polimerase após reação de transcriptase reversa (RT-PCR), que deve ser realizada em laboratórios de referência da rede do Sistema Único de Saúde (SUS). A detecção retrospectiva ou tardia do ZIKV é complicada, pois até o momento, não existem ensaios sorológicos comerciais que tenham sido exaustivamente validados para a detecção de anticorpos específicos para o ZIKV, haja vista a reação cruzada com DENV e outros flavivírus. Há, entretanto, um grande esforço dos laboratórios de referência e de centros de pesquisa para o desenvolvimento de plataformas para realização de provas sorológicas específicas (Brasil, 2015). Não existe no mercado vacinas ou antivirais específicos disponíveis para ZIKV. Recentemente, Larocca et al (2016) desenvolveram e validaram uma vacina de DNA contra ZIKV em camundongos Balb/c, C57BL/6 e SJL, expressando antígenos virais de ZIKV, como a proteína de envelope (Env) e/ou proteína pré membrana (prM) e também mutantes com deleções na prM, na região transmembrana (dTM) ou ENV. O intestino e a resposta imune: o efeito das infecções parasitárias e do Microbioma e viroma intestinal na resposta contra vírus A análise da complexa interação entre o organismo humano e os microrganismos que compõem sua microbiota tem se mostrado mais importante a cada dia. Apenas recentemente fomos capazes de estimar que o corpo humano é colonizado por aproximadamente 1014 células microbianas (Whitman et al, 1998) e 1015 partículas virais (Haynes et al, 2011). Mais recente ainda é a capacidade de correlacionarmos o impacto desta microbiota com a fisiologia e o funcionamento do organismo em geral. Apenas uma pequena parte dos microrganismos presentes são cultiváveis, e somente após o desenvolvimento e análise de técnicas de sequenciamento de larga escala foi possível estimar a complexidade dessa relação (Methé, 2012). Os microrganismos e os parasitas que compõem a microbiota humana desempenham um papel crucial na saúde do organismo estando envolvidos na modulação do sistema imune, o que inclui o desenvolvimento do tecido linfóide secundário, a expansão e diferenciação de células mielóides, a ativação de células T, a promoção de uma imunidade heteróloga contra vírus e a permeabilidade da barreira hematoencefálica (Chow J et al, 2010). Determinar quais são os constituintes comuns a uma microbiota saudável, assim como a variabilidade intrínseca a diferentes populações, tem sido tema de estudo de diferentes grupos (Methé et al, 2012; Peterson et al, 2009; Arumugam et al, 2011), gerando bancos de dados muito importantes para definir quais desvios populacionais podem estar associados à determinadas patologias. O Projeto Microbioma Humano (HMP) sequenciou a microbiota de diferentes pontos do corpo de 242 indivíduos saudáveis, gerando o maior reservatório de genes comuns ao microbioma humano (Peterson et al, 2009). A análise metagenômica do trato intestinal humano gerou o primeiro catálogo gênico microbiano do intestino humano e identificou enterotipos constantes ao microbioma, independentes da origem geográfica dos indivíduos. Estes e muitos outros estudos revisados (Clemente et al, 2012) tem tido sucesso em demonstrar que, embora exista uma grande variabilidade interpessoal na composição do microbioma, as pessoas compartilham um conjunto central de microrganismos, que quando sofre alterações específicas em sua composição predispõe a determinados quadros clínicos. Dentro desta perspectiva, alguns grupos têm buscado correlacionar de forma mais direta alterações no microbioma intestinal com o resultado clínico obtido após infecções com determinados agentes patogênicos (Clemente et al, 2012). Em trabalho recente um grupo da Washington University, usando modelos de camundongos C57BL, demonstrou que os componentes bacterianos do microbioma intestinal desempenham um papel essencial no estabelecimento ou não de infecções persistentes com norovirus murino. Como consequência, eles demonstraram que o uso de antibióticos pode alterar substancialmente a patogênese em infecções virais entéricas (Baldridge et al, 2015). Em outro trabalho, também muito recente, concluiu-se que a infecção por Influenza H7N9 e a administração de antibióticos tiveram um efeito significativo na microbiota intestinal, com uma diminuição da diversidade e aumento de espécies como Escherichia coli e Enterococcus faecium (Qin et al, 2015). Ainda nessa linha, estudos da microbiota intestinal de portadores do vírus HIV, mostraram uma alteração importante na composição da microbiota intestinal (Dillon et al, 2014) levando a ativação sistêmica e de

mucosa de células T, mediadas por células dendríticas intestinais, levando a um quadro inflamatório crônico (Dillon et al, 2015). Com isso, fica cada vez mais evidente o papel que a microbiota intestinal desempenha na modulação do sistema imunológico e na resposta contra infecções virais. Apesar de ainda não ter sido descrita nenhuma relação direta entre a composição do microbioma intestinal e a progressão de doenças provocadas por ZIKV, a cada dia novos trabalhos descrevendo a relação entre o microbioma e a modulação do sistema imune, e sua relação com a progressão de doenças virais, tem sido publicados (Baldridge et al, 2015; Dillon et al, 2014; Pfeiffer et al, 2016). Além disso, é conhecida a influência que o microbioma exerce na modulação de diversos tipos celulares que estão diretamente envolvidos na progressão da infecção pelo vírus da dengue (Schmid et al, 2014; Diamond et al, 2015). Além da microbiota, infecções parasitárias também possuem um papel essencial na imunomodulação em humanos. De fato, esses organismos acompanham a evolução de nossa espécie a milhares de anos, visto que eles já foram encontrados em fósseis de hominídeos (Zaiss et al, 2016; Araújo et al, 2008). Já se sabe, por exemplo, que a infecção por Heligmosomoides polygyrus é capaz de reduzir respostas alérgicas respiratórias estimuladas por células Th2 (Wilson et al, 2005). Também já foram feitos experimentos que mostraram que os parasitas podem induzir alterações benignas na microbiota, melhorando a sua diversidade (Zaiss et al, 2016) e reduzindo doenças inflamatórias crônicas (Zaiss et al, 2016; Ramanan et al, 2016). Por outro lado, há estudos mostrando que infecção por helmintos dificulta a eliminação de vírus pelo sistema imunológico (Mueller et al, 2014), e uma pesquisa recente concluiu que a infecção por Schistosoma mansoni favorece a reativação de gama-herpesvírus pela indução de IL-4 (Reese et al, 2014). Há ainda um estudo que concluiu que a modulação da resposta imune aos vírus pode ser independente da microbiota quando há co-infecção de vírus e helmintos (Osborne et al, 2014). A diferença na prevalência de anomalias fetais induzidas pelo ZIKV em diferentes regiões do globo, pode estar associada a outros fatores que não apenas o vírus. Diante do exposto, pode parecer promissor o estudo do papel da microbiota e das infecções parasitárias intestinais na infecção por ZIKV. É possível que modulações imunológicas específicas ocasionadas por populações microbianas (bactérias e vírus) e parasitárias intestinais possam alterar a permeabilidade da barreira hematoplacentária de algumas gestantes tornando-a mais permeável ao ZIKV, e levando, talvez, a uma maior susceptibilidade dos fetos expostos intra-útero. A metabolômica e sua possível relação com síndrome congênita do Zika A busca por fatores de risco que possam estar associados com o desenvolvimento da síndrome congênita do ZIKV passa pela dificuldade em relacionar o genótipo com o fenótipo (saúde ou doença), pois a interação dos produtos gênicos com os demais componentes intracelulares é a base do acesso aos sistemas biológicos (Kitano et al, 2002). O estudo dos componentes moleculares tem gerado diferentes "ômicas", como a proteômica, a transcriptômica e a metabolômica (Harkewicz et al, 2011). Esta última consiste no estudo de moléculas de baixo peso molecular e não proteicas que representam os produtos finais do metabolismo celular, como aminoácidos, açúcares e lipídeos (Gomase et al, 2008). Dentre estes, os lipídeos representam o maior grupo de moléculas de um metaboloma, e atuam não somente como constituintes de membrana, mas também podem apresentar diferentes funções como sinalização celular, estoque de energia e até mesmo funções de transporte (Navas-Iglesias et al, 2009). O estudo dos lipídeos de um organismo constitui a lipidômica que, juntamente com a metabolômica, pode fornecer informações úteis quando se comparam estados de saúde versus estado de doença (Harkewicz et al, 2011). Essa análise permite que se obtenha um perfil instantâneo da fisiologia celular (fenótipo), de acordo com a situação vigente (Harkewicz et al, 2011; Gomase et al, 2008). Atualmente, a tecnologia mais utilizada para estudos de metabolômica e lipidômica tem sido a espectrometria de massas, a qual possibilita aprimorar o conhecimento bioquímico em relação a diferentes tipos de doenças, dentre elas as doenças infecciosas (Gomase et al, 2008, Siuzdak et al, 1996). Crianças e gestantes que tiveram bebês com anomalias possivelmente associadas à infecção pré-natal pelo ZIKV podem apresentar diferenças que podem estar relacionadas à susceptibilidade à ação teratogênica desse vírus. Portanto, estudos de metabolômica, dentre eles de lipidômica, podem nos possibilitar compreender melhor os fatores que estejam associadas ao desenvolvimento da doença congênita causada pelo ZIKV.

Hipótese:

Os efeitos da infecção congênita pelo ZIKV devem estar associados a variações genéticas, bem como alterações do microbioma.

Objetivo Primário:

O objetivo geral desse projeto é investigar fatores (genéticos ou ligados ao microbioma ou à metabolômica) que possam induzir a uma maior susceptibilidade aos efeitos teratogênicos do ZIKV.

Objetivo Secundário:

1 Investigar fatores genéticos, comparando casos e controles, de modo a identificar variantes genéticas associadas à infeção congênita pelo ZIKV. 2 Caracterizar o papel da composição do microbioma intestinal materno (bactéria e vírus), em casos e controles, de modo a identificar uma possível associação ou susceptibilidade à infecção congênita pelo ZIKV. 3 Caracterizar o papel de infecções parasitárias intestinais em mães de casos e de controles, de modo a identificar uma possível associação ou susceptibilidade à infecção congênita pelo ZIKV. 4 Caracterizar os metabólitos maternos e de crianças afetadas pela síndrome congênita do ZIKA, bem como de crianças saudáveis, de modo a identificar possíveis fatores de risco relacionados à síndrome congênita por ZIKV.

Metodologia Proposta:

Desenho do Estudo: Estudo de coorte retrospectivo de uma série de crianças acometidas pela síndrome congênita do Zika e suas mães, oriundas de várias regiões do Brasil, sobretudo do nordeste brasileiro. A coleta dos materiais biológicos será realizada durante os mutirões nos respectivos locais onde contamos com médicos colaboradores do presente projeto, a saber Fortaleza, Recife, Rio de Janeiro e Jundiaí. Normalmente esses mutirões têm por finalidade a avaliação clínica e orientação das famílias. Para fins desse projeto incluiremos a informação sobre o TCLE e a coleta de exames. Dada as especificidades dos objetivos, apresentaremos a seguir a metodologia, critérios de inclusão e tamanho amostral referentes ao objetivo específico 1, e em seguida a metodologia a ser seguida para cumprir os demais objetivos (2, 3 e 4).I.1 Em relação ao objetivo específico 1 [Investigar fatores genéticos, comparando casos e controles, que possam indicar uma maior susceptibilidade à infeção congênita pelo ZIKV] Serão incluídas crianças com diagnóstico confirmado de síndrome congênita do Zika e crianças controles cujas gestações e partos ocorreram nos mesmos locais em que nasceram as crianças afetadas. Em relação às crianças afetadas, visto que o fenótipo associado ao ZIKV se caracteriza por um espectro, e dependendo desse fenótipo diferentes diagnósticos diferenciais podem ser considerados, a investigação dessas crianças seguirá o fluxograma apresentado no quadro 1. Todas as crianças afetadas serão selecionadas pelos colegas colaboradores e reavaliadas direta (reexame físico) ou indiretamente (reavaliação de dados clínicos, exames complementares, bem como por meio de fotos clínicas). Essa reavaliação dar-se-á por ocasião dos mutirões a serem realizados pelos colaboradores em datas específicas dentro do 1º semestre de realização do projeto. Para ilustração de como são realizados esses mutirões, o seguinte endereço (https://youtu.be/p3tTmUiMKh8), mostra um filme realizado num mutirão recentemente realizado na cidade de Fortaleza, no qual avaliamos conjuntamente, entre pediatras, neurologistas, geneticistas, oftalmologistas, fisioterapeutas e psicólogos, cerca de 60 crianças. A dinâmica dos mutirões, portanto, implicará na convocação prévia dos pacientes pelos colaboradores do projeto, avaliação das crianças por uma equipe médica, incluindo médicos geneticistas e a coordenadora do presente projeto, e coleta dos materiais biológicos. As crianças afetadas, cujo diagnóstico foi confirmado apenas pelos dados clínicos e dados de neuroimagem, uma amostra de sangue, para extração do soro também será coletada para realização de sorologia específica. As amostras das crianças controles deverão planejadas para serem coletadas também dentro do mesmo período de cada mutirão a ser realizado.Cálculo do tamanho amostral: Como se trata de um estudo de associação (de variações, provavelmente raras, do genoma com o fenótipo em questão), calculamos o tamanho amostral para modelo de estudo tipo caso-controle. Então para um gene (variação) com frequência alélica de 0,01, para detectar um risco de 3,5 serão necessários 276 casos e 276 controles.Coleta do material biológico: Serão coletadas amostras de sangue (dos casos e controles) em tubos Vacutainer com EDTA (tampa roxa) a partir de punção de sangue periférico.Métodos: Para extração do DNA serão utilizados kits apropriados. O DNA será armazenado em freezer até o envio para a realização do exoma.

Critério de Inclusão:

Em relação ao objetivo específico 1:Casos: serão considerados casos as crianças com diagnóstico confirmado da síndrome congênita do Zika, ou seja, com fenótipo dismorfológico típico e neuroimagem característica, tenham ou não confirmação laboratorial da infecção pré-natal pelo ZIKV. Controles: serão considerados controles crianças clinicamente normais nascidas (em proporção igual) nos mesmos locais que as crianças afetadas e dentro do mesmo período de tempo que nasceram as afetadas.Em relação aos objetivos específicos 2, 3 e 4:Serão incluídas mães e crianças saudáveis e com microcefalia cujas mães tiveram suspeita de ZIKV na gestação, numa doença caracterizada pela presença de exantema maculopapular pruriginoso associado ou não a: hiperemia conjuntival sem secreção e sem prurido, febre, poliartralgia e edema periarticular. Também será critério de inclusão aquelas mulheres e seus bebês que apresentaram na gestação febre de início súbito (38,5º C) e artralgia ou artrite intensa com início agudo não explicadas por outras condições. Incluiremos as mães e bebês que tiveram febre na gestação sem etiologia definida associada à mialgia, cefaleia, prostração e dor retro-orbitária. Por fim, incluiremos as mães e crianças com microcefalia sem causa conhecida.

Critério de Exclusão:

Serão considerados como critério de exclusão os casos de microcefalia de origem genética.

Riscos:

Os possíveis riscos ou desconfortos decorrentes da participação na pesquisa são relacionados ao pequeno desconforto na picada da agulha e, em alguns casos, poderá ocorrer a formação de uma pequena mancha roxa no local de onde foi retirado o sangue. As fotos clínicas das crianças sob estudo serão feitas mediante autorização dos responsáveis, não acarretando riscos. Da mesma forma, a coleta da amostra de fezes das mães não acarreta riscos para mãe.A análise do sequenciamento do exoma poderá, eventualmente, identificar variantes genéticas não relacionadas ao estudo, mas com alguma outra repercussão clínica (achados secundários). Embora esse não seja o foco do exame, cabe a você decidir se deseja receber essas informações. Sendo assim, solicitamos que preencha uma das opções a seguir: ( ) Desejo receber informações (uma listagem) com a inclusão dos achados secundários, caso sejam eventualmente identificados. ( ) Não desejo receber informações sobre achados secundários, caso sejam eventualmente identificados.

Benefícios:

O possível benefício decorrente da participação na pesquisa é o melhor conhecimento das consequências da infecção por Zika na gravidez, auxiliando na investigação e aconselhamento de famílias com este problema.

Metodologia de Análise de Dados:

A) EXOMA: A técnica escolhida como método de investigação e diagnóstico foi o exoma, pois com essa mesma técnica é possível avaliar os genes associados à microcefalia isolada ou a quadros sindrômicos no processo de realizar inicialmente os diagnósticos diferenciais e, em seguida os mesmos bancos de dados serão utilizados para a investigação de variantes associadas ao grupo de afetados (genes de susceptibilidade). O trabalho de bancada, ou seja, o diagnóstico das variantes genéticas de cada indivíduo que faz parte do sequenciamento do exoma deverá ser realizado em Laboratório externo, devido ao grande número de amostras e a necessidade de processar todas as amostras dentro de um mesmo período, condições importantes para a qualidade dos dados a serem analisados pela bioinformática. A identificação das variantes genéticas será realizada em dois tempos: 1. realizado num laboratório externo, e 2. O conjunto desses fatores genéticos (pesquisa de bioinformática) será realizado na Unicamp por um grupo de bioinformatas. Além de não dispormos de infra-estrutura nacional que atenda esses requisitos, a colaboração com a instituição externa é mais atrativa. A seguir, apresentamos dados que justificam a escolha da metodologia, bem como a sua realização no exterior. Em 2014, Kozlitina et al. apresentaram um estudo no qual identificam uma variante do TM6SF2 como gene de suscetibilidade para doença hepática não alcoólica por meio de sequenciamento completo de exoma (Whole Exome Sequencing, WES). Em 2015, Luzón-Toro et. al. identificam genes de suscetibilidade para Doença de Hirschsprung empregando esta mesma técnica. Cirulli et. al. (2015) utilizam WES para identificar genes de suscetibilidade associados a Esclerose Lateral Amiotrófica (ELA). Mais recentemente, Smith et. al. (2016) identificam genes de susceptibilidade para câncer pacreático de alto risco empregando sequenciamento de exoma. Também em 2016, Dai et. al. apresentam MST1R como gene de suscetibilidade para carcinoma de nasofaringe. Nesta proposta, também utilizaremos sequenciamento de exoma completo como ferramenta principal para a identificação de genes de susceptibilidade de infecções pelo vírus Zika (ZKV). Para tanto, aplicaremos ferramentas analíticas utilizadas nestes estudos de sucesso. Em particular, empregaremos técnicas de bioinformática para controle de qualidade e detecção de variantes, seguido por modelagens estatísticas para quantificação de evidências de associação destes marcadores moleculares com o fenótipo de interesse. A.1) Justificativa Execução do Sequenciamento no Exterior O sucesso de um projeto de pesquisa que utilize técnicas de sequenciamento como ferramenta essencial depende fortemente da qualidade de execução deste serviço. Adicionado a este fator, há também a questão de tempo necessário para a conclusão do sequenciamento, que em centros de menor capacidade de geração de dados pode durar até um ano. Num cenário simulado, no qual considera-se o sequenciamento 600 amostras para realização do exoma humano completo, apresentam-se abaixo as condições requeridas para execução no LaCTAD/UNICAMP, utilizando-se os cálculos providos pela Illumina (http://support.illumina.com/downloads/sequencing_coverage_calculator.html)Análise de Bioinformática: Fragmentos sequenciados por equipamentos Illumina são retornados ao pesquisador no formato FASTQ. Para cada amostra disponibilizada, há um par de arquivos FASTQ e este par de arquivos pode ocupar cerca de 5GB em disco. Dado o volume de dados requerido por todo o experimento (inicialmente da ordem de 3.5TB, mas chegando a 25TB ao fim de todas as análises), faz-se necessária a utilização de um ambiente computacional de alta performance com grande capacid

Desfecho Primário:

Produto "físico" não é o objetivo do projeto, no entanto, resultados desse projeto podem, a longo prazo, fornecer subsídio para o desenvolvimento de kits de diagnóstico para pacientes mais susceptíveis e probióticos que ajudem a prevenir a síndrome congênita por ZIKV. Os principais produtos esperados desse projeto, no entanto, são os trabalhos científicos de divulgação das pesquisas.

Tamanho da Amostra no Brasil: 552

Países de Recrutamento

País de Origem do Estudo	País	Nº de participantes da pesquisa
Sim	BRASIL	552

Outras Informações

Haverá uso de fontes secundárias de dados (prontuários, dados demográficos, etc)?

Sim

Detalhamento:

Apenas os prontuários dos participantes serão consultados.

Informe o número de indivíduos abordados pessoalmente, recrutados, ou que sofrerão algum tipo de intervenção neste centro de pesquisa:

552

Grupos em que serão divididos os participantes da pesquisa neste centro

ID Grupo	Nº de Indivíduos	Intervenções a serem realizadas
casos	276	análise do exoma
controles	276	análise do exoma

O Estudo é Multicêntrico no Brasil?

Não

Centros Coparticipantes

CNPJ	Nome da Instituição Co-participante	Nome do Responsável	Nome do Comitê de Ética	Instituição Selecionada Via Plataforma Brasil
06.279.103/0001-19	FUNDACAO UNIVERSIDADE FEDERAL DO MARANHAO	Antônio Augusto Moura da Silva	UFMA - Universidade Federal do Maranhão	Sim
04.102.843/0003-11	Instituto para o Desenvolvimento da Educação Ltda-IPADE/Faculdade Christus	Dra. Erlane Marques Ribeiro	Centro Universitário Christus - UNICHRISTUS	Sim

Propõe dispensa do TCLE?

Não

Haverá retenção de amostras para armazenamento em banco?

Sim

Justificativa:

Haverá retenção por enquanto dure o projeto conforme documento de biorepositório

Cronograma de Execução

Identificação da Etapa	Início (DD/MM/AAAA)	Término (DD/MM/AAAA)
Sequenciamento do microbioma/viroma dos casos e dos controles	01/10/2017	01/05/2018
Análise dos parasitas unicelulares e multicelulares nas fezes	01/05/2017	01/01/2018
Análise de Exoma	01/01/2018	01/05/2018
Sequenciamento do exoma dos casos e dos controles	01/10/2017	01/01/2018
Produção do relatório e artigos	01/05/2017	01/01/2019
Investigação dos casos sindrômicos por aCGH	01/10/2017	01/05/2018
Obtenção das amostras biológicas e dados clínicos (mutirões de avaliação e coleta) no Instituto para o Desenvolvimento da Educação-IPADE/Faculdade Christus	15/11/2017	15/11/2018
Extração dos DNAs, avaliação de qualidade e classificação das amostras	01/05/2017	01/10/2017
Geração das bibliotecas de 16S e de material genético enriquecido para vírus das fezes para análise de microbioma e viroma	01/05/2017	01/01/2018
Obtenção das amostras biológicas e dados clínicos (mutirões de avaliação e coleta) na Faculdade de Medicina de Jundiaí (FMJ)	15/11/2017	15/11/2018
Análise de Viroma	01/01/2018	01/05/2018
Obtenção das amostras biológicas e dados clínicos (mutirões de avaliação e coleta)	01/03/2017	30/09/2017
Obtenção das amostras biológicas e dados clínicos (mutirões de avaliação e coleta) na Fundação Universidade Federal do Maranhão, UFMA	15/11/2017	15/11/2018

Orçamento Financeiro

Identificação de Orçamento	Tipo	Valor em Reais (R$)
Diárias	Custeio	R$ 15.000,00
Material permanente	Capital	R$ 71.570,00
Bolsa DTI - Categoria A	Bolsas	R$ 96.000,00
Bolsa iniciação científca	Bolsas	R$ 9.600,00
Material de consumo	Custeio	R$ 304.314,83
Passagens	Custeio	R$ 20.000,00
Bolsas de pós-doutorado	Bolsas	R$ 305.100,00
bolsa doutorado	Bolsas	R$ 62.256,00
Material bibliográfico	Capital	R$ 6.186,00
Serviços de terceiros	Custeio	R$ 1.055.220,00
Total em R$		R$ 1.945.246,83

Bibliografia:

ABDEL-SALAM GM, ZAKI MS, SALEEM SN, GABER KR. Microcephaly, Malformation of Brain Development and Intracranial Calcification in Sibs: Pseudo-TORCH or a New Syndrome. Am J Med Genet A 2008;146A(22):2929-36. ARAÚJO A, REINHARD KJ, FERREIRA LF, GARDNER SL. Parasites as probes for prehistoric human migrations? Trends in Parasitology 2008; 24 (3): 112-115. ARUMUGAM M, RAES J, PELLETIER E, LE PASLIER D, YAMADA T, MENDE DR, ET AL. Enterotypes of the human gut microbiome. Nature 2011;473:174–80. doi:10.1038/nature09944. BALDRIDGE MT, NICE TJ, MCCUNE BT, YOKOYAMA CC, KAMBAL A, WHEADON M, ET AL. Commensal microbes and interferon- determine persistence of enteric murine norovirus infection. Science 2015;347:266–9. BARR C, WU T AND LAWRENCE M (2016). gmapR: An R interface to the GMAP/GSNAP/GSTRUCT suite. R package version 1.15.0. BESNARD M, LASTERE S, TEISSIER A, CAO-LORMEAU V, MUSSO D. Evidence of perinatal transmission of Zika virus, French Polynesia, December 2013 and February 2014. Euro Surveill 2014;19(14):01-05. BRASIL. Ministério da Saúde. Secretaria de Vigilância em Saúde. Boletim Epidemiológico Volume 47 N° 8 – 2016. http://portalsaude.saude.gov.br/images/pdf/2016/fevereiro/29/2016-006---Dengue-SE5-publica----o.pdfacessado em 28/3/2016 BROUTET, N. ET AL. Zika virus as a cause of neurologic disorders. N. Engl. J. Med 2016; 374: 1506–09. CARTEAUX G, MAQUART M, BEDET A, CONTOU D, BRUGIÈRES P, FOURATI S, ET AL. Zika Virus Associated with Meningoencephalitis. N Engl J Med 2016; 374(16):1595-6. CHOW J, LEE SM, SHEN Y, KHOSRAVI A, MAZMANIAN SK. Host–Bacterial Symbiosis in Health and Disease. Adv Immunol 2010;107:243-74. CIRULLI ET, LASSEIGNE BN, PETROVSKI S, SAPP PC, DION PA, ET AL. Exome sequencing in amyotrophic lateral sclerosis identifies risk genes and pathways. Science 2015;347(6229):1436-41. CLEMENTE JC, URSELL LK, PARFREY LW, KNIGHT R. The Impact of the Gut Microbiota on Human Health: An Integrative View. Cell 2012;148:1258–70. CUGOLA FR, FERNANDES IR, RUSSO FB, FREITAS BC, DIAS JL, GUIMARÃES KP, ET AL. The Brazilian Zika virus strain causes birth defects in experimental models. Nature 2016;534(7606):267-71. DAI W, ZHENG H, CHEUNG AK, TANG CS, KO JM, WONG BW, ET. Whole-exome sequencing identifies MST1R as a genetic susceptibility gene in nasopharyngeal carcinoma. Proc Natl Acad Sci USA 2016;113(12):3317-22. DEPRISTO M, BANKS E, POPLIN R, GARIMELLA K, MAGUIRE J, HARTL C, PHILIPPAKIS A, DEL ANGEL G, RIVAS MA, HANNA M, MCKENNA A, FENNELL T, KERNYTSKY A, SIVACHENKO A, CIBULSKIS K, GABRIEL S, ALTSHULER D, DALY M. A framework for variation discovery and genotyping using next-generation DNA sequencing data. Nature Genetics 43:491-498. DIAMOND MS, PIERSON TC. Molecular Insight into Dengue Virus Pathogenesis and Its Implications for Disease Control. Cell 2015;162:488–92. DILLON S, LEE E, KOTTER C, AUSTIN G, DONG Z, HECHT D, ET AL. An altered intestinal mucosal microbiome in HIV-1 infection is associated with mucosal and systemic immune activation and endotoxemia. Mucosal Immunol 2014; 7: 983–94. DILLON SM, LEE EJ, KOTTER C V, AUSTIN GL, GIANELLA S, SIEWE B, ET AL. Gut dendritic cell activation links an altered colonic microbiome to mucosal and systemic T-cell activation in untreated HIV-1 infection. Mucosal Immunol 2016;9(1):24-37. DRIGGERS RW, HO C-Y, KORHONEN EM, ET AL. Zika Virus Infection with Prolonged Maternal Viremia and Fetal Brain Abnormalities. N Engl J Med 2016;374: 2142–51. DUFFY MR, CHEN TH, HANCOCK WT. Zika virus outbreak on Yap Island, Federated States of Micronesia. N Engl J Med 2009; 360(24): 2536-43. EUROPEAN CENTRE FOR DISEASE PREVENTION AND CONTROL. Zika virus infection outbreak, Brazil and the Pacific region. 25 May 2015. Disponível em http://ecdc.europa.eu/en/publications/Publications/rapid-risk-assessment-Zika%20virus-south-america-Brazil-2015.pdf (acessado em 28/3/2016). GOMASE VS ET AL. Metabolomics. Current Drug Metabolism 2008;9: 89-98. HALL JG, ALDINGER KA, TANAKA KI. Amyoplasia revisited. Am J Med Part A 2014; 164A:700-730. HARKEWICZ, R. & DENNIS, E. A. Applications of mass spectrometry to lipids and membranes. Annual review of biochemistry 2011;80, 301. HAYNES M, ROHWER F. The Human Virome. Metagenomics Hum. Body. New York, NY: Springer New York; 2011; p. 63–77. HAZIN AN, PORETTI A, TURCHI MARTELLI CM, HUISMAN TA, MICROCEPHALY EPIDEMIC RESEARCH GROUP, DI CAVALCANTI SOUZA CRUZ D, ET AL. Computed Tomographic Findings in Microcephaly Associated with Zika Virus. N Engl J Med 2016;374(22):2193-5. INTERNATIONAL COMITTEE ON TAXONOMY OF VIRUSES. Virus taxonomy. 2014. Release 2015, http://www.ictvonline.org/virustaxonomy.asp (acesso 07.07.16). KITANO H. 2002. Systems biology: a brief overview. Science 295:1662–64. KOZLITINA J, SMAGRIS E, STENDER S, NORDESTGAARD BG, ZHOU HH, TYBJÆRG-HANSEN A, VOGT TF, HOBBS HH, COHEN JC. Exome-wide association study identifies a TM6SF2 variant that confers susceptibility to nonalcoholic fatty liver disease. Nat Genet 2014;46(4):352-6. LAROCCA RA, ABBINK P, PERON JP, ZANOTTO PM, IAMPIETRO MJ, BADAMCHI-ZADEH A, ET AL. Vaccine protection against Zika virus from Brazil. Nature 2016; [Epub ahead of print]. LUZÓN-TORO B, GUI H, RUIZ-FERRER M, SZE-MAN TANG C, FERNÁNDEZ RM, ET AL. Exome sequencing reveals a high genetic heterogeneity on familial Hirschsprung disease. Sci Rep 2015;5:16473. MAHMOOD S, AHMAD W, HASSAN MJ. Autosomal Recessive Primary Microcephaly (MCPH): clinical manifestations, genetic heterogeneity and mutation continuum. Orphanet J Rare Dis 2011;6:39. MARRS C, OLSON G, SAADE G, HANKINS G, WEN T, PATEL J, WEAVER S. Zika Virus and Pregnancy: A Review of the Literature and Clinical Considerations. Am J Perinatol 2016;33(7):625-39. MCKENNA A, HANNA M, BANKS E, SIVACHENKO A, CIBULSKIS K, KERNYTSKY A, GARIMELLA K, ALTSHULER D, GABRIEL S, DALY M, DEPRISTO MA. The Genome Analysis Toolkit: a MapReduce framework for analyzing next-generation DNA sequencing data. Genome Research 2010;20:1297-303. MCLAREN W, GIL L, HUNT SE, RIAT HS, RITCHIE GR, THORMANN A, FLICEK P, CUNNINGHAM F. The Ensembl Variant Effect Predictor. Genome Biology 2016;17(1):122. METHÉ B A., NELSON KE, POP M, CREASY HH, GIGLIO MG, HUTTENHOWER C, ET AL. A framework for human microbiome research. Nature 2012;486:215–21. MINER JJ, CAO B, GOVERO J, SMITH AM, FERNANDEZ E, CABRERA OH, ET AL. Zika Virus Infection during Pregnancy in Mice Causes Placental Damage and Fetal Demise. Cell 2016;165(5):1081-91. MLAKAR J, KORVA M, TUL N, POPOVI M, POLJŠAK-PRIJATELJ M, MRAZ J, ET AL. Zika Virus Associated with Microcephaly. N Engl J Med 2016;374(10):951-8. MORRIS-ROSENDAHL DJ, KAINDL AM. What next-generation sequencing (NGS) technology has enabled us to learn about primary autosomal recessive microcephaly (MCPH). Mol Cell Probes 2015;29(5):271-8. MUELLER KL. Parasites make it hard to fight viruses. Science. 2014;

345 (6198): 526. NAVAS-IGLESIAS, N., CARRASCO-PANCORBO, A. & CUADROS-RODRÍGUEZ, L. From lipids analysis towards lipidomics, a new challenge for the analytical chemistry of the 21st century. Part II: Analytical lipidomics. TrAC Trends in Analytical Chemistry 2009;28, 393-403. OLIVEIRA MELO AS, MALINGER G, XIMENES R, SZEJNFELD PO, ALVES SAMPAIO S, BISPO DE FILIPPIS AM. Zika virus intrauterine infection causes fetal brain abnormality and microcephaly: tip of the iceberg? Ultrasond in Obstetrics & Gynecology 2016;47(1):6-7. ONLINE MENDELIAN INHERITANCE IN MAN, OMIM®. Johns Hopkins University, Baltimore, MD. MIM Number: #251200: 12/08/2015.URL: http://omim.org/ OSBORNE LC, MONTICELLI LA, NICE TJ, SUTHERLAND TE, SIRACUSA MC, HEPWORTH MR, ET AL. Virus-helminthcoinfection reveals a microbiota-independent mechanism of immunomodulation. Science 2014;345(6196):578-582. PASSEMARD S, VERLOES A, BILLETTE DE VILLEMEUR T, BOESPFLUG-TANGUY O, HERNANDEZ K ET AL. Abnormal spindle-like microcephaly-associated (ASPM) mutations strongly disrupt neocortical structure but spare the hippocampus and longterm memory. Cortex 2016;74:158-76 PETERSON J, GARGES S, GIOVANNI M, MCINNES P, WANG L, SCHLOSS JA, ET AL. The NIH Human Microbiome Project. Genome Res 2009;19:2317–23. PFEIFFER JK, VIRGIN HW. Transkingdom Control of Viral Infection and Immunity in the Mammalian Intestine. Science 2016;351:240. PIERSON, T.C.; DIAMOND, M.S. Flaviviruses. In: KNIPE, D.M.; HOWLEY, P.M. eds. Fields virol. 6th ed. Philadelphia: Lippincott Williams & Wilkins. 2013;p.747-94. QIN N, ZHENG B, YAO J, GUO L, ZUO J, WU L, ET AL. Influence of H7N9 virus infection and associated treatment on human gut microbiota. Sci Rep 2015;5:14771. RAMANAN D, BOWCUTT3 R, LEE S.C., TANG M.S., KURTZ ZD ET AL. Helminth infection promotes colonization resistance via type 2 immunity. Science. 2016; 352(6285):608-12. RASMUSSEN SA, JAMIESON DJ, HONEIN MA, PETERSEN LR. Zika Virus and Birth Defects--Reviewing the Evidence for Causality. N Engl J Med 2016; 374(20):1981-7. RAVENSCROFT G, THOMPSON EM, TODD EJ, YAU KS, KRESOJE N, SIVADORAI P. Whole exome sequencing in foetal akinesia expands the genotype-phenotype spectrum of GBE1 glycogen storage disease mutations. Neuromuscul Disord 2013;23(2):165-9 REESE TA, WAKEMAN BS, CHOI HS, ET AL. Coinfection. Helminth infection reactivates latent gamma-herpesvirus via cytokine competition at a viral promoter. Science 2014;345: 573–577. ROLFE AJ, BOSCO DB, WANG J, NOWAKOWSKI RS, FAN J, REN Y. Bioinformatic analysis reveals the expression of unique transcriptomic signatures in Zika virus infected human neural stem cells. Cell Biosci 2016;6:42 RUMP P, JAZAYERI O, VAN DIJK-BOS KK, JOHANSSON LF, VAN ESSEN AJ, VERHEIJ JB, ET AL. Whole-exome sequencing is a powerful approach for establishing the etiological diagnosis in patients with intellectual disability and microcephaly. BMC Med Genomics 2016;9:7. SARNO M, SACRAMENTO GA, KHOURI R, ROSÁRIO MS. Zika Virus Infection and Stillbirths: A Case of Hydrops Fetalis , Hydranencephaly and Fetal Demise. PLos Negl Trop Dis 2016;10: 5–9. SCHMID MA, DIAMOND MS, HARRIS E. Dendritic cells in dengue virus infection: targets of virus replication and mediators of immunity. Front Immunol 2014;5:647. SCHULER-FACCINI L, RIBEIRO EM, FEITOSA IML, HOROVITZ DDG, CAVALCANTI DP. Possible Association Between Zika Virus Infection and Microcephaly —. MMWR Morb Mortal Wkly Rep. 2016; 65: 59–62. SHEPARD TH. "Proof" of human teratogenicity. Teratology 1994;50(2):97-8. SIUZDAK G ET AL. Mass spectrometry and viral analysis. Chemistry & Biology. 1996;3: 45-48. SMITH AL, ALIREZAIE N, CONNOR A, CHAN-SENG-YUE M, GRANT R, SELANDER I, ET AL. Candidate DNA repair susceptibility genes identified by exome sequencing in high-risk pancreatic cancer. Cancer Lett 2016; 370(2):302-12. SOUZA W, CARVALHO BS, LOPES-CENDES I. Rqc: a Bioconductor package for quality control and assessment of high-throughput sequencing data. Journal of Statistical Software 2016a [submitted]. SOUZA W AND CARVALHO B. Rqc: Quality Control Tool for High-Throughput Sequencing Data. 2016b R package version 1.6.2, https://github.com/labbcb/Rqc. TIBSHIRANI, R. Regression shrinkage and selection via the lasso. J. Royal. Statist Soc B 1996;58(1);267-288. VASCO ARAGAO MF, VAN DER LINDEN V, BRAINER-LIMA AM, COELI RR, ROCHA MA, SOBRAL DA SILVA P, ET AL. Clinical features and neuroimaging (CT and MRI) findings in presumed Zika virus related congenital infection and microcephaly: retrospective case series study. BMJ 2016;353:i1901. VOGT J, MORGAN NV, MARTON T, MAXWELL S, HARRISON BJ, BEESON D, MAHER ER. Germline mutation in DOK7 associated with fetal akinesia deformation sequence. J Med Genet. 2009;46(5):338-40. WANG K, LI M, HAKONARSON H. ANNOVAR: Functional annotation of genetic variants from next-generation sequencing data. Nucleic Acids Research 2010; 38:e164. WHITMAN WB, COLEMAN DC, WIEBE WJ. Prokaryotes: the unseen majority. Proc Natl Acad Sci USA 1998; 95: 6578–83. WILSON, M. S., TAYLOR, M. D., BALIC, A., FINNEY, C. A., LAMB, J. R., AND MAIZELS, R. M. (2005). Suppression of allergic airway nflammation by helminth induced regulatory T cells. J. Exp. Med. 202, 1199–1212. ZAISS MM, HARRIS NL. Interactions between the intestinal microbiome and helminth parasites. Parasite Immunology 2016;38, 5–11. ZANLUCA, C.; DOS SANTOS.; C.N.D. Zika virus: an overview. Microb Infect May, 2016;18(5):295-301.

Upload de Documentos

Arquivo Anexos:

Tipo	Arquivo
TCLE / Termos de Assentimento / Justificativa de Ausência	TERMOCONEPZIKVControle.docx
TCLE / Termos de Assentimento / Justificativa de Ausência	TERMODERECONSENTIMENTO_ZIKV_Casos.docx
TCLE / Termos de Assentimento / Justificativa de Ausência	TERMODERECONSENTIMENTOZIKVCasosmarcado.docx
Outros	CooperationCovenant_Engl.pdf
Projeto Detalhado / Brochura Investigador	Projeto.docx
Outros	cartaemendaoutubro2018vf.docx
Cronograma	CronogramaDeAtividades.pdf
Informações Básicas do Projeto	PB_INFORMAÇÕES_BÁSICAS_1151695_E3.pdf
Folha de Rosto	Folha_Rosto_Plataforma_Br.pdf
TCLE / Termos de Assentimento / Justificativa de Ausência	UnichristusTCLE_ProjetoZIKV_casos_VersaoFinal.pdf
Declaração de Manuseio Material Biológico / Biorepositório / Biobanco	acordodetransferencia.doc
TCLE / Termos de Assentimento / Justificativa de Ausência	TERMOCONEPZIKVCasos.docx
Folha de Rosto	Folha_Rosto_Plataforma_Br.pdf
Declaração de Manuseio Material Biológico / Biorepositório / Biobanco	Transferencia.doc
Folha de Rosto	Folha_Rosto_Plataforma_Br.pdf
Projeto Detalhado / Brochura Investigador	Projeto_SindCong_Zika_05092017EmendaOutubro2017.pdf

Comprovante de Recepção	PB_COMPROVANTE_RECEPCAO_1151695.pdf
TCLE / Termos de Assentimento / Justificativa de Ausência	TERMODERECONSENTIMENTO_ZIKV_Casos.docx
Declaração de Manuseio Material Biológico / Biorepositório / Biobanco	acordodetransferencia.doc
TCLE / Termos de Assentimento / Justificativa de Ausência	TERMODERECONSENTIMENTO_ZIKV_Controle.docx
TCLE / Termos de Assentimento / Justificativa de Ausência	TERMODERECONSENTIMENTO_ZIKV_Controle.docx
TCLE / Termos de Assentimento / Justificativa de Ausência	TERMODERECONSENTIMENTOZIKVCasos.docx
TCLE / Termos de Assentimento / Justificativa de Ausência	TERMODERECONSENTIMENTO_ZIKV_Casos.docx
Projeto Detalhado / Brochura Investigador	Projeto_SindCong_Zika_05092017EmendaOutubro2017.pdf
Outros	cartaemendaoutubro2018vf.docx
Declaração de Manuseio Material Biológico / Biorepositório / Biobanco	Biorepositorio.docx
Declaração de Manuseio Material Biológico / Biorepositório / Biobanco	Transferencia.doc
Projeto Detalhado / Brochura Investigador	Projetomarcado.docx
Comprovante de Recepção	PB_COMPROVANTE_RECEPCAO_896437.pdf
TCLE / Termos de Assentimento / Justificativa de Ausência	TERMODERECONSENTIMENTO_ZIKV_Casos.docx
Outros	emenda.docx
Declaração de Pesquisadores	UnichristusCartaDeclaracaoIslane.pdf
TCLE / Termos de Assentimento / Justificativa de Ausência	TERMODERECONSENTIMENTO_ZIKV_Controle.docx
Outros	emenda.docx
Outros	emenda.docx
Informações Básicas do Projeto	PB_INFORMAÇÕES_BÁSICAS_1151695_E3.pdf
TCLE / Termos de Assentimento / Justificativa de Ausência	TERMOCONEPZIKVControle.docx
Comprovante de Recepção	PB_COMPROVANTE_RECEPCAO_1015585.pdf
Comprovante de Recepção	PB_COMPROVANTE_RECEPCAO_823978.pdf
Informações Básicas do Projeto	PB_INFORMAÇÕES_BÁSICAS_1151695_E3.pdf
Comprovante de Recepção	PB_COMPROVANTE_RECEPCAO_1151695.pdf
Outros	UnichristusCartaEmendaOutubro_2017vf.pdf
Declaração de Pesquisadores	UnichristusTermoDeCompromissoDoAluno.pdf
Declaração de Manuseio Material Biológico / Biorepositório / Biobanco	Biorepositorio.docx
Projeto Detalhado / Brochura Investigador	Projeto.docx
TCLE / Termos de Assentimento / Justificativa de Ausência	TERMOCONEPZIKVCasos.docx
Projeto Detalhado / Brochura Investigador	Projeto_SindCong_Zika_05092017EmendaOutubro2017.pdf
Declaração de Manuseio Material Biológico / Biorepositório / Biobanco	regulamentoBiorepositorio.docx
Outros	CooperationCovenant_Port.pdf
Declaração de Pesquisadores	UnichristusCartaColaboracaoErlane.pdf
Declaração de Manuseio Material Biológico / Biorepositório / Biobanco	Transferencia.doc
Projeto Detalhado / Brochura Investigador	Projeto.docx
Declaração de Pesquisadores	UnichristusTermoDeCompromissoDoDesquisador.pdf
Outros	CartaResposta.docx
Comprovante de Recepção	PB_COMPROVANTE_RECEPCAO_1151695.pdf
Declaração de Manuseio Material Biológico / Biorepositório / Biobanco	regulamentoBiorepositorio.docx
Comprovante de Recepção	PB_COMPROVANTE_RECEPCAO_1151695.pdf
TCLE / Termos de Assentimento / Justificativa de Ausência	TERMODERECONSENTIMENTO_ZIKV_Controle.docx

Comprovante de Recepção	PB_COMPROVANTE_RECEPCAO_1151695.pdf
Folha de Rosto	Folha_Rosto_Plataforma_Br.pdf
TCLE / Termos de Assentimento / Justificativa de Ausência	UnichristusTCLE_ProjetoZIKV_controles_VersaoFinal.pdf
Declaração de Manuseio Material Biológico / Biorepositório / Biobanco	Biorepositorio.docx
Outros	Materialtransferagreement.pdf

Finalizar

Manter sigilo da integra do projeto de pesquisa: Sim

Prazo: Até a publicação dos resultados

Justificativa da Emenda:

Introduzo essa resposta para nova avaliação com o objetivo de atender as pendências referentes ao parecer 3.125.908

ANEXO 2: CEP - Circulação e diversidade genética e molecular dos vírus Dengue, Chikungunya e Zika, e outras arboviroses na região metropolitana de Campinas-SP.

COMITÊ DE ÉTICA EM PESQUISA DA UNICAMP - CAMPUS CAMPINAS

PARECER CONSUBSTANCIADO DO CEP

DADOS DO PROJETO DE PESQUISA

Título da Pesquisa: Circulação e diversidade genética e molecular dos vírus Dengue, Chikungunya e Zika, e outras arboviroses na região metropolitana de Campinas-SP.

Pesquisador: Clarice Weis Arns

Área Temática:

Versão: 1

CAAE: 56793516.0.0000.5404

Instituição Proponente: Instituto de Biologia - Unicamp

Patrocinador Principal: Universidade Estadual de Campinas - UNICAMP

DADOS DO PARECER

Número do Parecer: 1.611.423

Apresentação do Projeto:

Os pesquisadores esclarecem que este projeto temático translacional visa caracterizar aspectos básicos e patogênicos da infecção pelo vírus Zika, sendo previsto o desenvolvimento de seis subprojetos. Informam que o Zika virus (ZIKV) é um membro da família Flaviviridae que causa doença febril aguda e outras complicações em humanos, isolado no final da década de 40 na África tendo sido associado a epidemia de grandes proporções na Polinésia Francesa em 2013. A descrição de casos autóctones no Brasil ocorreu no início de 2015 e desde então um número significativo de casos da doença tem sido descrito no nordeste brasileiro com extensão para todo o território nacional. Enquanto cerca de 80% de todas pessoas infectadas são assintomáticas, 20% de todos os humanos com infecção pelo virus Zika desenvolvem uma doença aguda febril ou não exantemática. Dentre as manifestações clássicas estão incluídos os seguintes sinais e sintomas: febre, cefaleia, artralgia, mialgia, exantema maculo-papular quadro clínico similar ao de outras arboviroses como a da Dengue e da febre pelo vírus Chikungunya exigindo a necessidade de investigação laboratorial para o diagnóstico diferencial. Embora a doença pelo ZIKV seja autolimitada, casos de manifestações neurológicas e síndrome de Guillain-Barré foram descritos na Polinésia Francesa e no Brasil durante as epidemias de Zika. Publicações recentes sugerem ainda que o ZIKV pode ser teratogênico e capaz de induzir o desenvolvimento de defeitos fetais,

Endereço: Rua Tessália Vieira de Camargo, 126
Bairro: Barão Geraldo **CEP:** 13.083-887
UF: SP **Município:** CAMPINAS
Telefone: (19)3521-8936 **Fax:** (19)3521-7187 **E-mail:** cep@fcm.unicamp.br

como microcefalia. Apesar deste grande impacto do vírus Zika em saúde pública, pouco se sabe sobre os mecanismos virais associados com o desenvolvimento desta doença. Assim, este esforço colaborativo feito por pesquisadores da Universidade de Campinas (Unicamp) pretende caracterizar aspectos básicos e patogênicos da infecção pelo vírus Zika. O presente subprojeto (denominado "1" ou "circulação e diversidade genética do Zika virus") visa realizar a investigação da infecção por ZIKV em indivíduos com suspeita clínica de acordo com a definição da Organização Mundial de Saúde através de reação em cadeia da polimerase em tempo real; além de sequenciar as cepas do ZIKV detectado, analisar a relação filogenética do ZIKV em circulação na região de Campinas e detectar variantes do ZIKV associado às diferentes síndromes clínicas apresentadas. Para tanto, soro, sangue total e urina serão obtidos dos pacientes incluídos neste estudo mediante termo de consentimento livre e esclarecido. A detecção do vírus Zika nestas amostras será realizada por qPCR de acordo com o protocolo descrito por Lanciotti e colaboradores. Para o grupo de adolescentes e menores de 12 anos, os procedimentos compreendem entrevista e coleta de amostras de sangue (10 ml), saliva, urina e fezes, sendo esses últimos de forma espontânea, bem como consultas mensais de seguimento clínico durante um ano. Para o grupo de gestantes e puérperas, além da amostra de sangue haverá coleta de uma amostra de placenta, em ocasião única, sendo ainda prevista a participação de um grupo controle não infectado pelo ZIKV. Para o grupo adulto, além da coleta de sangue, eventualmente haverá coleta de líquor, porém somente em situações em que houver alterações neurológicas que indiquem esse procedimento, a ser feito sob anestesia e pelo médico assistente responsável pelo atendimento. Os pacientes serão selecionados no Hospital de Clínicas da Unicamp e no Centro de Atenção Integral à Saúde da Mulher, hospitais de ensino vinculados à Faculdade de Ciências Médicas da Universidade Estadual de Campinas. Serão incluídos 300 sujeitos com suspeita clínica de arbovirose, dengue, Zika vírus ou febre de chikungunya segundo as definições da Organização Mundial de Saúde, 2016. Também serão utilizadas fontes secundárias de dados como fichas de notificação dos casos, prontuários médicos, boletins de atendimento de urgência e dados do sistema informatizado do HC-Unicamp e do CAISM-Unicamp.

Objetivo da Pesquisa:

Realizar a investigação da infecção por ZIKV em indivíduos com suspeita clínica de acordo com a definição da Organização Mundial de Saúde através de reação em cadeia da polimerase em tempo real; - sequenciar as cepas do ZIKV detectado; - analisar a relação filogenética do ZIKV em circulação na região de Campinas; detectar variantes do ZIKV associado às diferentes síndromes clínicas apresentadas.

Avaliação dos Riscos e Benefícios:

Como a maior parte do estudo será realizado "in vitro", o protocolo é avaliado como de baixo risco aos participantes. Os maiores desconfortos se referem à coleta de sangue periférico, a ser realizado por profissional habilitado. No caso da coleta de líquor pode ocorrer dor no local e dor de cabeça após o procedimento, porém nem sempre essa coleta está prevista e será realizada por indicação clínica, não para finalidades exclusivas do estudo. No caso de coletas de saliva, urina e fezes, a mesma será natural, ou seja, sem o uso de equipamentos. Não haverá benefícios diretos, mas há potenciais benefícios coletivos no âmbito da saúde pública no Brasil.

Comentários e Considerações sobre a Pesquisa:

Estudo monocêntrico no Brasil, compreendendo projeto temático translacional que visa caracterizar aspectos básicos e patogênicos da infecção pelo vírus Zika. Serão desenvolvidos seis subprojetos. Subprojeto 1. Circulação e diversidade genética do Zika virus: estudo transversal; Subprojeto 2. Modelo de infecção de Zika virus camundongo adulto: estudo experimental com animais; Subprojeto 3. Efeitos da infecção por vírus zika sobre a interação leucócito-endotelio: estudo experimental in vitro; Subprojeto 4. Efeito do Zika vírus durante a embriogênese neural in vivo e in vitro: experimental com animais, serão utilizados tecidos provenientes de natimortos; Subprojeto 5. Neuroproteômica durante a infecção pelo vírus Zika; Subprojeto 6. O microbioma intestinal durante a infecção por Zika virus: estudo transversal clínico. O estudo é relevante e há potencial benefício coletivo relacionado à saúde pública.

Considerações sobre os Termos de apresentação obrigatória:

Projeto de pesquisa encaminhado nos moldes da PB com todos os itens preenchidos, incluindo orçamento e cronograma, além de brochura dos pesquisadores com o detalhamento do estudo. Também foi anexada folha de rosto assinada pela pesquisadora responsável e pela pró-reitora de pesquisa da Unicamp, uma vez que há previsão de outras etapas a serem realizadas, além do envolvimento diretamente de pacientes atendidos no HC e no CAISM. Também há previsão de armazenamento de material biológico com detalhamento no item "justificativa" das informações básicas do projeto gerada pela PB. Foram anexados quatro modelos de TCLE, sendo um para indivíduos adultos, um para menores, um para adolescentes (termo de assentimento) e outro para gestantes e puérperas, nesse último incluindo indivíduos controle.

Recomendações:

1. No TCLE destinado para o grupo de participantes adultos, na penúltima linha da primeira folha é mencionada a resolução 196/96, porém a mesma foi revogada pela resolução 466/2012 CNS, de

modo que essa informação necessita ser atualizada.
2. O cronograma mostra sobreposição entre a previsão de início dos procedimentos do estudo e o período de apreciação ética. Observar que os procedimentos só poderão ser iniciados após a aprovação final pelo CEP.

Conclusões ou Pendências e Lista de Inadequações:
Aprovado com recomendações.

Considerações Finais a critério do CEP:
- O sujeito de pesquisa deve receber uma via do Termo de Consentimento Livre e Esclarecido, na íntegra, por ele assinado (quando aplicável).

- O sujeito da pesquisa tem a liberdade de recusar-se a participar ou de retirar seu consentimento em qualquer fase da pesquisa, sem penalização alguma e sem prejuízo ao seu cuidado (quando aplicável).

- O pesquisador deve desenvolver a pesquisa conforme delineada no protocolo aprovado. Se o pesquisador considerar a descontinuação do estudo, esta deve ser justificada e somente ser realizada após análise das razões da descontinuidade pelo CEP que o aprovou. O pesquisador deve aguardar o parecer do CEP quanto à descontinuação, exceto quando perceber risco ou dano não previsto ao sujeito participante ou quando constatar a superioridade de uma estratégia diagnóstica ou terapêutica oferecida a um dos grupos da pesquisa, isto é, somente em caso de necessidade de ação imediata com intuito de proteger os participantes.

- O CEP deve ser informado de todos os efeitos adversos ou fatos relevantes que alterem o curso normal do estudo. É papel do pesquisador assegurar medidas imediatas adequadas frente a evento adverso grave ocorrido (mesmo que tenha sido em outro centro) e enviar notificação ao CEP e à Agência Nacional de Vigilância Sanitária – ANVISA – junto com seu posicionamento.

- Eventuais modificações ou emendas ao protocolo devem ser apresentadas ao CEP de forma clara e sucinta, identificando a parte do protocolo a ser modificada e suas justificativas e aguardando a aprovação do CEP para continuidade da pesquisa. Em caso de projetos do Grupo I ou II apresentados anteriormente à ANVISA, o pesquisador ou patrocinador deve enviá-las também à mesma, junto com o parecer aprovatório do CEP, para serem juntadas ao protocolo inicial.

- Relatórios parciais e final devem ser apresentados ao CEP, inicialmente seis meses após a data deste parecer de aprovação e ao término do estudo.

-Lembramos que segundo a Resolução 466/2012 , item XI.2 letra e, "cabe ao pesquisador apresentar dados solicitados pelo CEP ou pela CONEP a qualquer momento".

Este parecer foi elaborado baseado nos documentos abaixo relacionados:

Tipo Documento	Arquivo	Postagem	Autor	Situação
Informações Básicas do Projeto	PB_INFORMAÇÕES_BASICAS_DO_PROJETO_726200.pdf	25/05/2016 23:10:56		Aceito
Projeto Detalhado / Brochura Investigador	ProjetoRedeZikaUnicampCEPAbril2016.pdf	25/05/2016 23:08:37	Clarice Weis Arns	Aceito
TCLE / Termos de Assentimento / Justificativa de Ausência	TCLEPaisResponsaveisLegais.pdf	25/05/2016 23:07:17	Clarice Weis Arns	Aceito
TCLE / Termos de Assentimento / Justificativa de Ausência	TCLEGestantesPuerperas.pdf	25/05/2016 23:06:22	Clarice Weis Arns	Aceito
TCLE / Termos de Assentimento / Justificativa de Ausência	TCLEAdulto.pdf	25/05/2016 23:05:59	Clarice Weis Arns	Aceito
TCLE / Termos de Assentimento / Justificativa de Ausência	TCLEAdolescentes.pdf	25/05/2016 23:05:42	Clarice Weis Arns	Aceito
Folha de Rosto	FOLHA_DE_ROSTO_DCZ.pdf	25/05/2016 23:04:09	Clarice Weis Arns	Aceito

Situação do Parecer:
Aprovado

Necessita Apreciação da CONEP:
Não

Endereço: Rua Tessália Vieira de Camargo, 126
Bairro: Barão Geraldo **CEP:** 13.083-887
UF: SP **Município:** CAMPINAS
Telefone: (19)3521-8936 **Fax:** (19)3521-7187 **E-mail:** cep@fcm.unicamp.br

CAMPINAS, 28 de Junho de 2016

Assinado por:
Renata Maria dos Santos Celeghini
(Coordenador)

Endereço: Rua Tessália Vieira de Camargo, 126
Bairro: Barão Geraldo **CEP:** 13.083-887
UF: SP **Município:** CAMPINAS
Telefone: (19)3521-8936 **Fax:** (19)3521-7187 **E-mail:** cep@fcm.unicamp.br